

Conference and Advanced School on Low-Dimensional Quantum Systems



13 - 24 March 2023
An ICTP Meeting
Santiago, Chile



Institut Català
de Nanociència
i Nanotecnologia



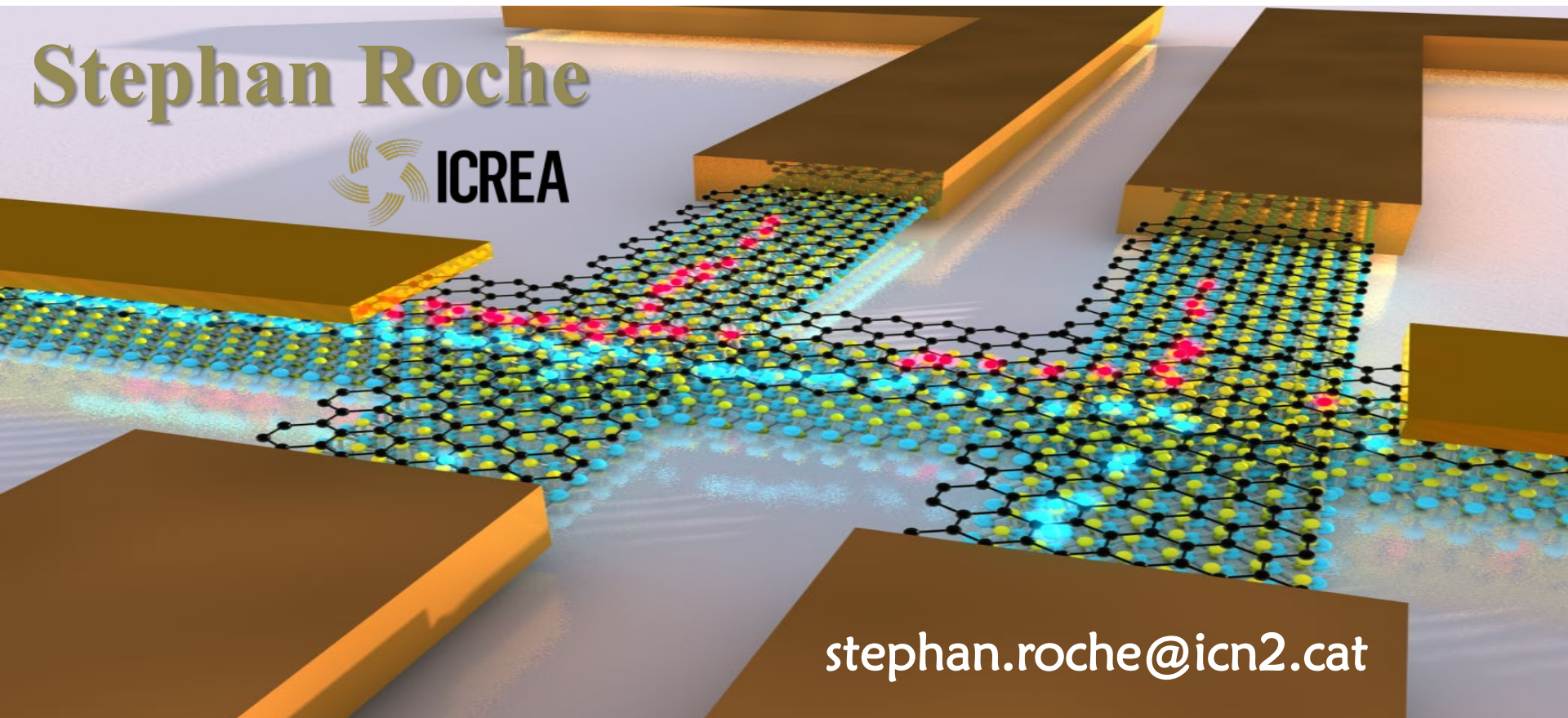
EXCELENCIA
SEVERO
OCHOA

BIST

Barcelona Institute of
Science and Technology

Topological Spin Transport in *Quantum Materials & Entanglement Dynamics*

Stephan Roche



stephan.roche@icn2.cat

Institute of Nanoscience & Nanotechnology

Barcelona Institute of Science & Technology

bist.eu



Quantum Materials @ICN2

www.icn2.cat



Institut Català
de Nanociència
i Nanotecnologia

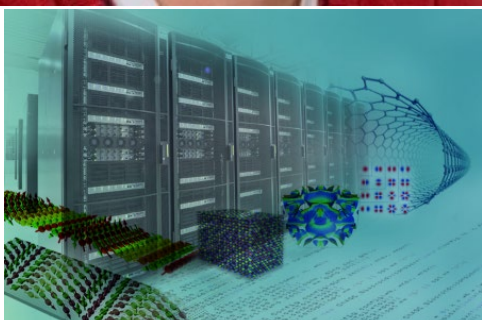
Sergio Valenzuela



ates.org/... Energy Converter SPICE

S DIRECTORY CAREERS RESEARCH INDUSTRY & SERVICES OUTREACH

RESEARCH

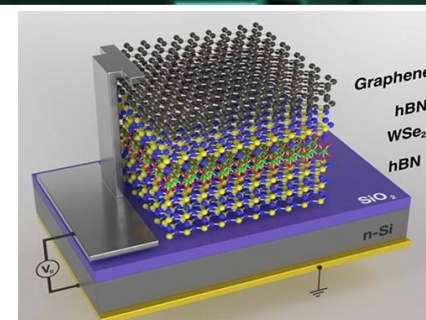


TRENDING TOPICS

QUANTUM MATERIALS

Shaping the materials for quantum technologies

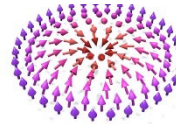
More trending topics coming soon



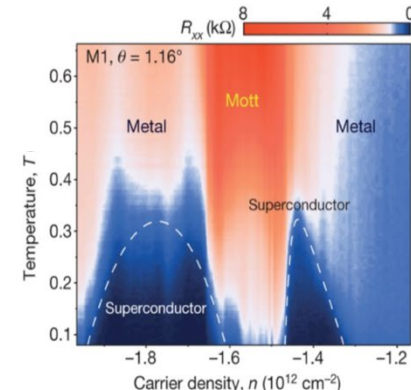
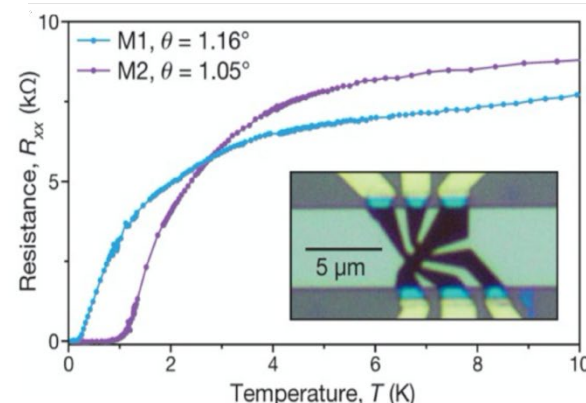
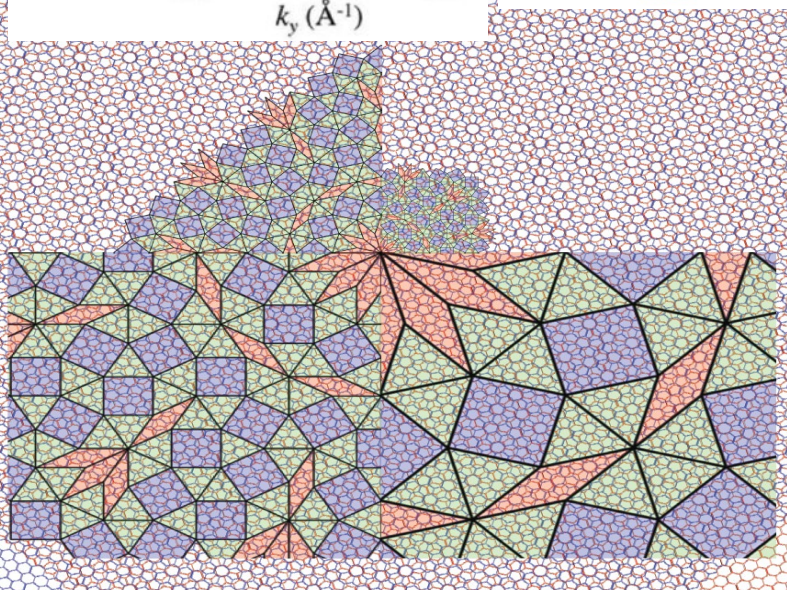
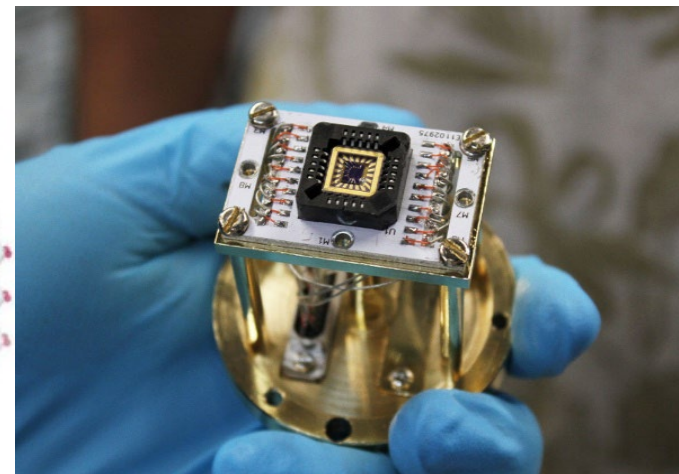
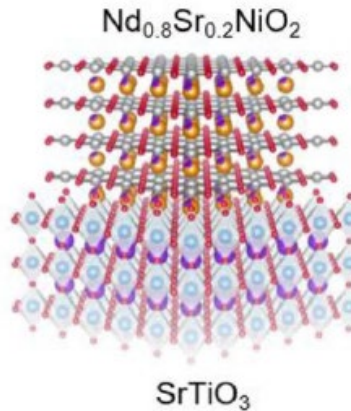
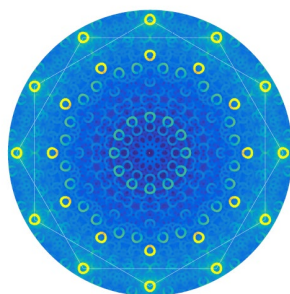
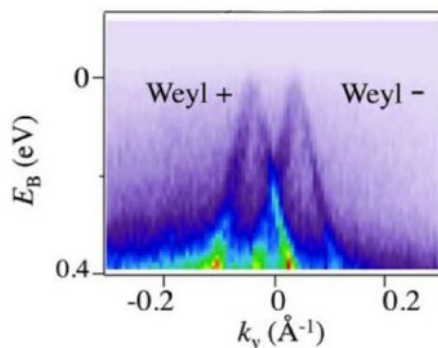


ROADMAP

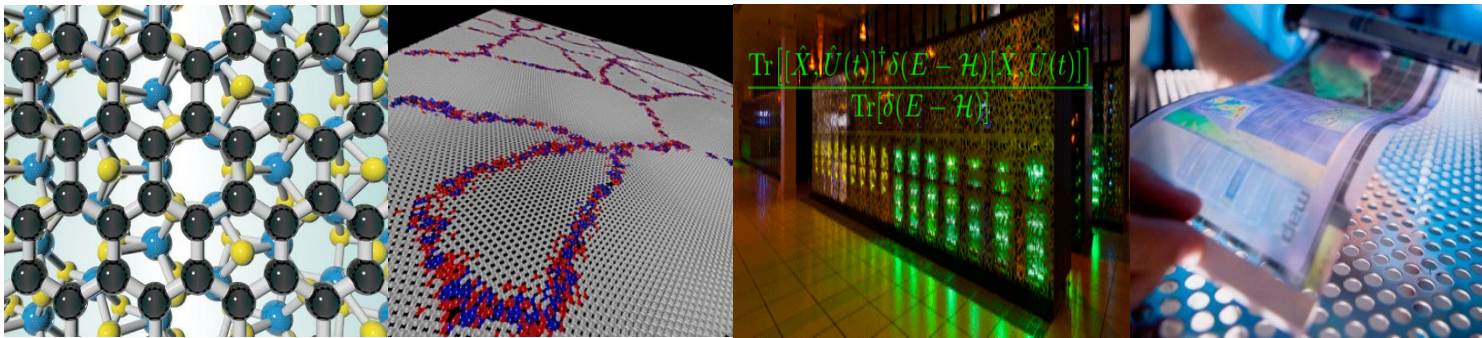
The 2021 quantum materials roadmap



Feliciano Giustino^{1,2} , Jin Hong Lee³, Felix Trier³ , Manuel Bibes³ , Stephen M Winter⁴, Roser Valenti⁴ , Young-Woo Son⁵, Louis Taillefer^{6,7}, Christoph Heil⁸ , Adriana I Figueroa⁹ , Bernard Plaçais¹⁰ , QuanSheng Wu¹¹, Oleg V Yazyev¹¹ , Erik P A M Bakkers¹², Jesper Nygård¹³, Pol Forn-Díaz^{14,15}, Silvano De Franceschi¹⁶, J W McIver¹⁷ , L E F Foa Torres¹⁸ , Tony Low¹⁹, Anshuman Kumar²⁰, Regina Galceran⁹ , Sergio O Valenzuela^{9,21}, Marius V Costache⁹ , Aurélien Manchon²², Eun-Ah Kim²³ , Gabriel R Schleder^{24,25} , Adalberto Fazzio^{24,25} and Stephan Roche^{9,21}



Theoretical & Computational Nanoscience



Members

Stephan Roche (head)
Aron W. Cummings (staff)
José H. Garcia (staff)
Thomas Galvani (Pdoc)
Isaac Alcón (Pdoc)
Luis Manuel Canonico (Pdoc)
Joaquin Medina Dueñas (PhD)
Onurcan Kaya (PhD)
Pedro Alcazar (PhD)
Jorge Ramírez and Jaime Garrido
(Master students)

Past members

José-Eduardo Barrios
Bruna Gabrielly
Pablo Piskunow
Antonio Benitez
Aleandro Antidormi
Nicolas Leconte
Dinh Van Tuan
Frank Ortmann
David Soriano
Stephen Power



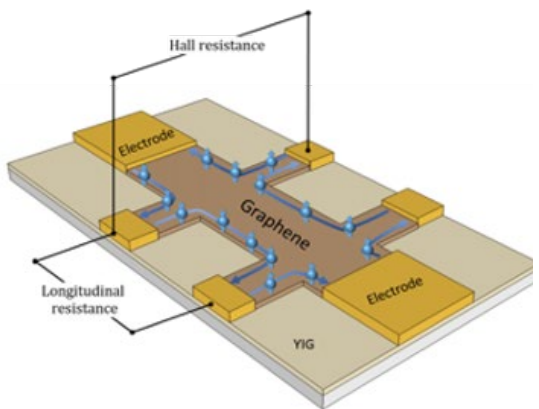
Topological Quantum Matter

Forefront Research

Topological Physics Fundamental

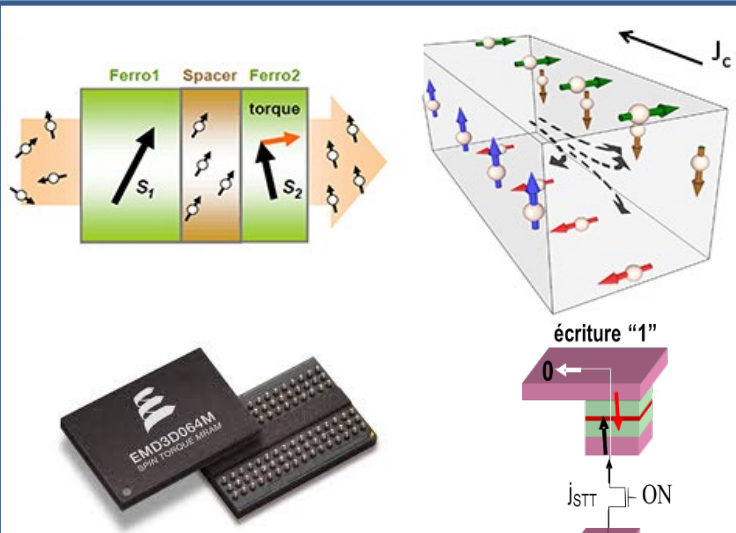
Spin Manipulation Memory Techs

Entanglement Quantum info manipulation

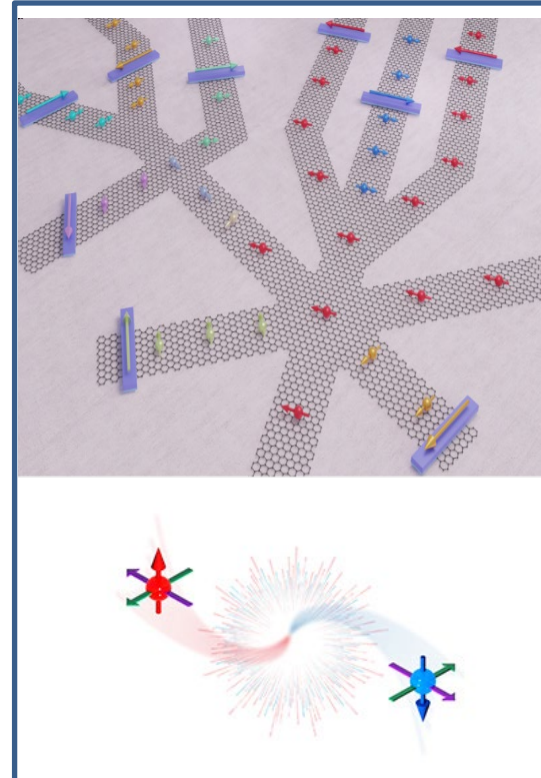


Non-local transport measurements

QHE (resistance standard)
QSHE (Topological insulators)
QAHE (magnetism/SOC)
...



Generation of spin current and
Manipulation of magnets
Spin-orbit torque
(STT-MRAM and SOT-MRAM)



SYNOPSIS

“Quo Vadis 2D Spintronics?”

Linear scaling quantum transport methods

Low symmetry topological insulators

- persistent

“SPUKHAFTE
FERNWIRKUNG!”

Multiple conduction bands

Spin Hall Effect

(MoTe₂ monolayer)

Giant SHE

$$\lambda_s \theta_{sH}^\alpha \sim 10 - 50 \text{ nm}$$

Quantum Spin Hall Effect
(WTe₂ monolayer)

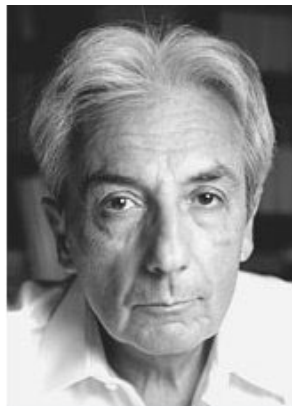
*Electrically tunable
spin polarized topological currents*

*Higher resilience to disorder scattering (long spin lifetimes)
& to Rashba SOC (inversion symmetry breaking)*

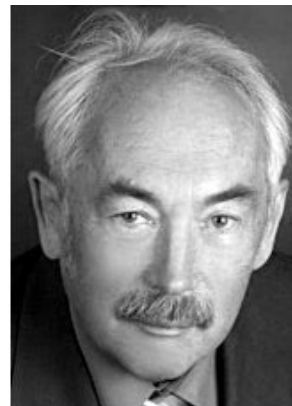
„Quo vadis
2D Spintronics?“

Spintronics and its industrial/Societal impact

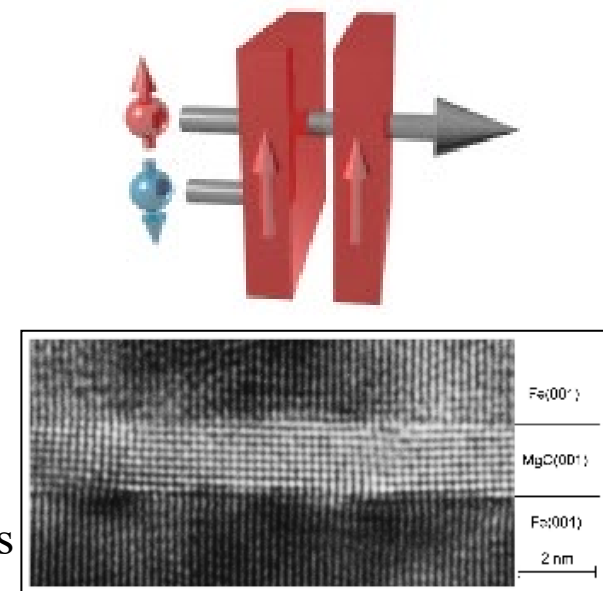
Albert Fert



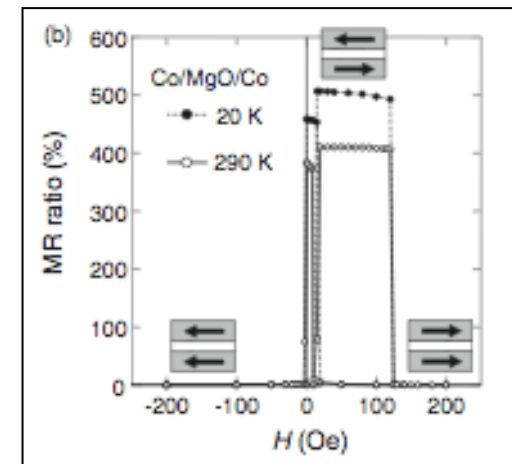
Peter Grünberg



2007 Physics Nobel Laureates



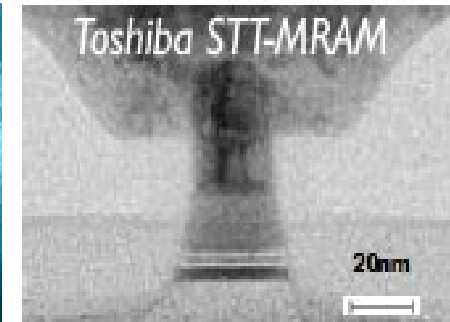
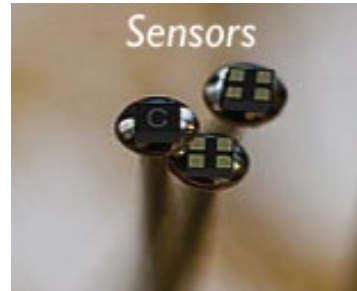
$$MR = \frac{R_{AP} - R_P}{R_P}$$



Magnetic field sensors used to read data in hard disk drives, microelectromechanical systems (MEMS), minimally invasive surgery
Automotive sensors for fuel handling system, Anti-skid system, speed control & navigation

Magnetoresistive random-access memory (MRAM)

Spin transfer Torque MRAM



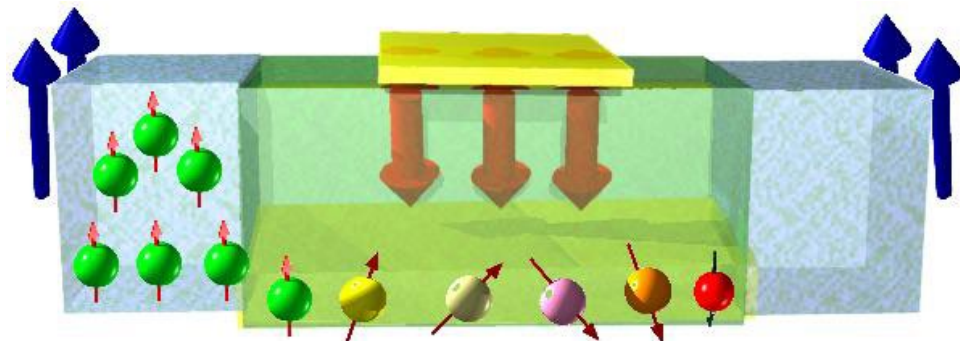
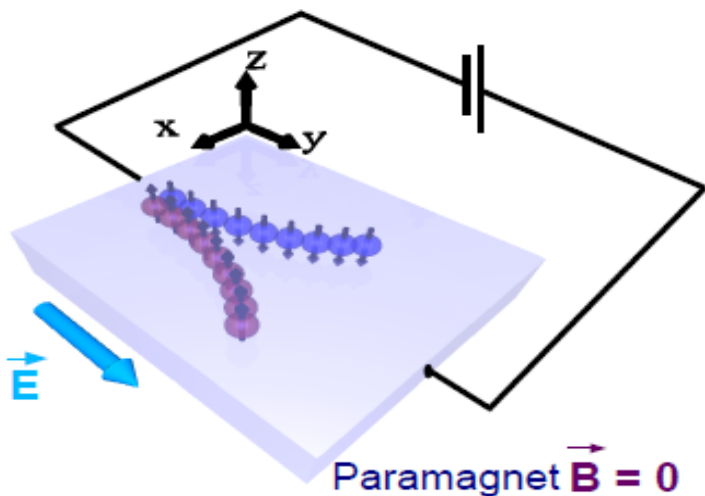
Spin-based information processing ?

Need for spin information transport on long distance (room T)

Spin injection and detection (ferromagnets/nonmagnetic materials)

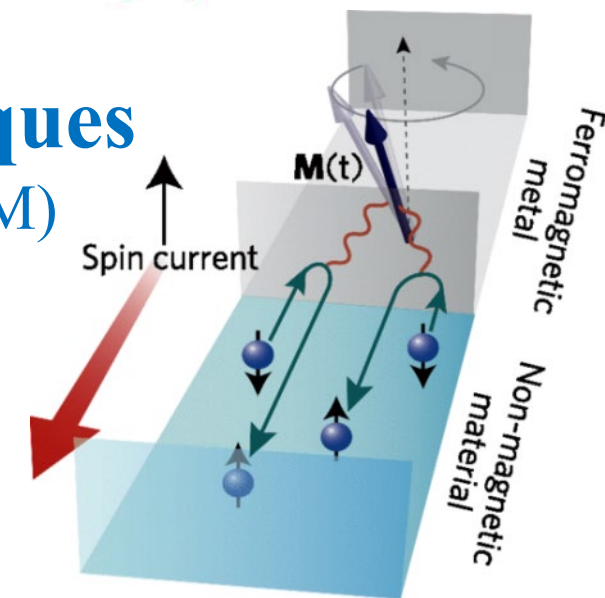
Active devices based on **Spin manipulation** ?

Datta-Das spin transistor



Spin torques
(SOT-MRAM)

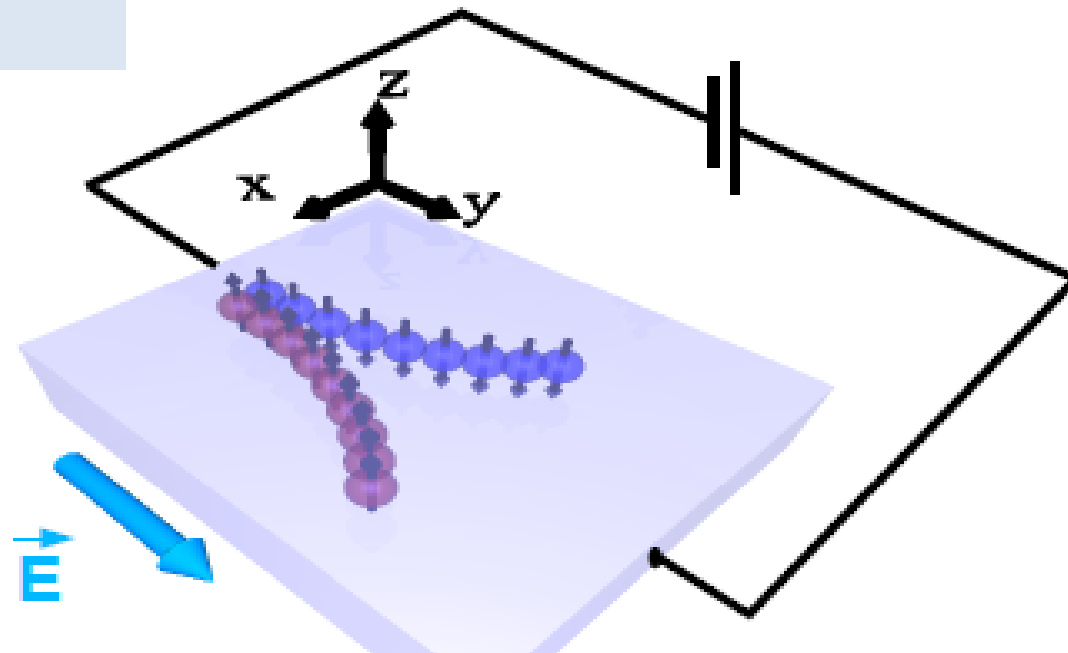
Spin Hall Effect



Spin Hall effect

(Pure) spin current generation,
manipulation & detection

(strong spin-orbit coupling materials)



Spin-orbit coupling fields

(effective magnetic field)

Generates (bulk)
transversal spin current

(spin polarization orthogonal
to both currents)

$$\vec{J}_s = \theta_{sH} \vec{\sigma} \wedge \vec{J}$$

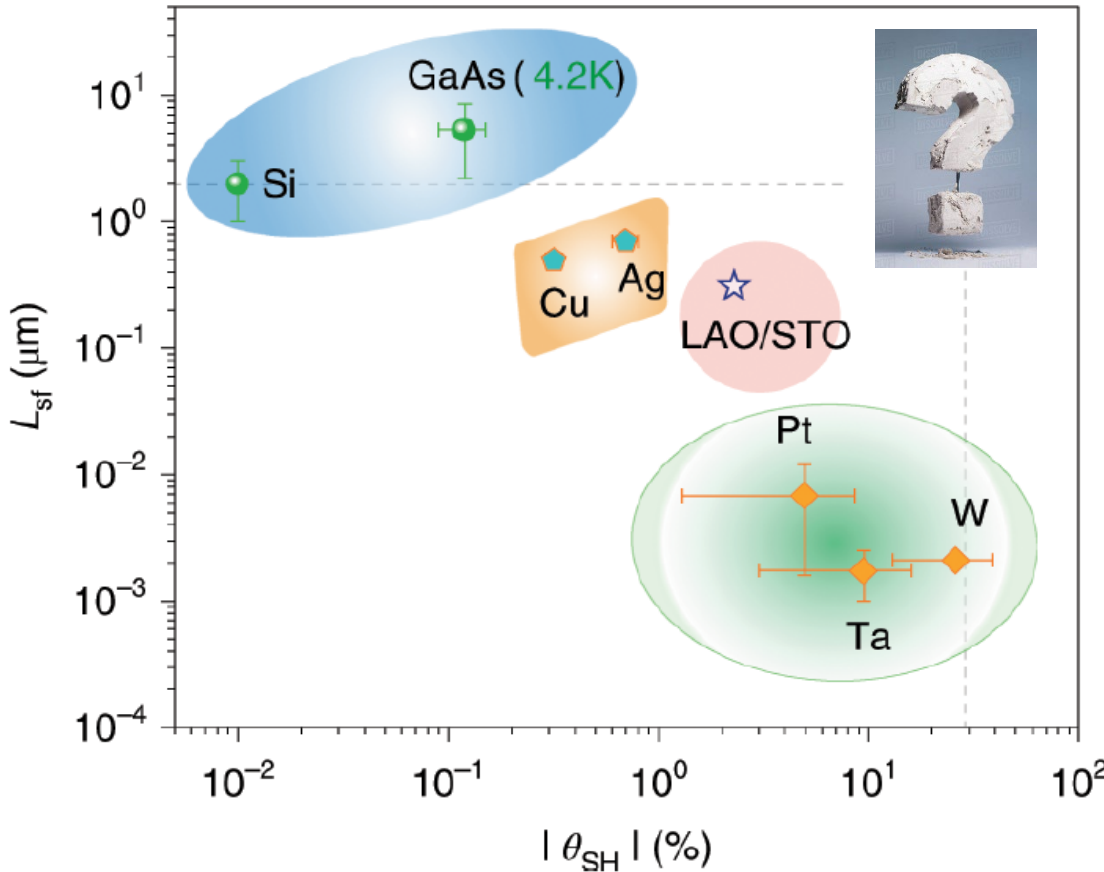
Spin Hall angle :

measures how much spin current
is generated from a charge current

$$\theta_{sH} \sim \frac{|J_s|}{|J_c|}$$

Long sought-after spintronic materials

λ_s **Spin diffusion length** : measures upper limit for spin transmission



Problem !

SOC \nearrow

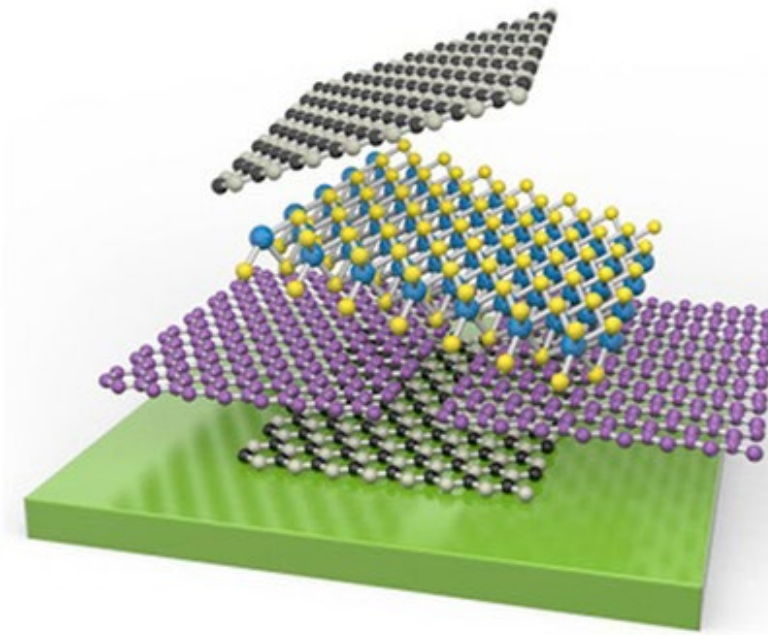
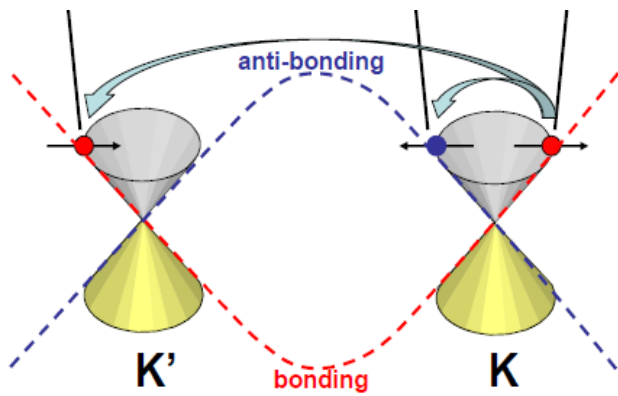
θ_{SH} \nearrow

λ_s \searrow

$$\lambda_s \cdot \theta_{SH} \sim 0.1 - 0.2 \text{ nm} \quad (\text{Pt, } \beta - W, \text{ } \beta\text{-Ta or Au})$$

Could graphene solve such conundrum?

- Ambipolar/tunable transport
 - Large mobilities (> 100k cm²/V.s at RT, 1M cm²/V.s at 4K)
 - Low spin-orbit interaction
- Graphene properties can be tailored by proximity effects



magnetizing graphene, generating spin currents, and fabricating “active spin devices, etc...

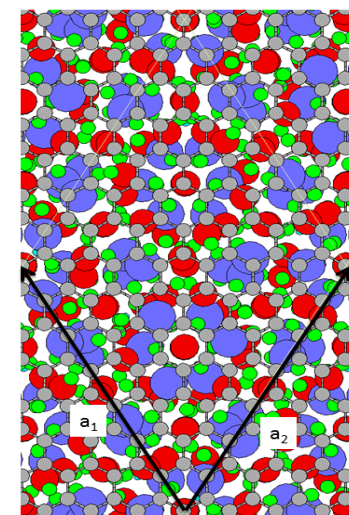
Graphene/Magnetic insulators



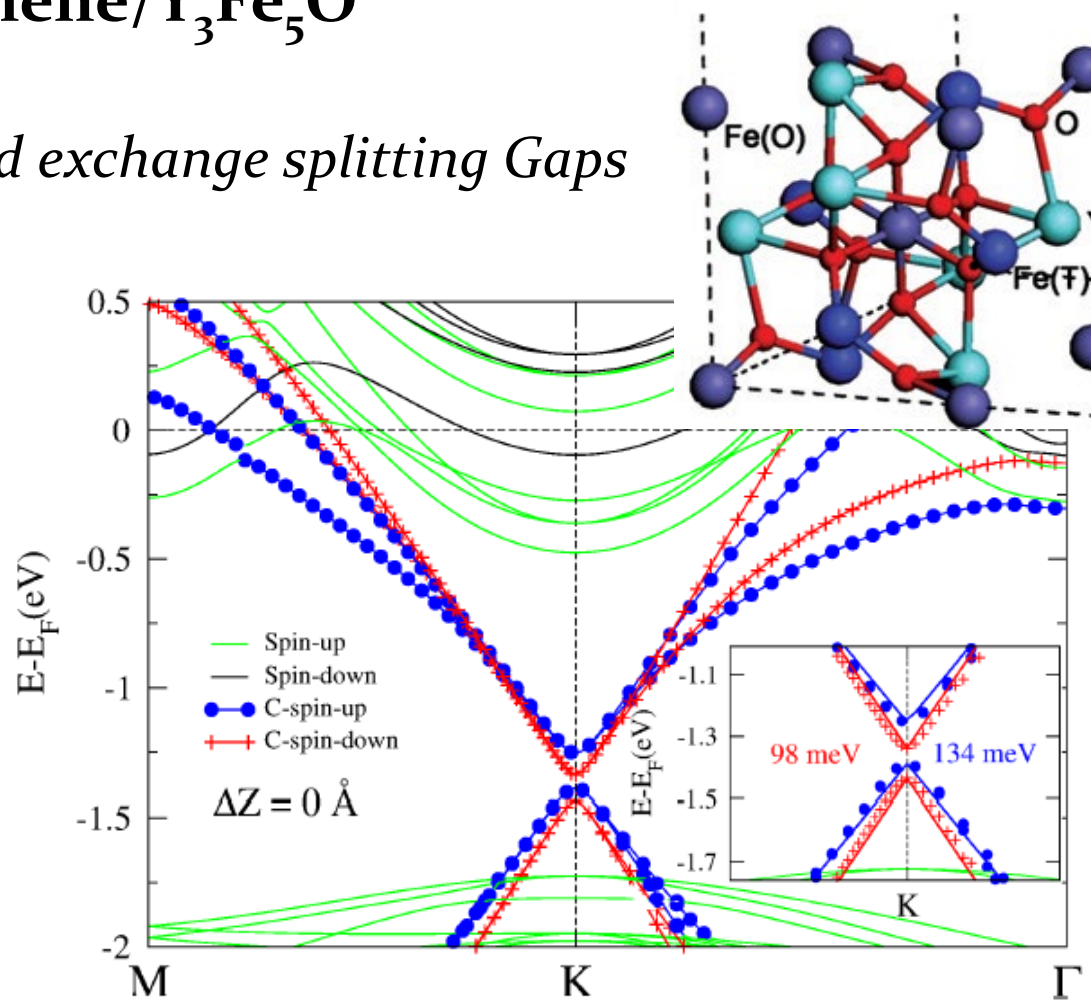
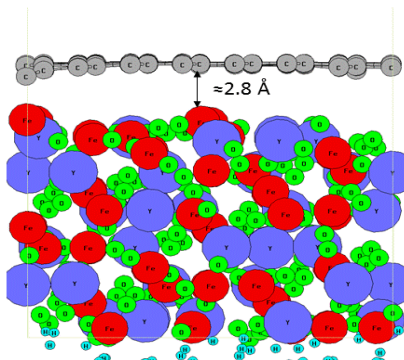
DE LA RECHERCHE À L'INDUSTRIE



Graphene/EuO and Graphene/Y₃Fe₅O



Spin filtering and exchange splitting Gaps



Exchange splitting
(G/YIG) = 40 meV

Yang, Hallal, Waintal, Roche, M. Chshiev, PRL 110, 046603 (2013)
Hallal et al. M. Chshiev, 2D materials 4 , 025074 (2017)



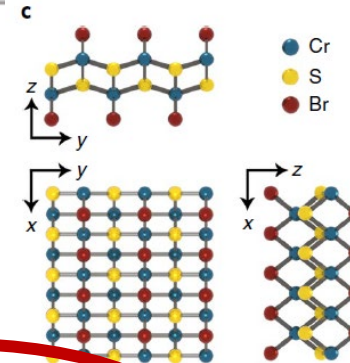
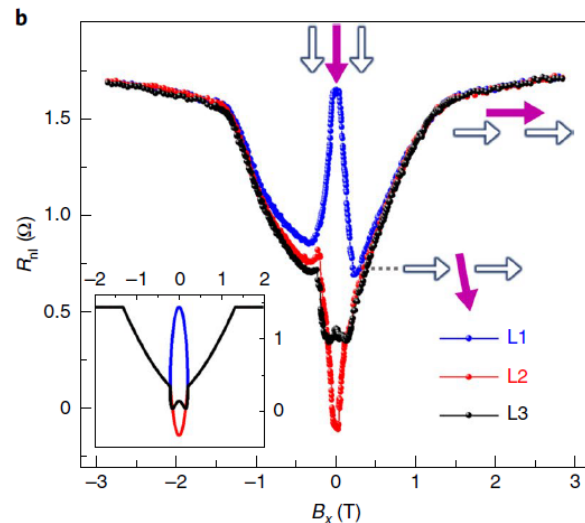
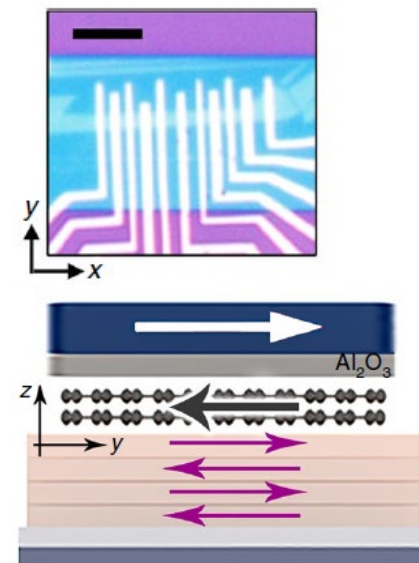
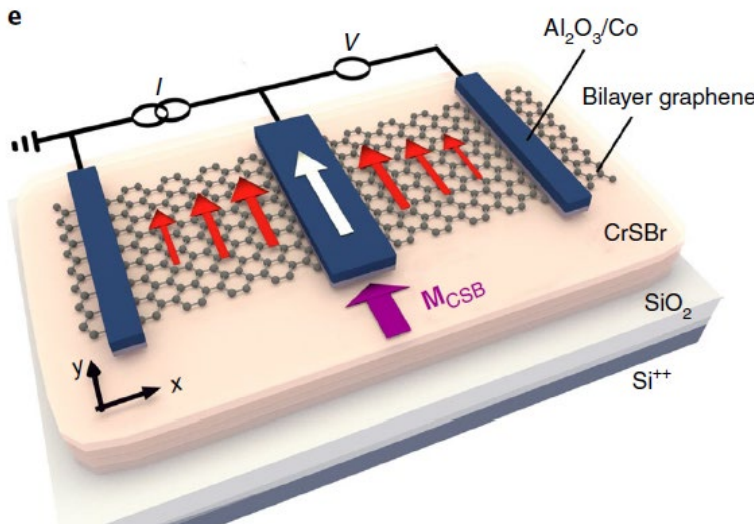
Electrical and thermal generation of spin currents by magnetic bilayer graphene

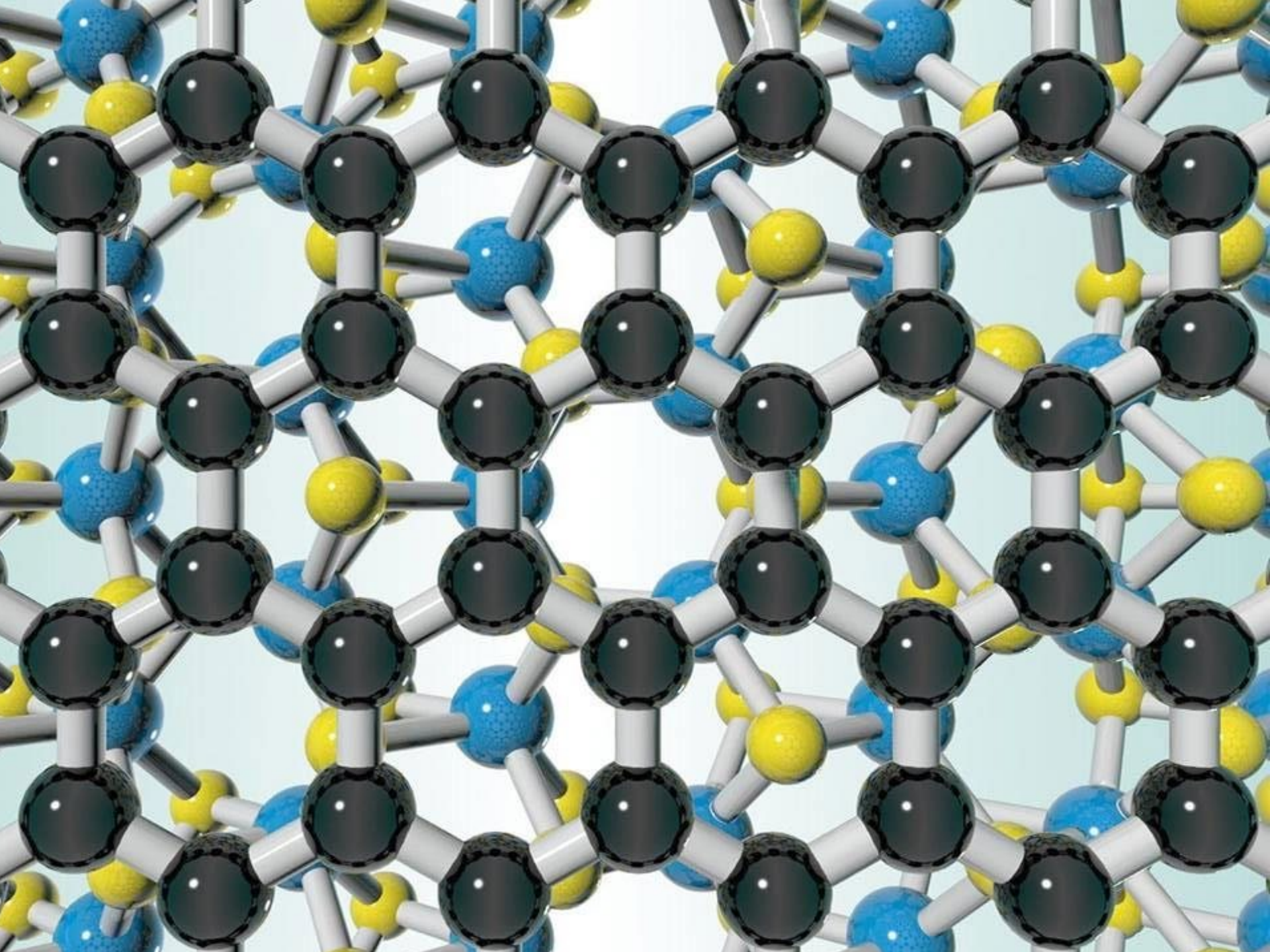
Talieh S. Ghiasi¹, Alexey A. Kaverzin¹, Avalon H. Dismukes², Dennis K. de Wal¹, Xavier Roy² and Bart J. van Wees¹

$$P_{Gr} \approx 14\%$$

Exchange splitting to be $\Delta \approx 20\text{meV}$, which corresponds to $B_{exch} \approx 170\text{T}$

Generation of the spin currents by the magnetized graphene should persist up to the Néel temperature of **CrSBr** ($T_N \approx 132\text{K}$) *interlayer antiferromagnet chromium sulfide bromide*

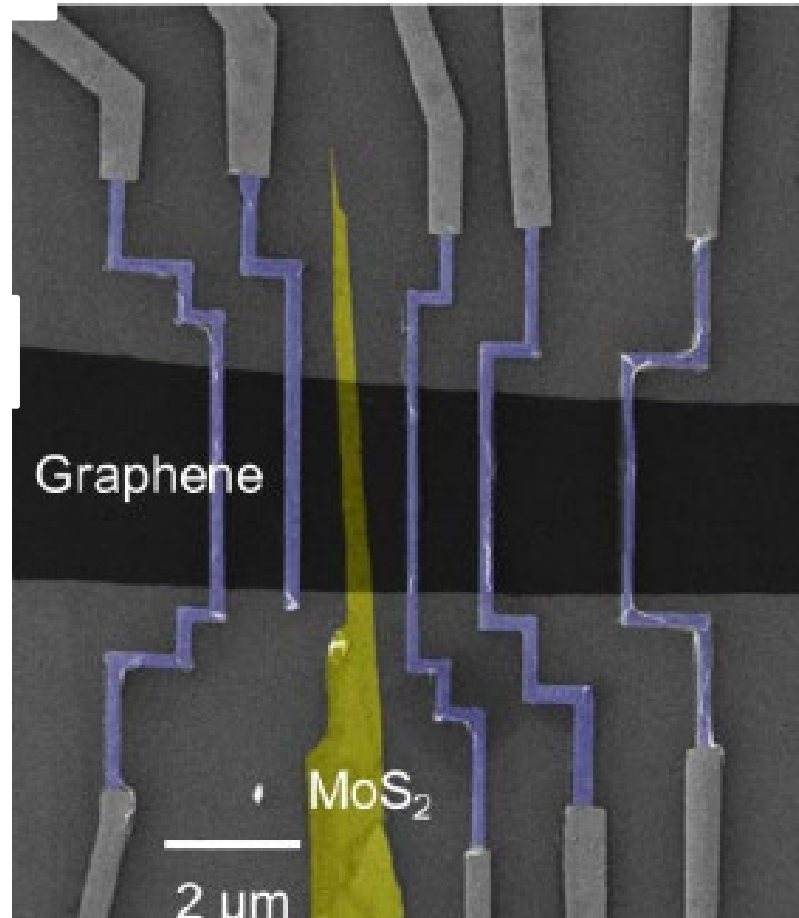
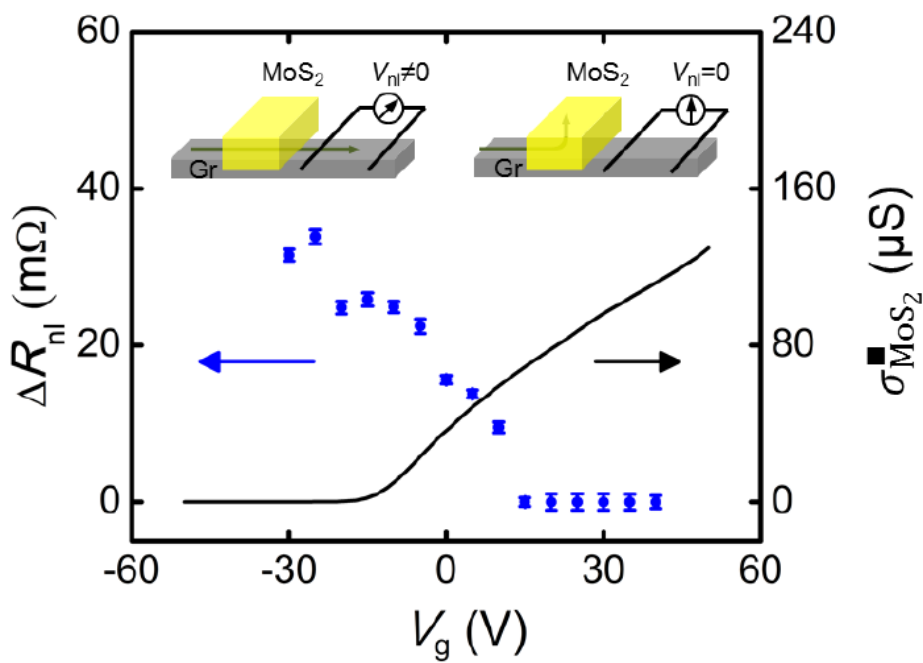
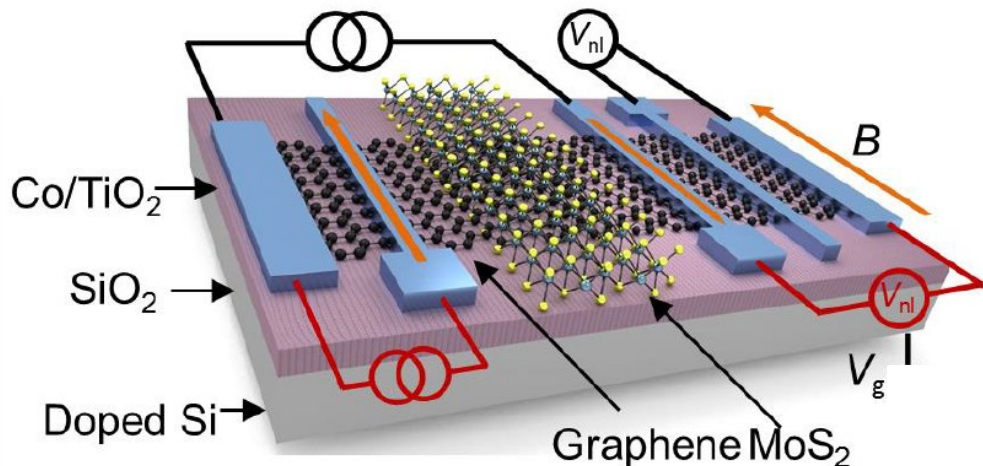




Two-dimensional spin field-effect switch

W. Yan, O. Txoperena, R. Llopis, H. Dery, Luis E. Hueso & Felix Casanova

Nature Comm. 7, 13372 (2016)

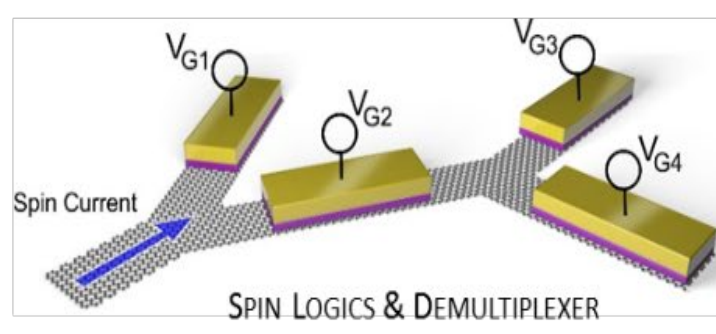
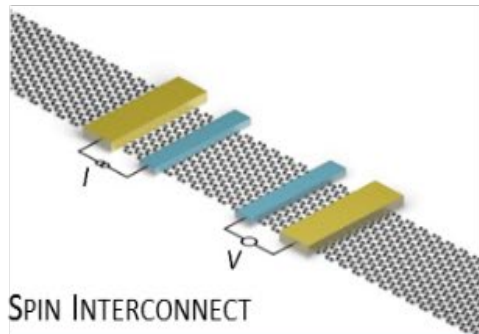


SPIN COMMUNICATION

WEAK SOC

Xenes

(multilayer) Graphene,
black phosphorous...



SPIN INJECTION & DETECTION

2D MAGNETS, CSI, OPTOSPINTRONICS

FM/AFM

CrI_3 , VSe_2 , CrSe_2 , $\text{Cr}_2\text{Ge}_2\text{Te}_6$, MnPSe_3 ...

Insulators

hBN

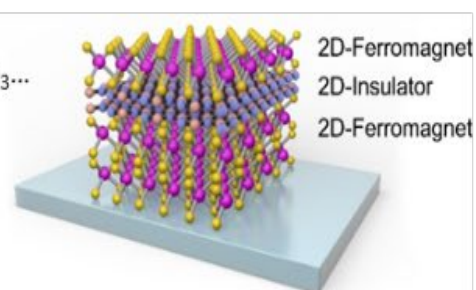
TMDCs

MoS_2 , MoSe_2 , WTe_2 ...

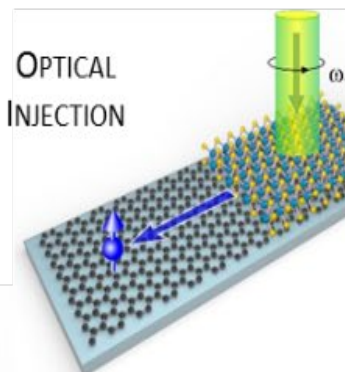
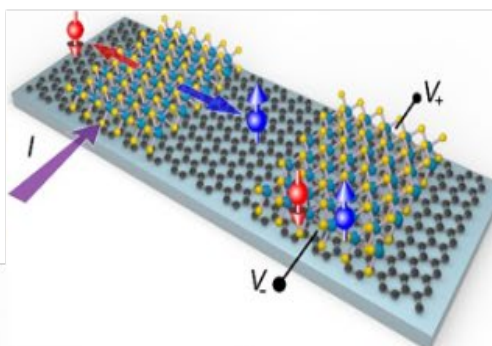
Topological Insulators

2D: Heavy Xenes
3D: $(\text{Bi}, \text{Sb})_2(\text{Te}, \text{Se})_3$, $\alpha\text{-Sn}$...

MAGNETIC TUNNEL JUNCTION



CHARGE-SPIN INTERCONVERSION



SPIN MANIPULATION & CONTROL

STRONG SOC

FM/AFM

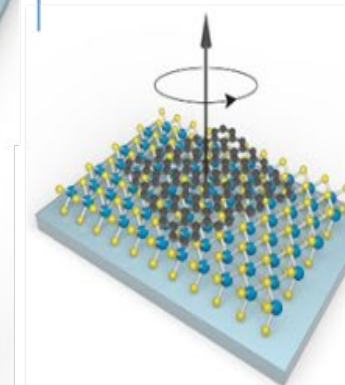
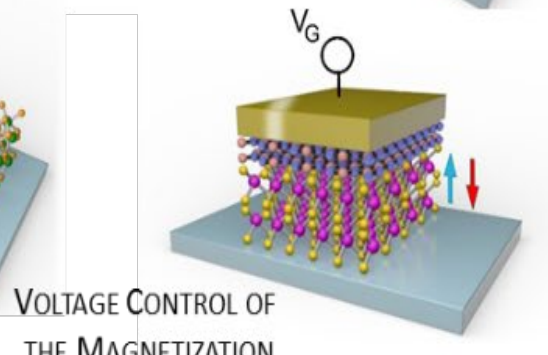
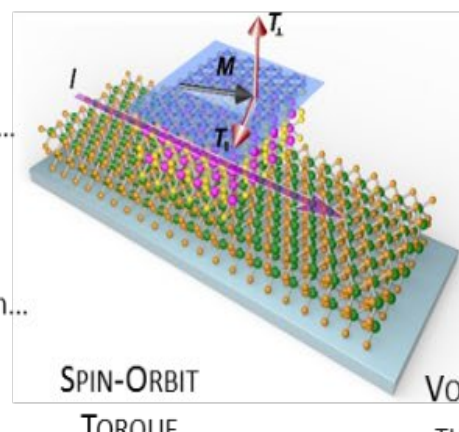
CrI_3 , VSe_2 , CrSe_2 , $\text{Cr}_2\text{Ge}_2\text{Te}_6$, MnPSe_3 ...

TMDCs

MoS_2 , MoSe_2 , WTe_2 ...

Topological Insulators

2D: Heavy Xenes
3D: $(\text{Bi}, \text{Sb})_2(\text{Te}, \text{Se})_3$, $\alpha\text{-Sn}$...



TWIST ANGLE &
STACKING

J.F. Sierra et al

Nature Nanotech. 16, 856–868 (2021)



“Race” to understand & tailor proximity effects

PHYSICAL REVIEW B **100**, 085128 (2019)

Editors' Suggestion

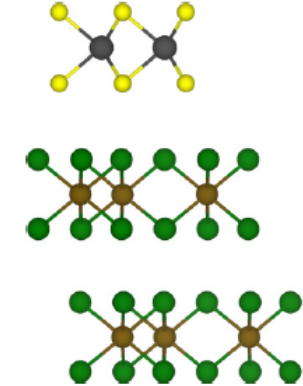
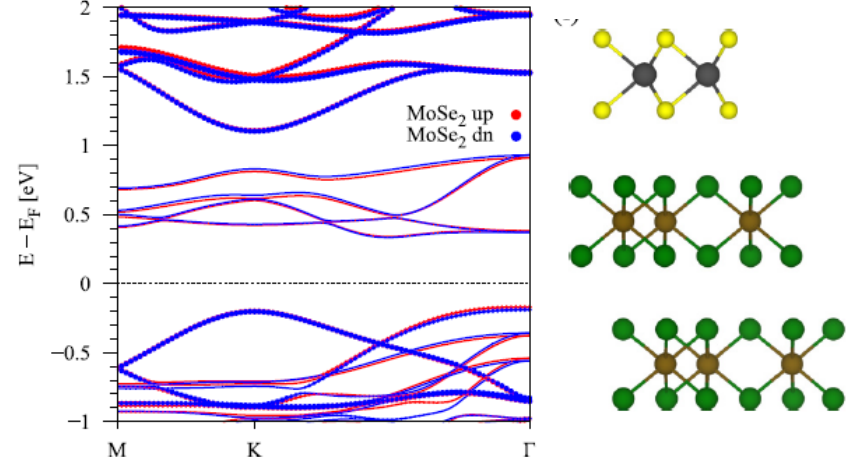
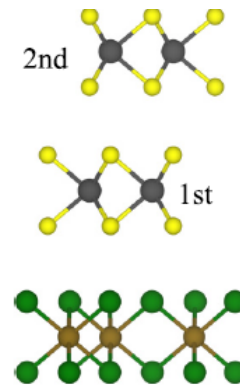
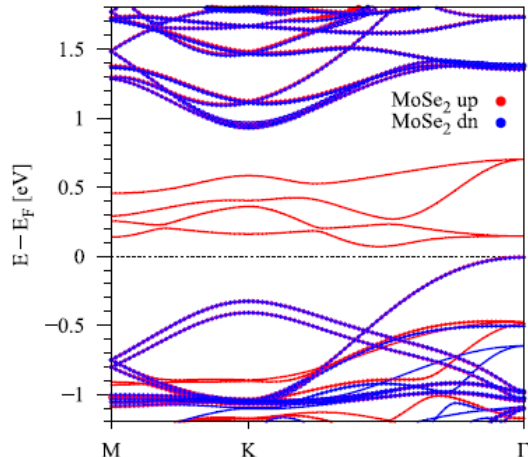
Proximity exchange effects in MoSe₂ and WSe₂ heterostructures with CrI₃: Twist angle, layer, and gate dependence

Klaus Zollner[✉],* Paulo E. Faria Junior, and Jaroslav Fabian

Institute for Theoretical Physics, University of Regensburg, 93040 Regensburg, Germany



(Received 24 June 2019; revised manuscript received 1 August 2019; published 16 August 2019)



Roadmap of 2D-based spintronics

Perspective

Two-dimensional materials prospects for non-volatile spintronic memories

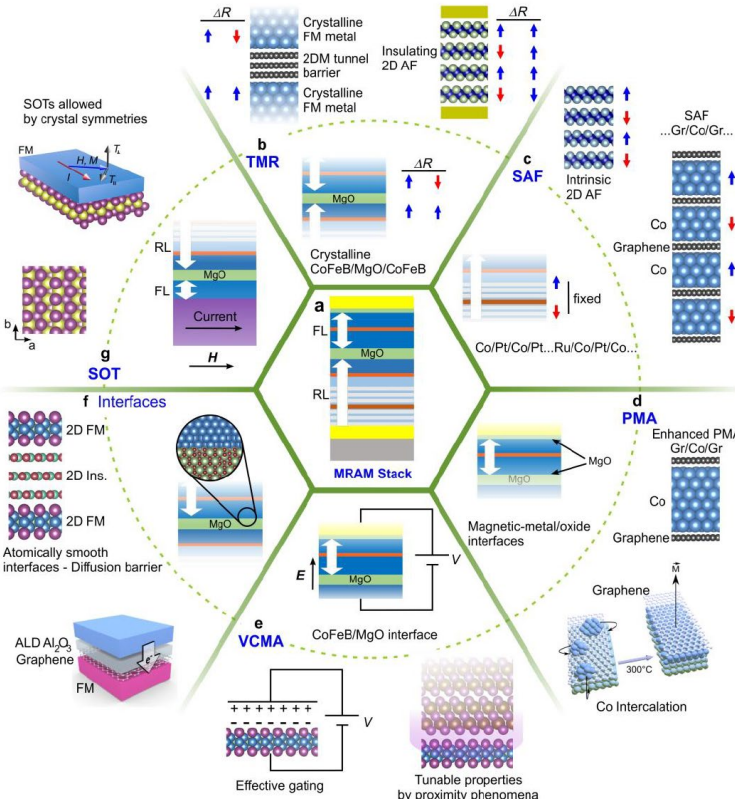


<https://doi.org/10.1038/s41586-022-04768-0>

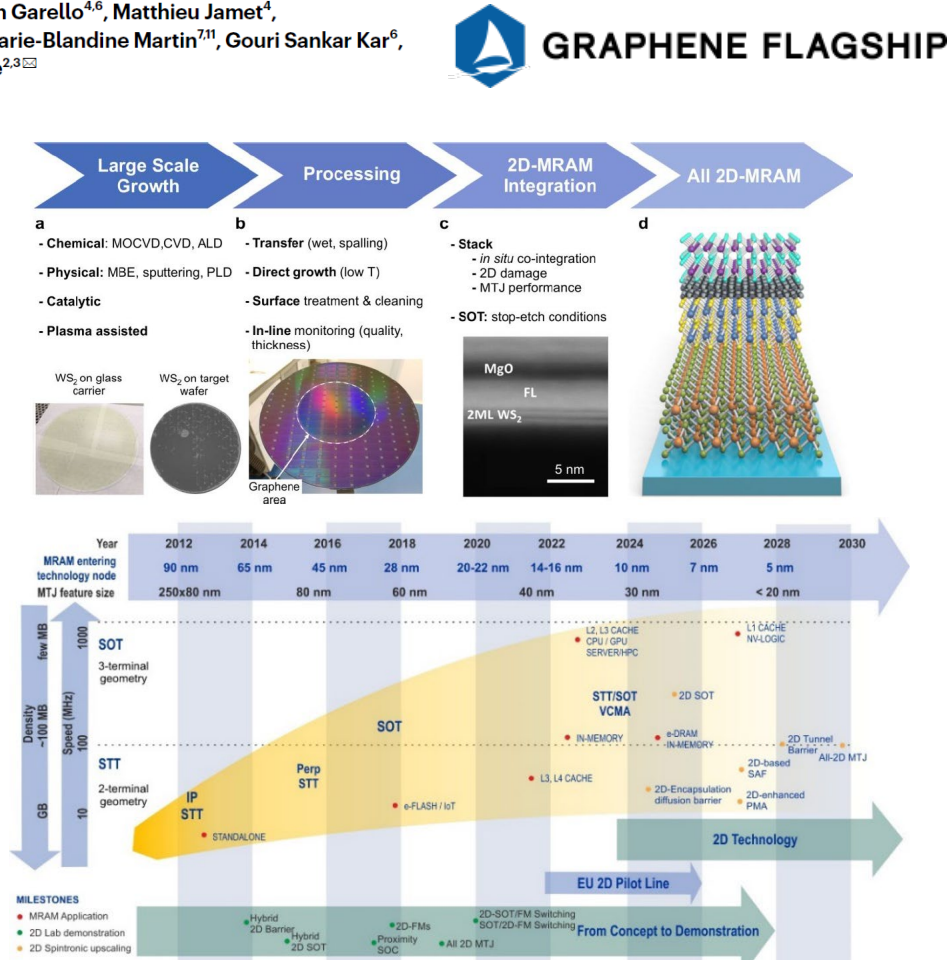
Received: 7 July 2020

Accepted: 19 April 2022

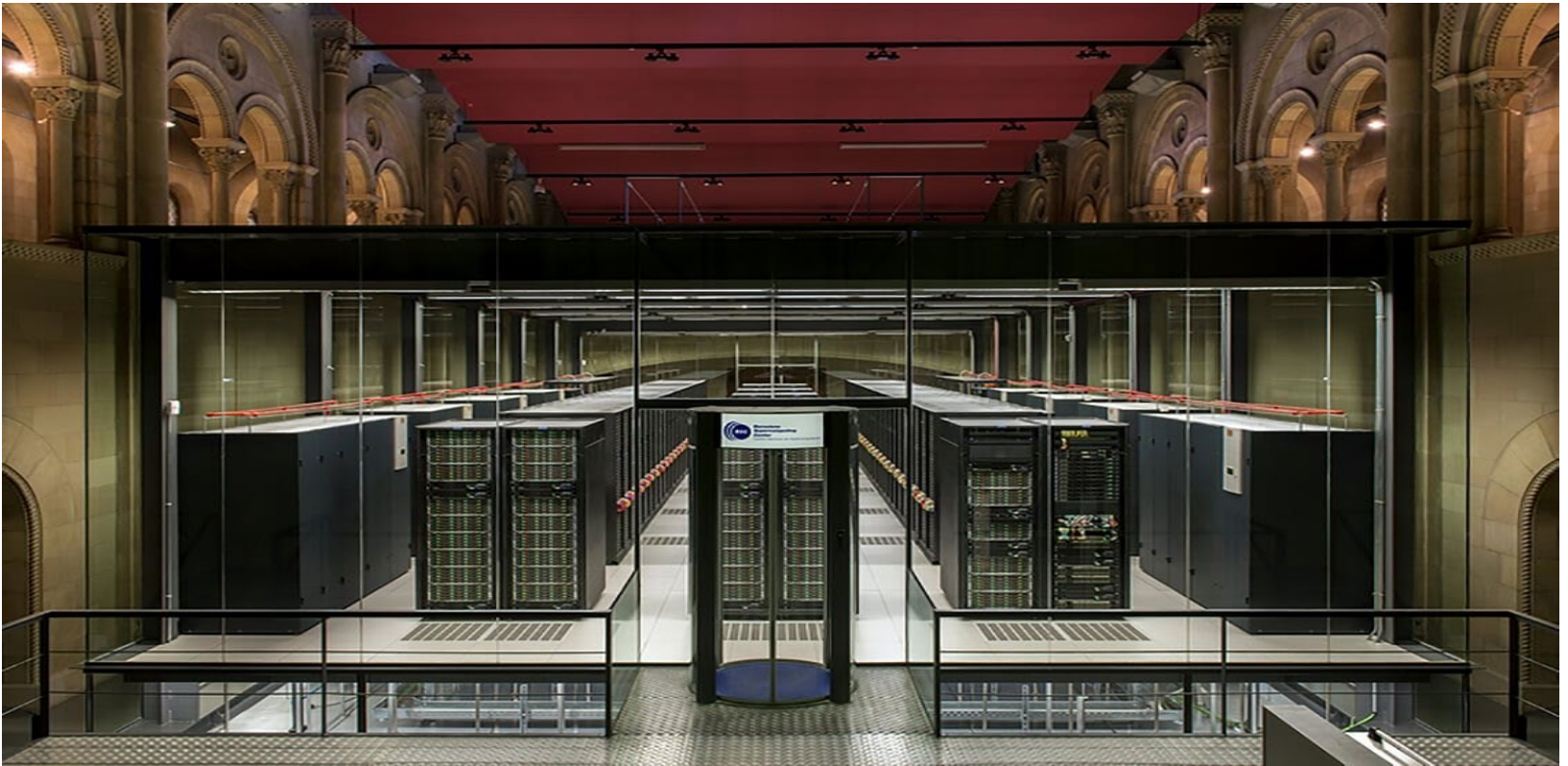
Nature 606 (7915), 663-673 (2022)



Hyunsoo Yang¹, Sergio O. Valenzuela^{2,3}, Mairbek Chshiev^{4,5}, Sébastien Couet⁶, Bernard Dieny⁴, Bruno Dlubak⁷, Albert Fert⁷, Kevin Garello^{4,6}, Matthieu Jamet⁴, Dae-Eun Jeong⁸, Kangho Lee⁹, Taeyoung Lee¹⁰, Marie-Blandine Martin^{7,11}, Gouri Sankar Kar⁶, Pierre Sénoré⁷, Hyeon-Jin Shin¹² & Stephan Roche^{2,3}



Linear scaling quantum transport methods



Linear scaling quantum transport methods

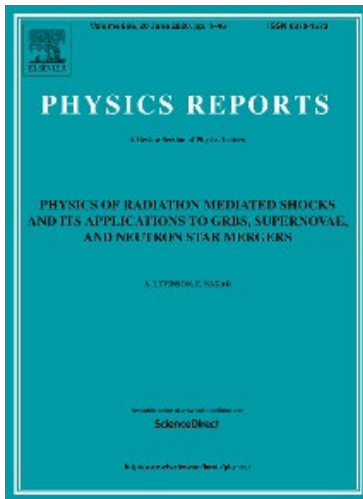
(Kubo, (Spin)-Hall Kubo, Landauer-Büttiker, spin dynamics)

Billion atoms scale / disordered models

Linear scaling quantum transport methodologies

Phys. Rep. 903, 1 (2021)

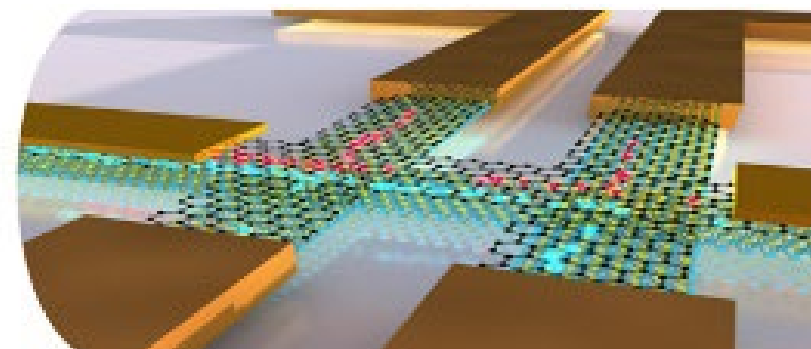
Zheyong Fan ^{a,b,1}, José H. Garcia ^{c,1}, Aron W. Cummings ^{c,1},
Jose Eduardo Barrios-Vargas ^d, Michel Panhans ^{e,f}, Ari Harju ^b, Frank Ortmann ^{e,f},
Stephan Roche ^{c,g,*}



*Disorder systems, Magnetic fields,
Charge transport
Thermal transport (phonon dynamics-harmonic approx.)
Spin transport (SOC effects)
Electron-phonon coupling (molecular dynamics, T-dependence)
Polaron transport
Non equilibrium transport...*

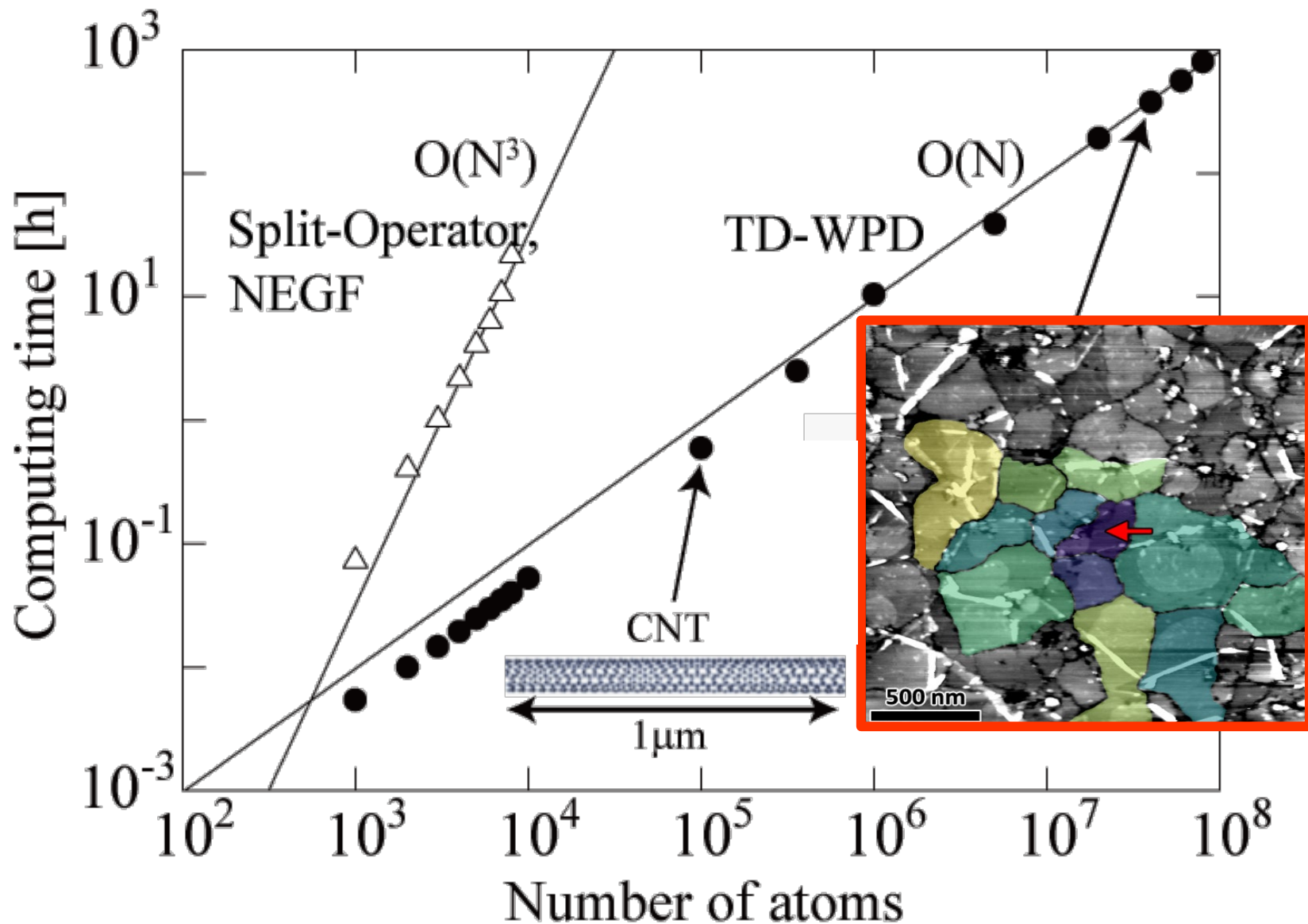
 **LSQUANT**
LINEAR SCALING QUANTUM TRANSPORT

www.lsquant.org



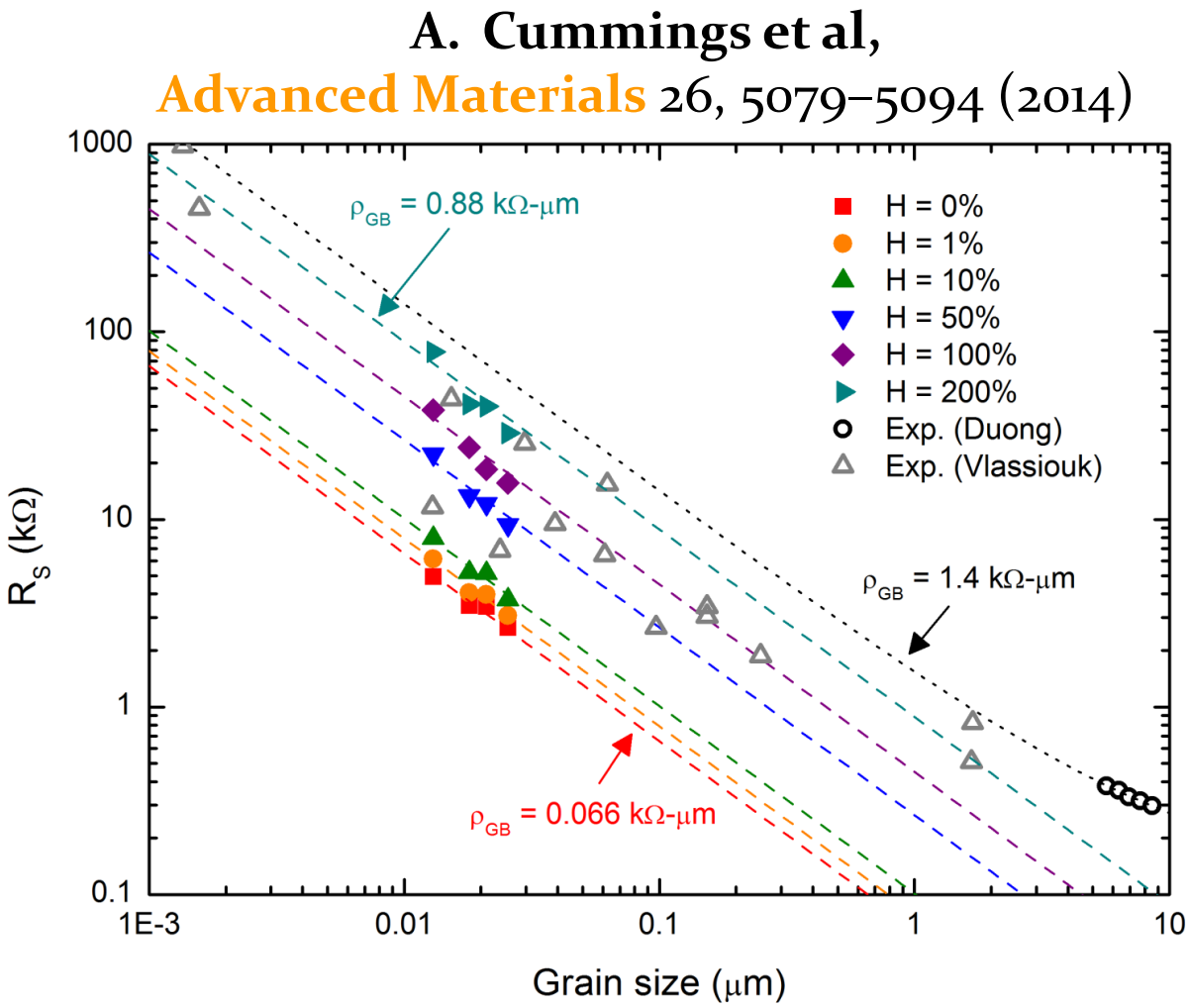
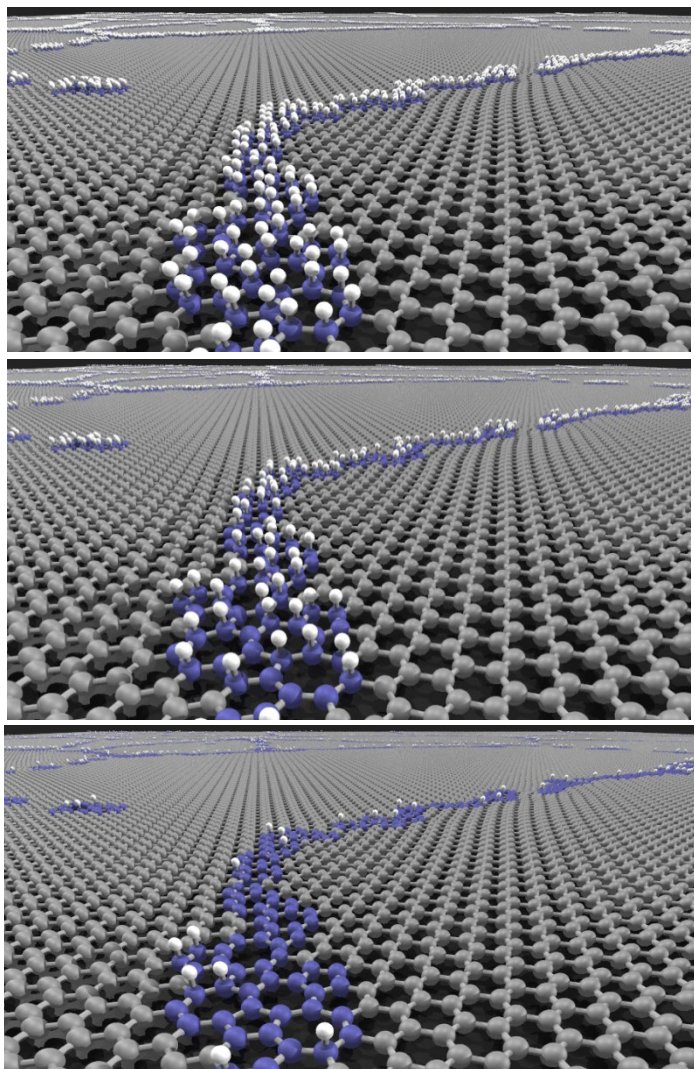
3 weeks versus 1 billion years....

“Advantage” of linear scaling quantum transport



Sheet resistance scaling law

Sheet resistance vs. grain size in chemically disordered CVD graphene



Significant increase in R_s with GB adsorbates

Kubo-Greenwood formula for quantum conductivity

$$\Re e\sigma(\omega) = \frac{2\pi e^2 \hbar}{\Omega} \int_{-\infty}^{+\infty} dE \frac{f(E) - f(E + \hbar\omega)}{\hbar\omega} \text{Tr}[\hat{V}_x \delta(E - \hat{\mathcal{H}}) \hat{V}_x \delta(E - \hat{\mathcal{H}})]$$

R Kubo, **Rep. Prog. Phys.** **29** 255-284 (1966)



Linear Response - Non-interacting electrons
Treat all multiple scattering phenomena

Give access to semiclassical transport
(*Mean free path, charge mobility*)

Non-perturbative regimes (disorder + B,...)

Beyond usual treatment semi-classical Bloch-Boltzmann
Weak localization/strong localization

Generalization to Hall effects (topological physics)

$$\Re e \sigma_{xx}(\omega) = \frac{2\pi e^2 \hbar}{\Omega} \int_{-\infty}^{+\infty} dE \frac{f(E) - f(E + \hbar\omega)}{\hbar\omega} \text{Tr}[\hat{V}_x \delta(E - \hat{\mathcal{H}}) \hat{V}_x \delta(E - \hat{\mathcal{H}})]$$

$$\sigma_{dc} = e^2 n(E_F) \lim_{t \rightarrow \infty} \frac{d}{dt} \Delta X^2(E_F, t) = e^2 n(E_F) \lim_{t \rightarrow \infty} D(t)$$

Linear scaling algorithm

$$D(t) = \frac{\text{Tr}[[\hat{X}, \hat{U}(t)]^\dagger \delta(E - \mathcal{H}) [\hat{X}, \hat{U}(t)]]}{\text{Tr}[\delta(E - \mathcal{H})]}$$

$$\frac{\langle \tilde{\varphi}_{RP}(t) | \delta(E - \mathcal{H}) | \tilde{\varphi}_{RP}(t) \rangle}{\langle \varphi_{RP} | \delta(E - \mathcal{H}) | \varphi_{RP} \rangle}$$

$$|\tilde{\varphi}_{RP}(T)\rangle = [\hat{X}, \hat{U}(t)] |\varphi_{RP}\rangle \simeq \sum_{n=0}^N c_n(T) [\hat{X}, P_n(H)] |\varphi_{RP}\rangle$$

$$\langle \varphi_{RP} | \delta(E - \hat{\mathcal{H}}) | \varphi_{RP} \rangle = -\frac{1}{\pi} \lim_{\eta \rightarrow 0} \Im m \langle \varphi_{RP} | \frac{1}{E + i\eta - \hat{\mathcal{H}}} | \varphi_{RP} \rangle,$$

No matrix inversion

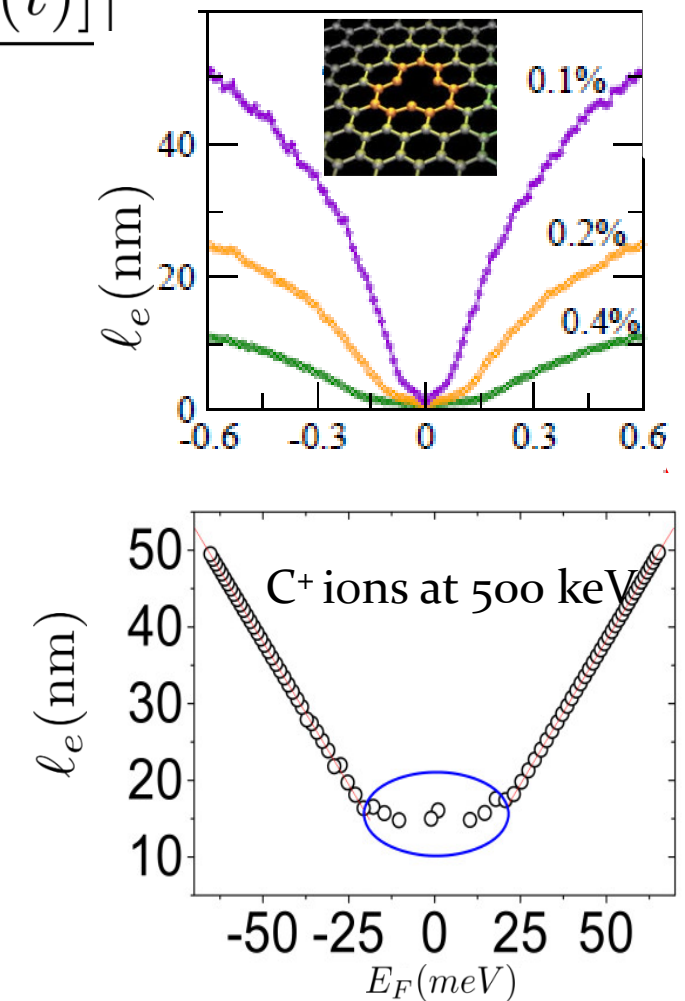
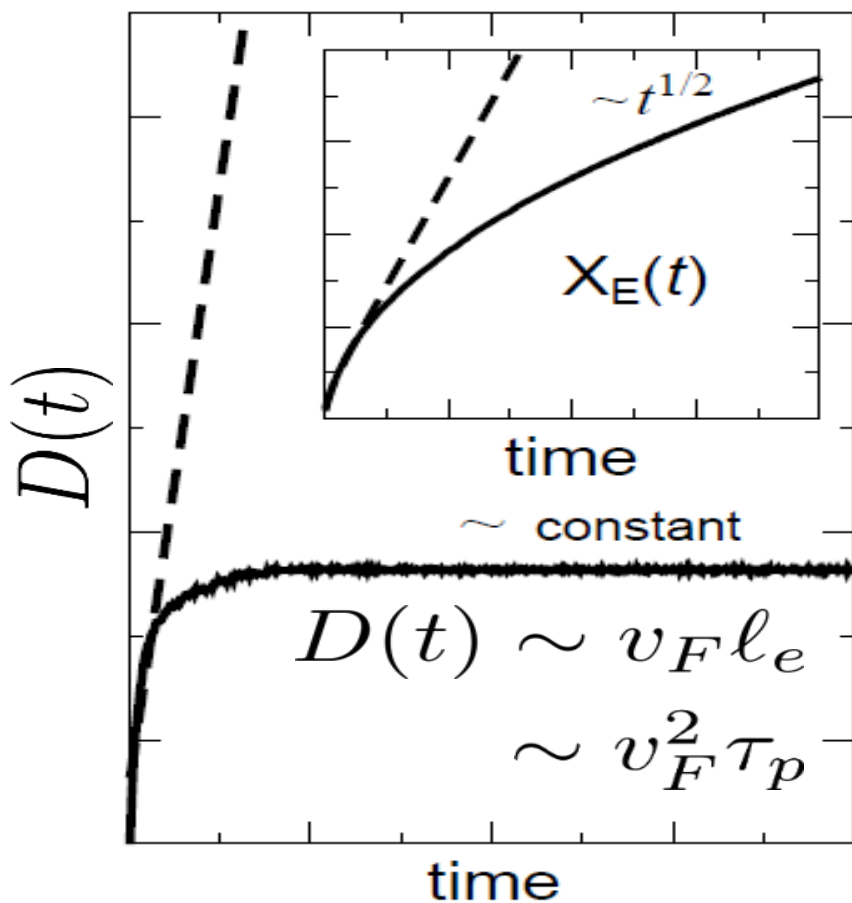
$$\begin{aligned} & \frac{1}{E + i\eta - a_1 - \frac{b_1^2}{E + i\eta - a_2 - \frac{b_2^2}{\ddots E + i\eta - a_N - b_N^2 \Sigma(\omega)}}}} \end{aligned}$$

S. Roche & D Mayou **Phys. Rev. Lett.** (1997)

S. Roche **Phys. Rev. B** (1999)

Quantum dynamics & scaling analysis

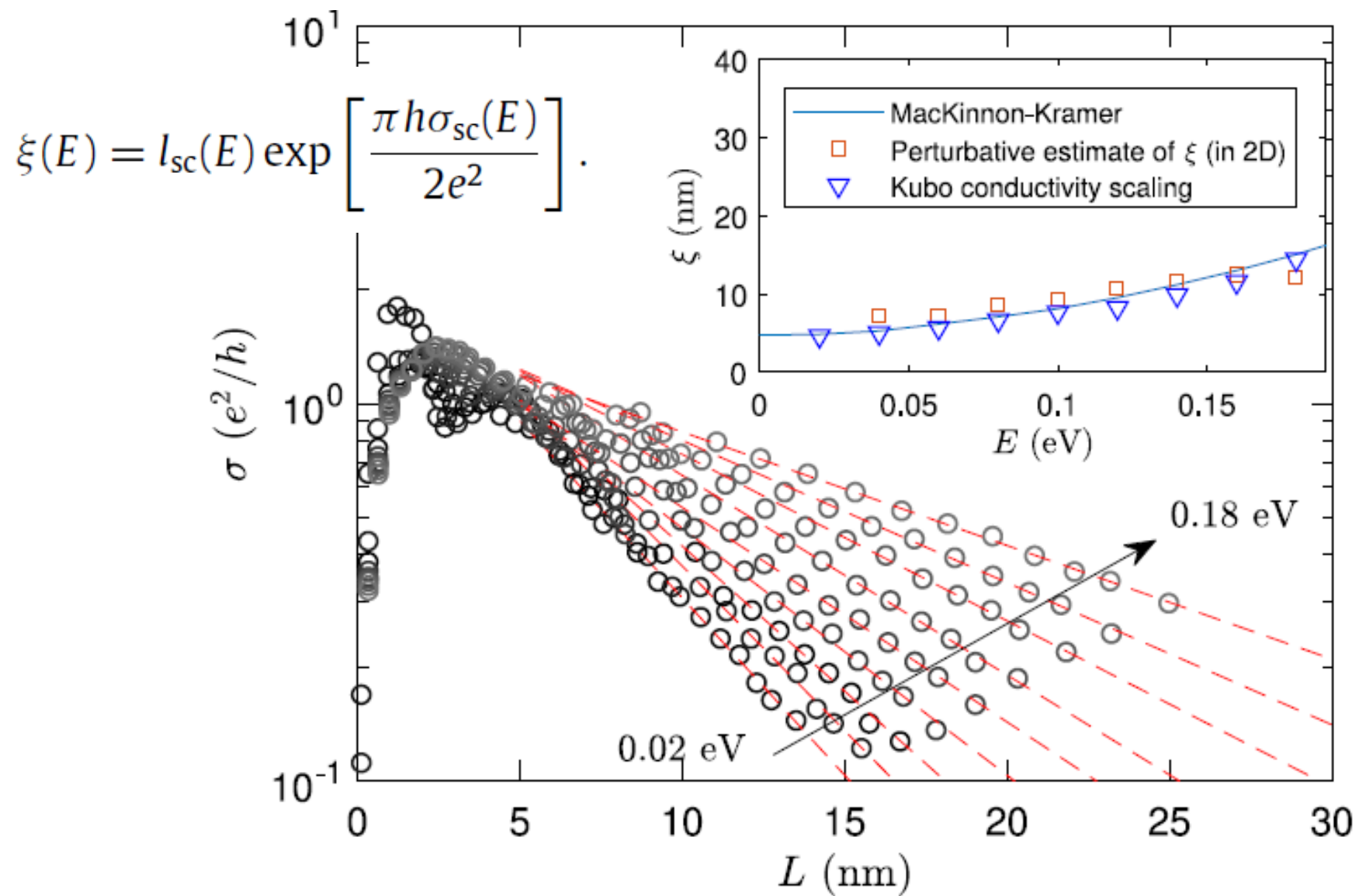
$$D(t) = \frac{\text{Tr}[[\hat{X}, \hat{U}(t)]^\dagger \delta(E - \mathcal{H}) [\hat{X}, \hat{U}(t)]]}{\text{Tr}[\delta(E - \mathcal{H})]}$$



F. Giannazzo et al,
Nanoscale Res.Lett.6, 109 (2011)

From weak to strong (Anderson) localization

disordered graphene lattice (lattice vacancies)



Hall Kubo-Streda formalism

Hall Kubo formula for real space implementation
(10^6 atoms- disorder – $B=1\text{mT}$ - 60T)

$$\sigma_{xy}(E) = -\frac{2}{\Omega} \int_0^{+\infty} dt e^{-\eta t/\hbar} \int_{-\infty}^{+\infty} dE' f(E' - E) \\ \times \Re e \left[\langle \varphi_{RP} | \delta(E' - \hat{\mathcal{H}}) \hat{J}_y \frac{1}{E' - \hat{\mathcal{H}} + i\eta} \hat{J}_x(t) | \varphi_{RP} \rangle \right]$$

Magnetic field modeled by Peierls' phase:

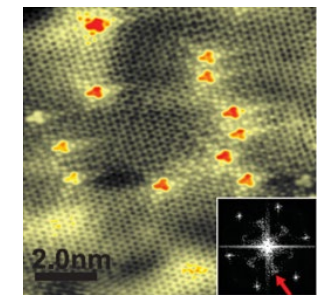
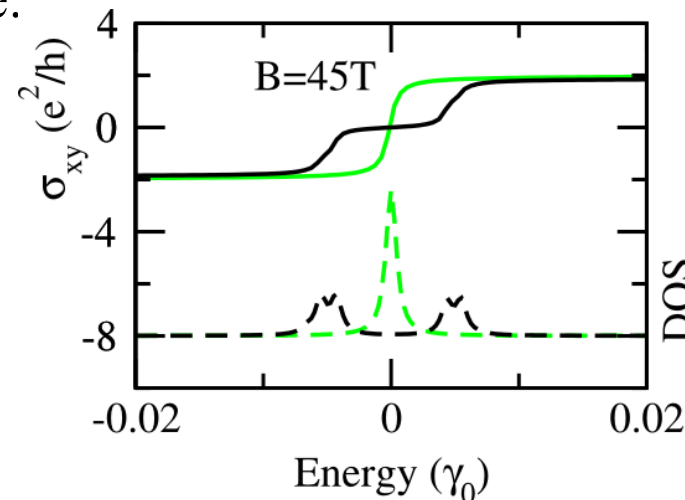
$$\gamma_{ij} = \gamma_0 e^{i\Phi_{ij}} \quad \Phi_{ij} = \frac{e}{\hbar} \int_i^j d\mathbf{s} \mathbf{A}(\mathbf{s})$$

F. Ortmann & S. Roche

Phys. Rev. Lett 110, 086602 (2013)

F. Ortmann, N. Leconte, S. Roche

Phys. Rev. B 91, 165117 (2015)



L. Zhao *et al.*
Science 333, 999 (2011)

Spin dynamics of propagating wavepacket



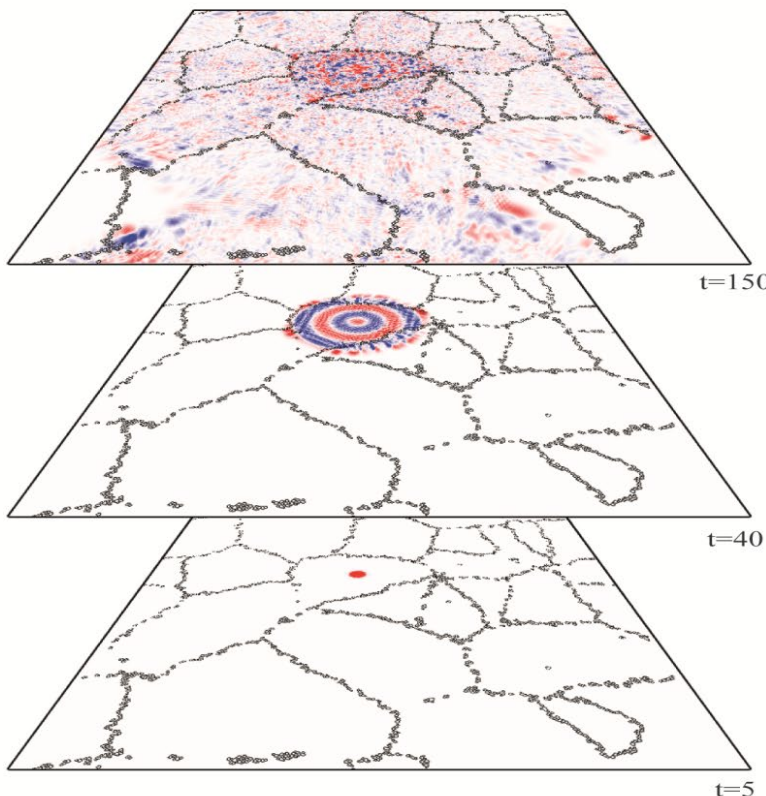
$$|\Psi_{\perp}(0)\rangle = \begin{pmatrix} 1 \\ 0 \end{pmatrix} |\varphi_{RP}\rangle$$

$$|\Psi(t)\rangle = e^{-i\hat{\mathcal{H}}t/\hbar} |\Psi(0)\rangle$$

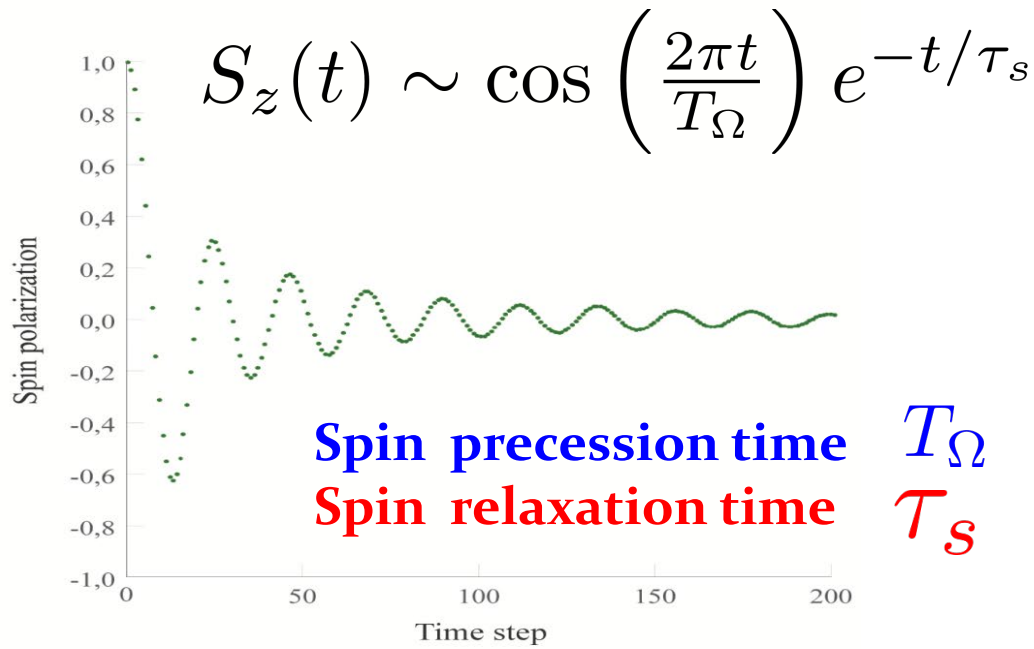
$$s_i(t) = |\Psi_i^{\uparrow}(t)|^2 - |\Psi_i^{\downarrow}(t)|^2$$

(time-dependent)

Local spin density in real space



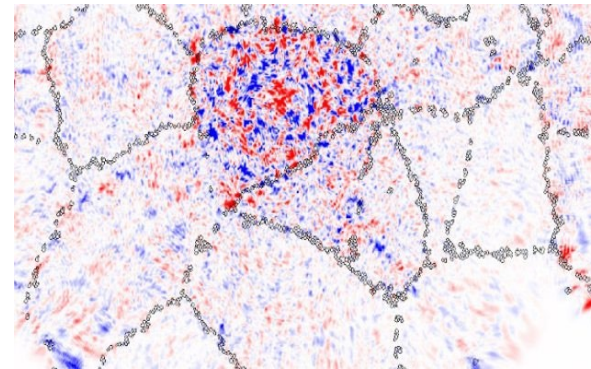
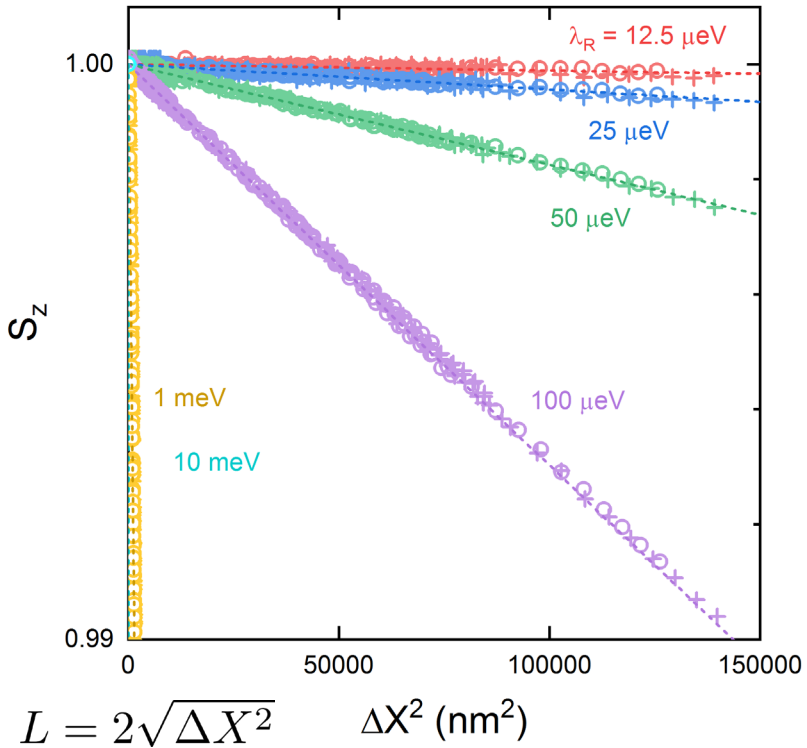
$$\frac{\langle \Psi(t) | \sigma_z \delta(E - \hat{\mathcal{H}}) + \delta(E - \hat{\mathcal{H}}) \sigma_z | \Psi(t) \rangle}{2 \langle \Psi(t) | \delta(E - \hat{\mathcal{H}}) | \Psi(t) \rangle}$$



Universal spin diffusion length



AW Cummings et al **Nano lett. 19, 7418 (2019)**



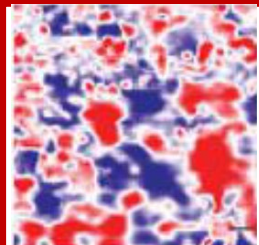
Spin polarization vs mean square displacement

$$S_z(X) = \exp(-\Delta X^2/L_s^2)$$

No dependence on grain size (!!!)

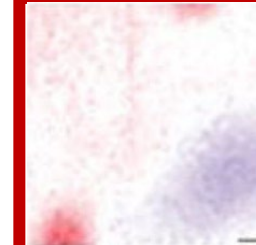
10 nm or 100 microns

$$L_s = \frac{\hbar v_F}{2\lambda_R}$$



Rashba SOC = 25 μ eV

$$L_s = 10 \mu\text{m}$$



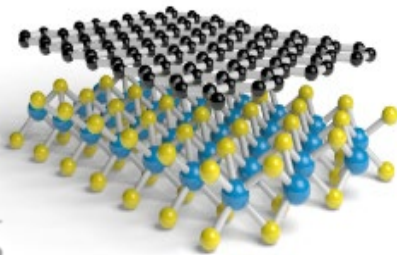
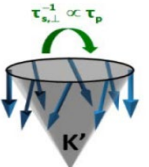
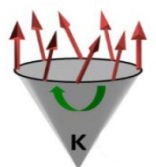
Rashba SOC = 5 μ eV

$$L_s = 50 \mu\text{m}$$

Giant Spin lifetimes Anisotropy

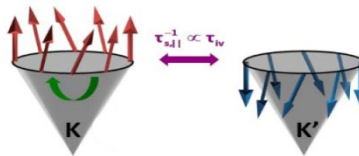
AW Cummings, JH Garcia, J Fabian, S Roche

Phys. Rev. Lett. 119 (20), 206601 (2017)

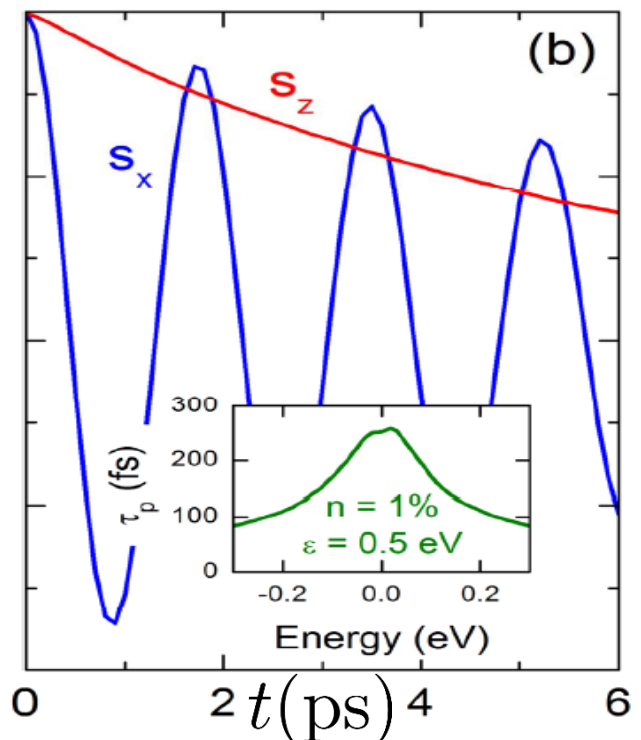


Intravalley scattering

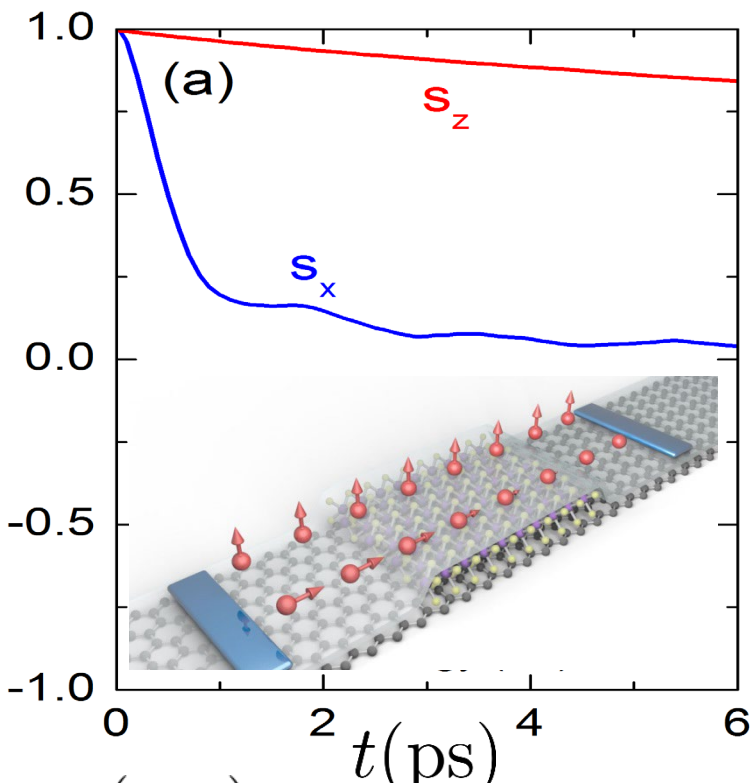
$$\frac{\tau_{s,\perp}}{\tau_{s,\parallel}} = 10 - 100$$



Strong valley mixing



$$S_\alpha \simeq \exp(-t/\tau_{s,\alpha}) \cos(\omega_z t)$$





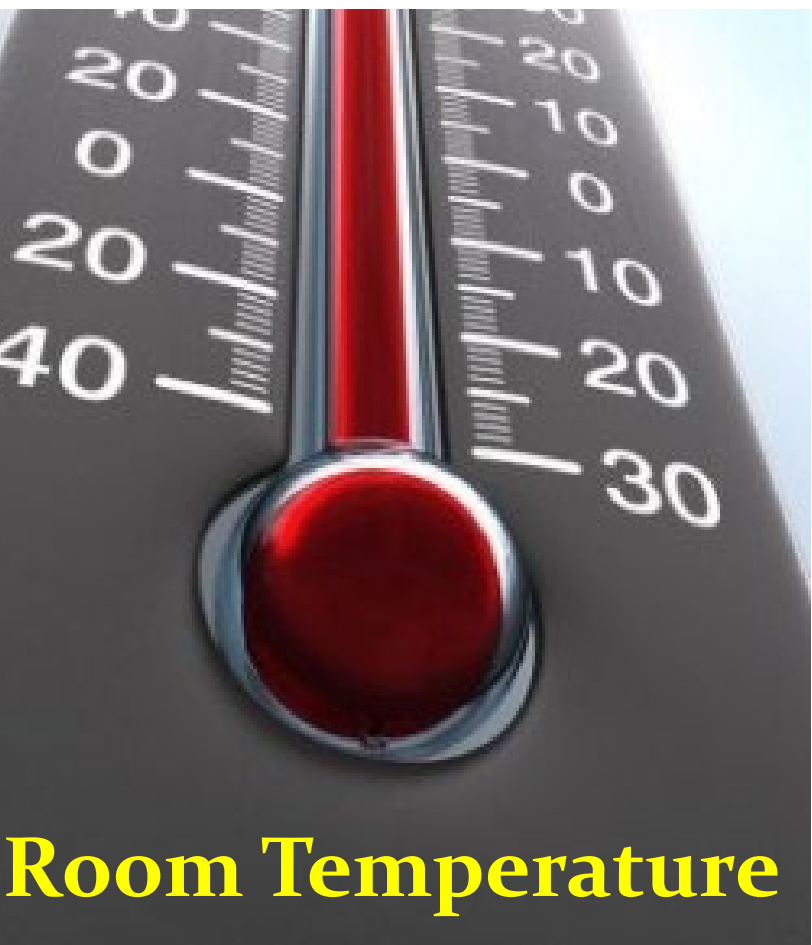
GRAPHENE FLAGSHIP

Experimental confirmation

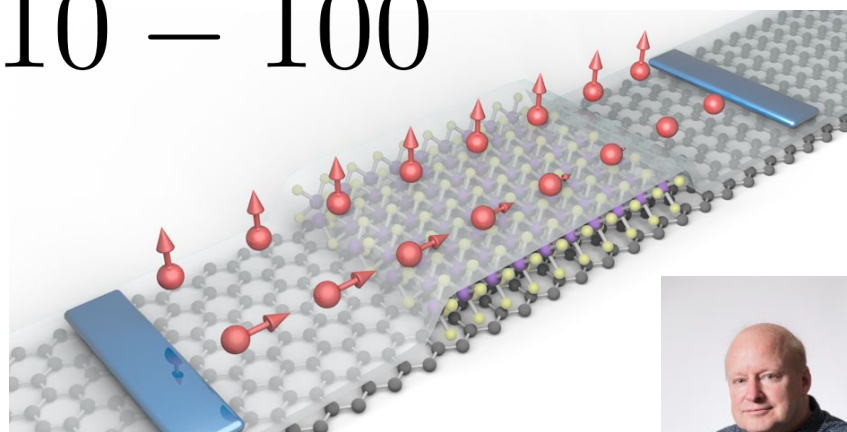


university of
groningen

ICN2^R



$$\frac{\tau_{s,\perp}}{\tau_{s,\parallel}} = 10 - 100$$



NANO
LETTERS

Cite This: *Nano Lett.* XXXX, XXX, XXX–XXX

Large Proximity-Induced Spin Lifetime Anisotropy in Transition-Metal Dichalcogenide/Graphene Heterostructures

Talieh S. Ghiasi,* Josep Inglá-Aynés, Alexey A. Kaverzin, and Bart J. van Wees

Physics of Nanodevices, Zernike Institute for Advanced Materials, University of Groningen, Groningen, 9747 A

nature
physics

<https://doi.org/10.1038/nphys3711>



Strongly anisotropic spin relaxation in graphene-transition metal dichalcogenide heterostructures at room temperature

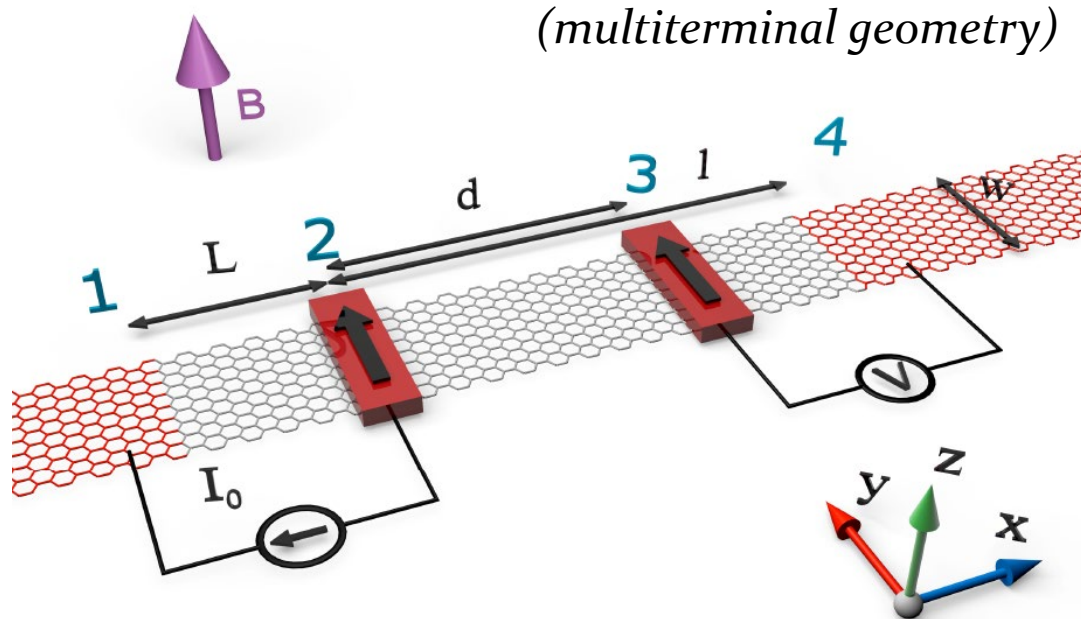
L. Antonio Benítez^{1,2*}, Juan F. Sierra¹, Williams Savero Torres¹, Aloïs Arrighi^{1,2}, Frédéric Bonell¹, Marius V. Costache¹ and Sergio O. Valenzuela^{1,3*}

Room Temperature

Nonlocal spin transport

charge current injected from lead 2 to 1 while a non-local voltage I_0

$$R_{NL} = (V_3 - V_4)/I_0$$



Charge current

$$I_p = \sum_q G_{pq} (V_p - V_q)$$

[kwant](#)

$$G_{pq} = \frac{e^2}{h} \int dE \text{Tr}[\mathbf{t}_{pq} \mathbf{t}_{pq}^\dagger] (-\partial f / \partial E)$$

Spin current

\mathbf{t}_{pq} the transmission matrix between transverse propagating modes within semi-infinite leads p and q

$$I_p^{s_\alpha}$$

$$G_{pq}^{s_\alpha} = \frac{e^2}{h} \int dE \text{Tr}[s_\alpha \mathbf{t}_{pq} \mathbf{t}_{pq}^\dagger] (-\partial f / \partial E)$$

$$\theta_{sH} = \frac{I_z^{s_\alpha}}{I_0}$$

Spin Hall Effect and Origins of Nonlocal Resistance in Adatom-Decorated Graphene

D. Van Tuan,^{1,2} J. M. Marmolejo-Tejada,^{3,4} X. Waintal,⁵ B. K. Nikolić,^{3,*} S. O. Valenzuela,^{1,6} and S. Roche^{1,6,†}

¹Catalan Institute of Nanoscience and Nanotechnology (ICN2), CSIC and The Barcelona Institute of Science and Technology, Campus UAB, Bellaterra, 08193 Barcelona, Spain

²Department of Electrical and Computer Engineering, University of Rochester, Rochester, New York 14627, USA

³Department of Physics and Astronomy, University of Delaware, Newark, Delaware 19716-2570, USA

⁴School of Electrical and Electronics Engineering, Universidad del Valle, Cali AA 25360, Colombia

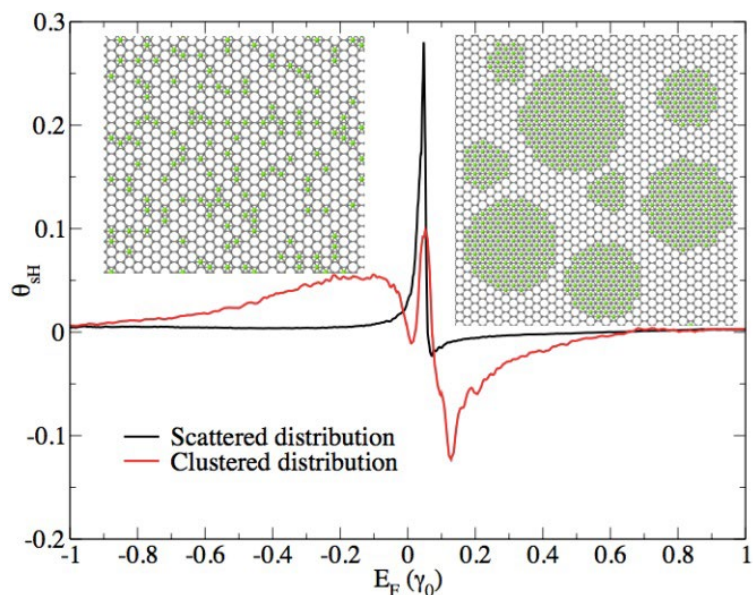
⁵Univ. Grenoble Alpes, INAC-PHELIQS, F-38000 Grenoble, France and CEA, INAC-PHELIQS, F-38000 Grenoble, France

⁶ICREA—Institució Catalana de Recerca i Estudis Avançats, 08010 Barcelona, Spain

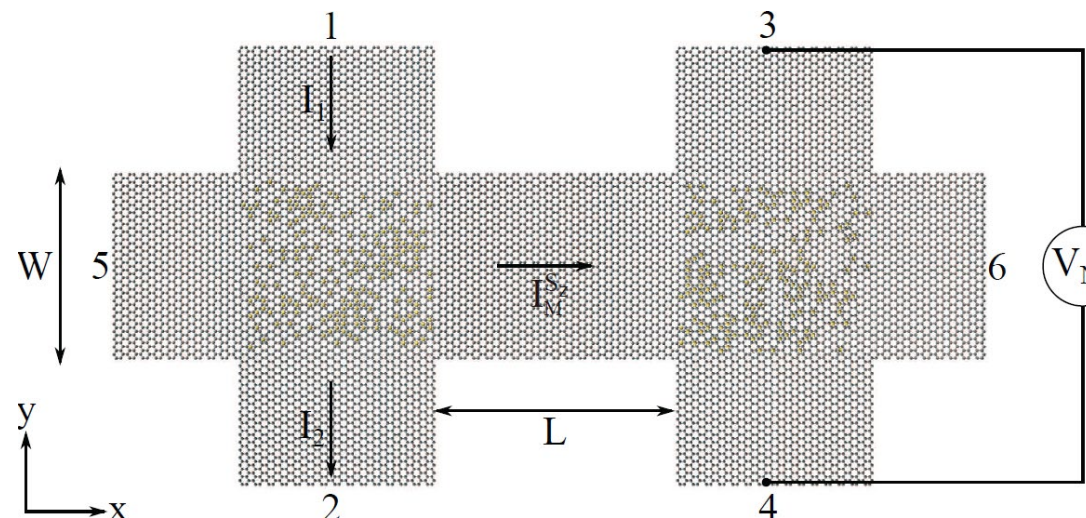
(Received 19 February 2016; published 20 October 2016)

Kubo formalism

(dissipative & Hall conductivities)



Multiterminal Landauer-Büttiker formalism

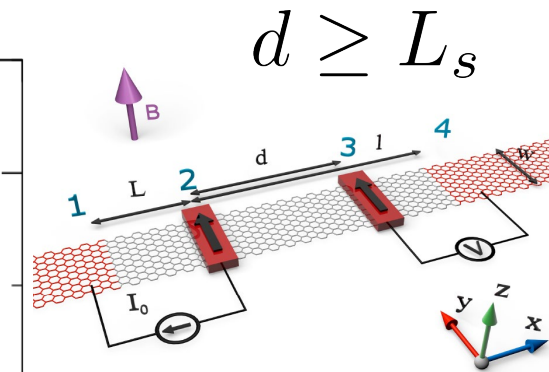
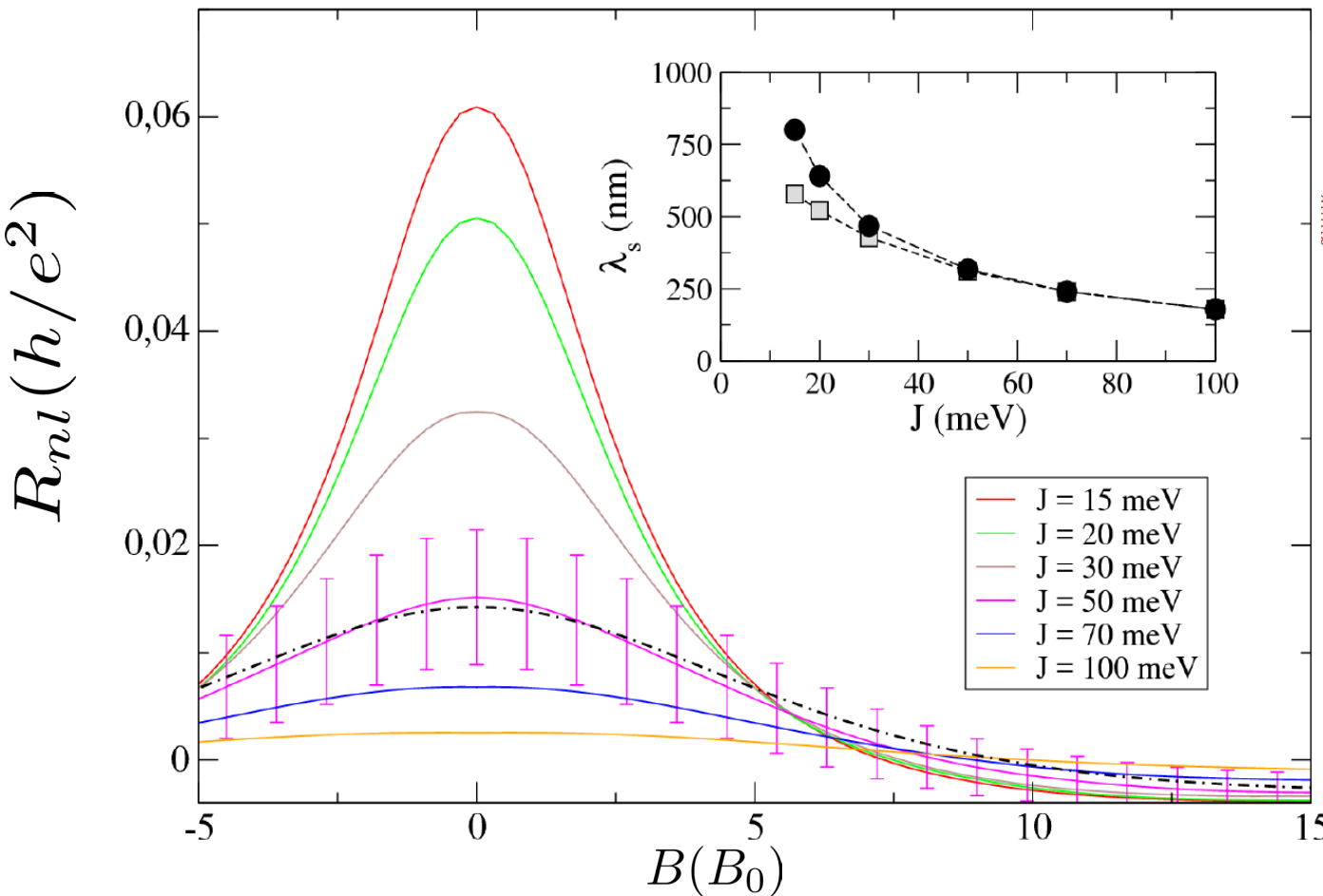


$$\theta_{\text{SH}} = \sigma_{\text{SH}} / \sigma_{xx}$$

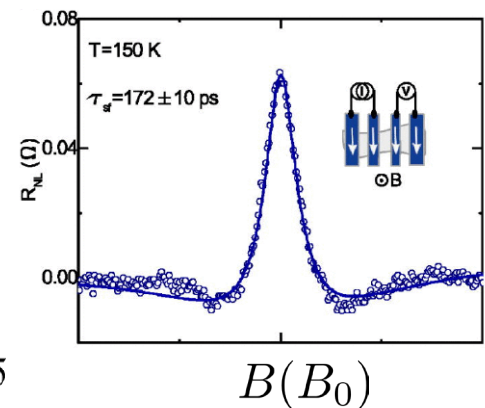
$$\theta_{\text{SH}} = I_5^{sz} / I_1$$

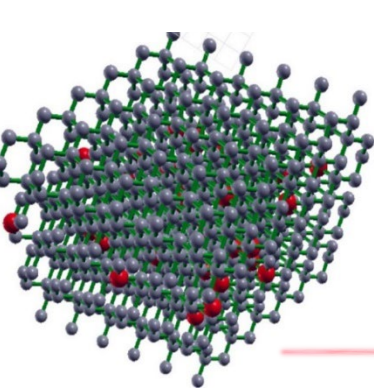
Hanle spin precession simulations

Graphene with random magnetic impurities



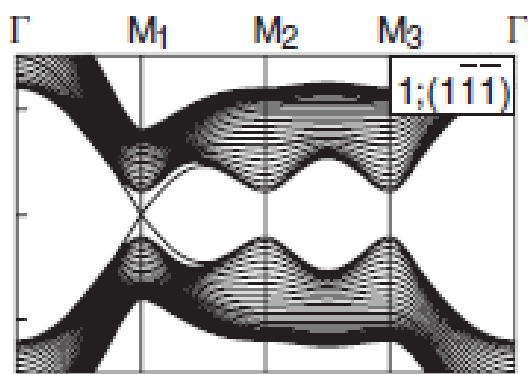
Consistent extrapolation
of spin diffusion length





Transport properties in High-dimensionality, disordered topological materials

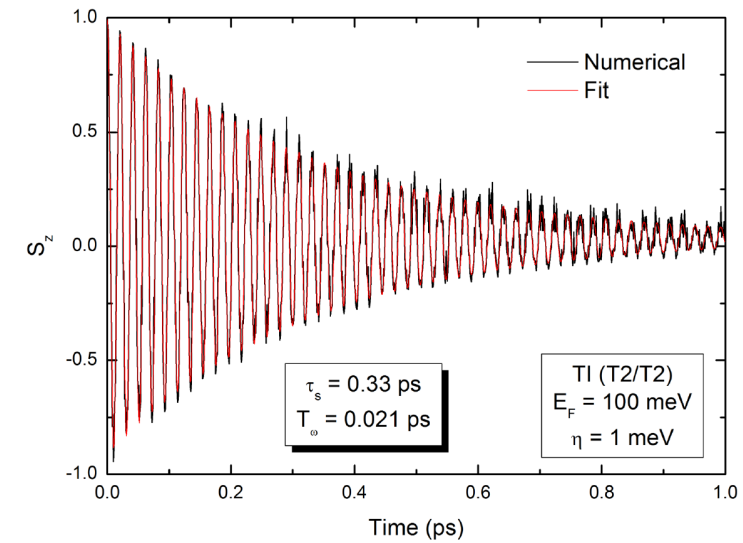
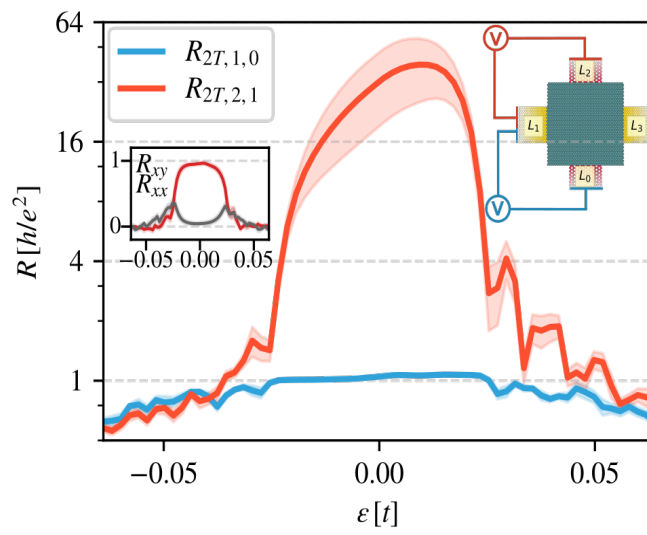
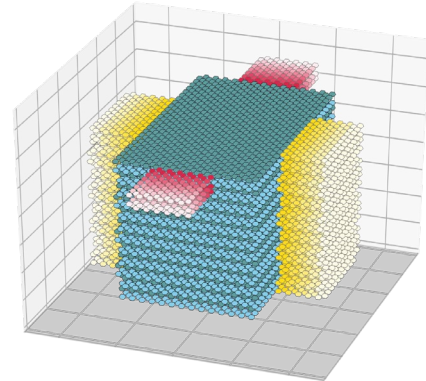
Pablo Piskunow

*3D Fu-Kane-Mele Hamiltonian for topological insulators
With magnetic impurities (proximity effects)*

$$\mathcal{H} = \sum_{\langle ij \rangle} t_{ij} c_i^\dagger c_j + i(4\hbar\lambda_{SO}/a^2) \sum_{\langle\langle ij \rangle\rangle} c_i^\dagger \boldsymbol{\sigma} \cdot (\mathbf{d}_{ij}^1 \times \mathbf{d}_{ij}^2) c_j$$

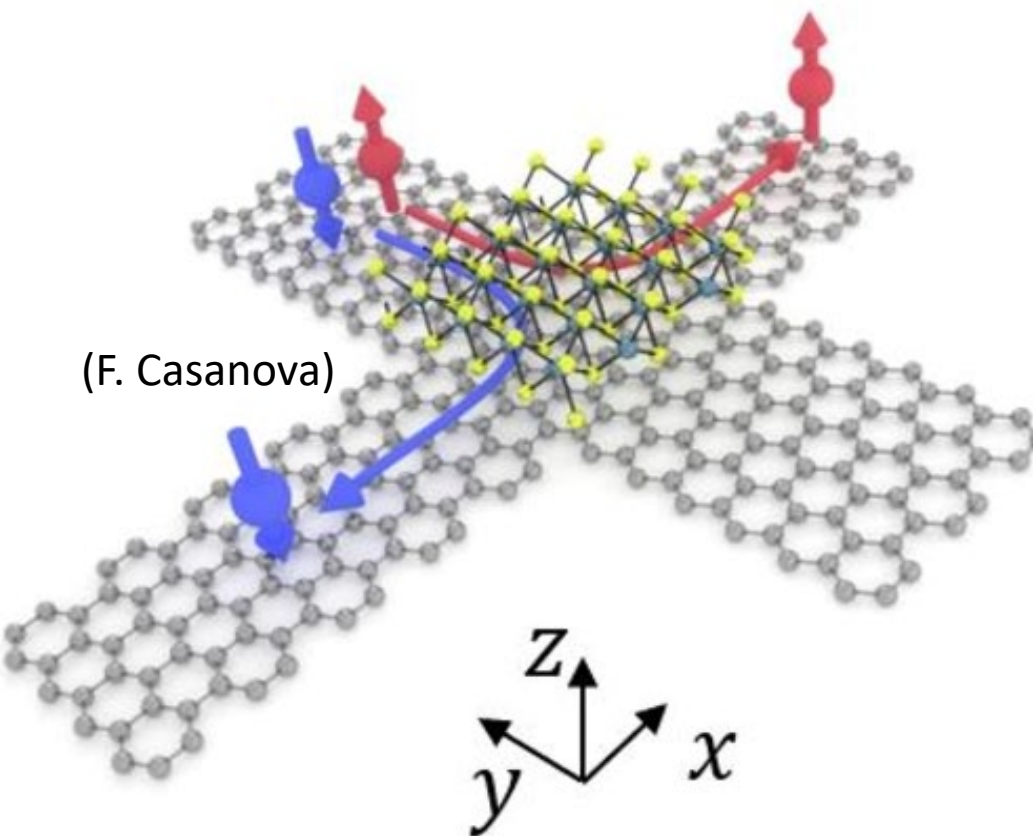
$$\mathcal{H}_Z = \sum_{i,\alpha,\beta} c_{i,\alpha}^\dagger [(m_i + \delta m_i) \hat{\mathbf{z}} \cdot \mathbf{s}]_{\alpha,\beta} c_{i,\beta}$$



Low symmetry topological materials

Multiple components
Spin Hall Effect
(MoTe₂ monolayer)

“Spin currents by proximity effect”



Using strong SOC
Spin Hall Effect

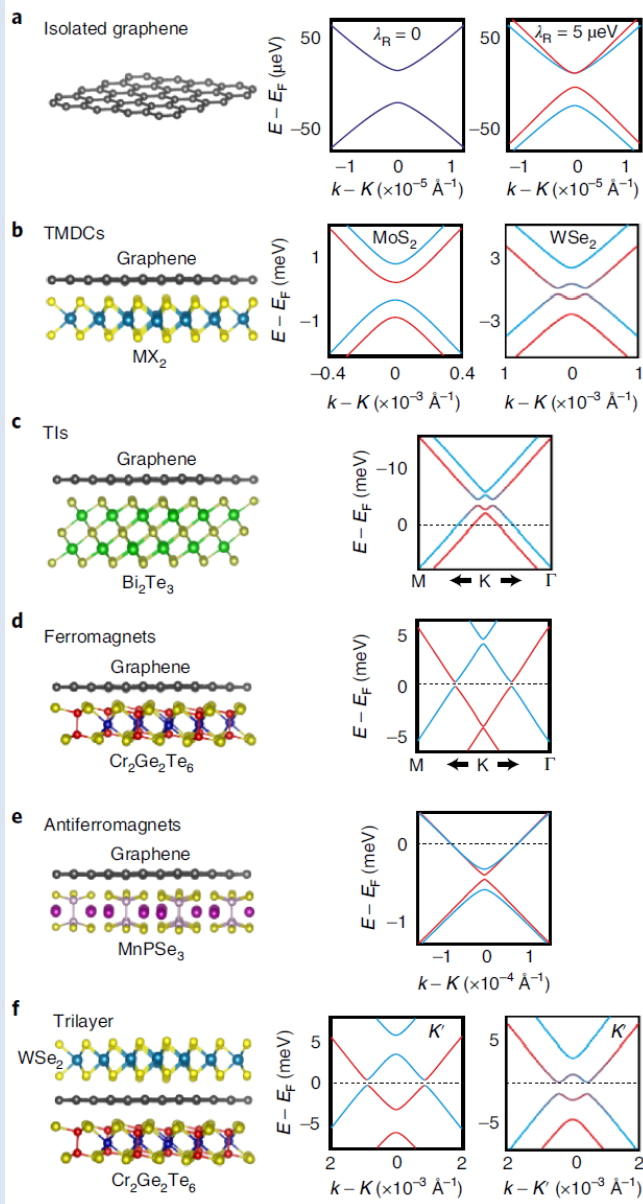
$$\theta_{sH} = \frac{|J_s^z|}{|J_c|}$$

Spin Hall angle

*efficiency of converting
charge current to spin current*

Can we use proximity effects to generate and control spin currents?

Emergent Hamiltonian in proximitized graphene



$$H = H_0 + H_\Delta + H_I + H_{\text{VZ}} + H_R + H_{\text{PIA}} + H_{\text{EX}}$$

$$H_0 = \hbar v_F (\tau k_x \sigma_x + k_y \sigma_y)$$

$$H_I = \lambda_I \tau \sigma_z s_z$$

$$H_R = \lambda_R (\tau \sigma_x s_y - \sigma_y s_x)$$

$$H_{\text{VZ}} = \lambda_{\text{VZ}} \tau \sigma_0 s_z$$

$$H_{\text{PIA}} = \alpha (\lambda_{\text{PIA}} \sigma_z + \Delta_{\text{PIA}}) (k_x s_y - k_y s_x)$$

$$H_{\text{EX}} = \lambda_{\text{EX}} s_z + \lambda_{\text{EX}}^{\text{AF}} \sigma_z s_z$$

J.F. Sierra, J. Fabian, R Kawakami, S. Roche, SO Valenzuela

Nature Nanotech. 16 (8), 856-868 (2021)

Spin Hall Kubo conductivity

(SHE in dissipative regime)

$$\sigma_{\text{sH}} = \frac{e\mu}{\Omega} \sum_{m,n} \frac{f(E_m) - f(E_n)}{E_m - E_n} \frac{\mathcal{Im}[\langle m | J_x^z | n \rangle \langle n | v_y | m \rangle]}{E_m - E_n + i\eta},$$

$J_x^z = \frac{\hbar}{4} \{ \sigma_z, v_x \}$ is the spin current operator

$$\sigma_{\text{sH}} = \frac{e\hbar}{\Omega} \int du dv \frac{f(u) - f(v)}{(u - v)^2 + \eta^2} j(u, v),$$

$$\theta_{sH} = \frac{\sigma_{xy}^z}{\sigma_{xx}}$$

$$j(u, v) = \sum_{m,n} \mathcal{Im}[\langle m | J_x^z | n \rangle \langle n | v_y | m \rangle] \delta(u - E_m) \delta(v - E_n)$$

$$= \sum_{m,n}^M (4\mu_{mn} g_m g_n T_m(\hat{u}) T_n(\hat{v})) / ((1 + \delta_{m,0})(1 + \delta_{n,0})\pi^2 \sqrt{(1 - \hat{u}^2)(1 - \hat{v}^2)}),$$

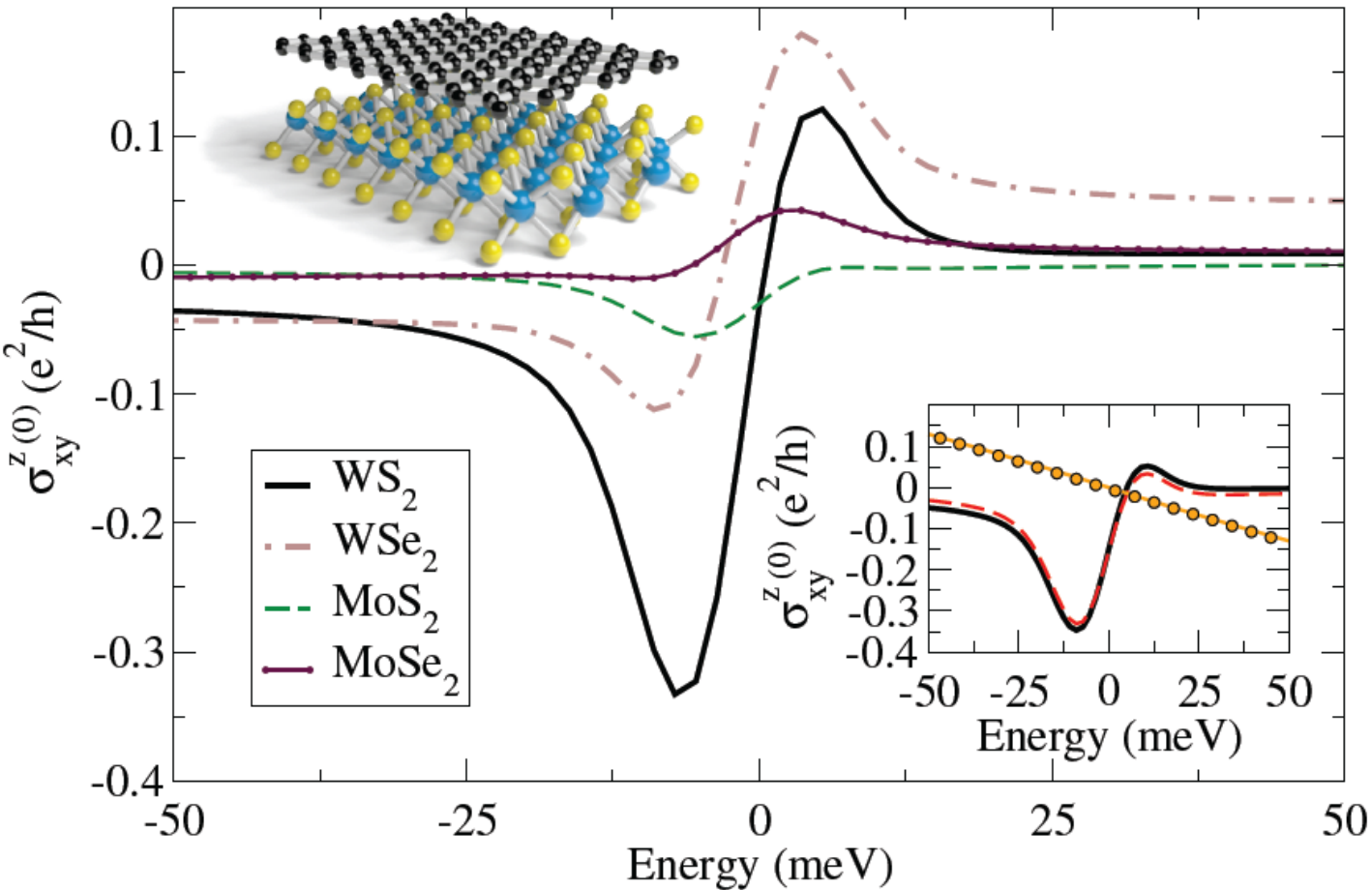
$$\mu_{mn} = \frac{4}{\Delta E^2} \mathcal{Im}[Tr[J_x^z T_n(\hat{H}) v_y T_m(\hat{H})]]$$

The trace in μ_{mn} is computed by the average on a small number $R \ll N$ of random phase vectors $|\varphi\rangle$

$$\sigma_{xx} = \frac{2\hbar e^2}{\pi\Omega} \sum_{m,n=0}^M \mathcal{Im}[g_m(\epsilon + i\eta)] \mathcal{Im}[g_n(\epsilon + i\eta)] \mu_{mn}$$

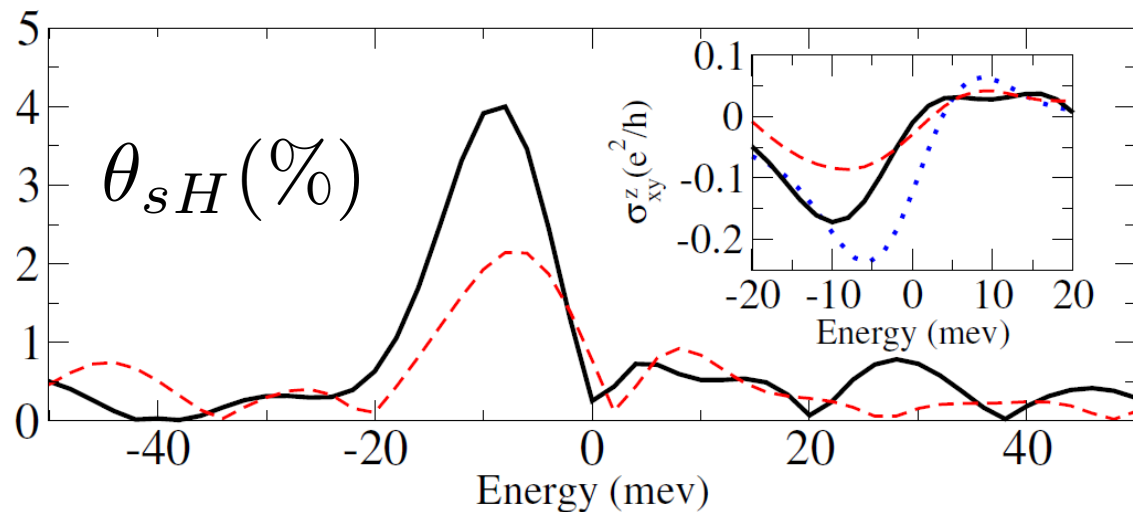
dc-Kubo
conductivity

Spin Hall Kubo conductivity in clean graphene/TMDC interfaces

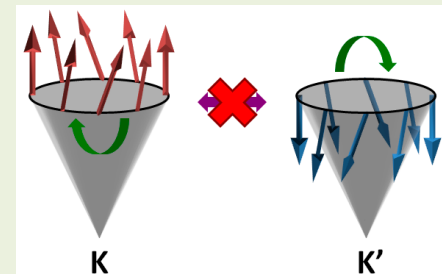


Upper limit Spin Hall Effect

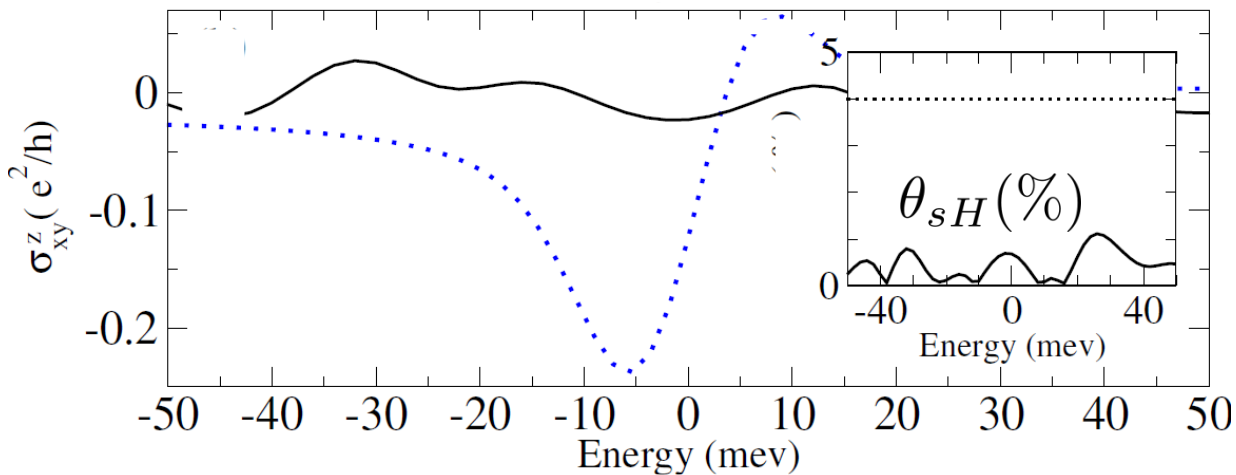
in disordered graphene/TMDC interfaces



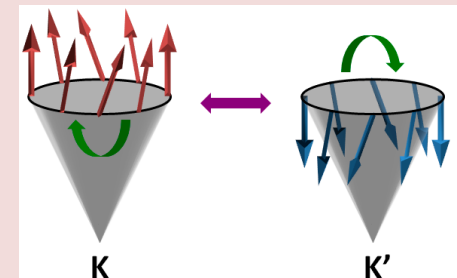
$$\theta_{sH}(\%) \simeq 4\%$$



Intravalley
scattering



$$\theta_{sH}(\%) \ll 1\%$$



Intervalley
scattering

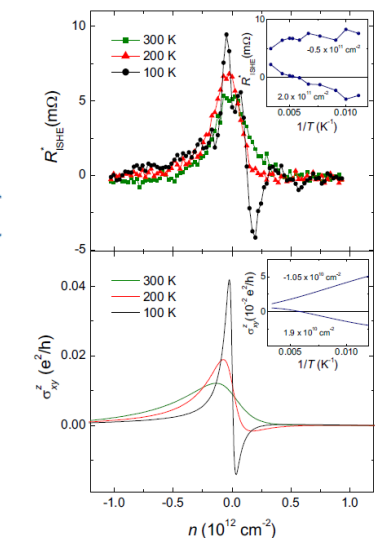
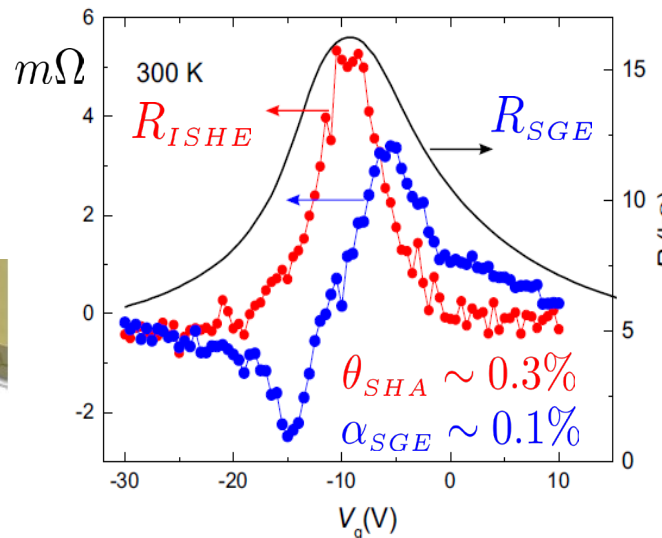
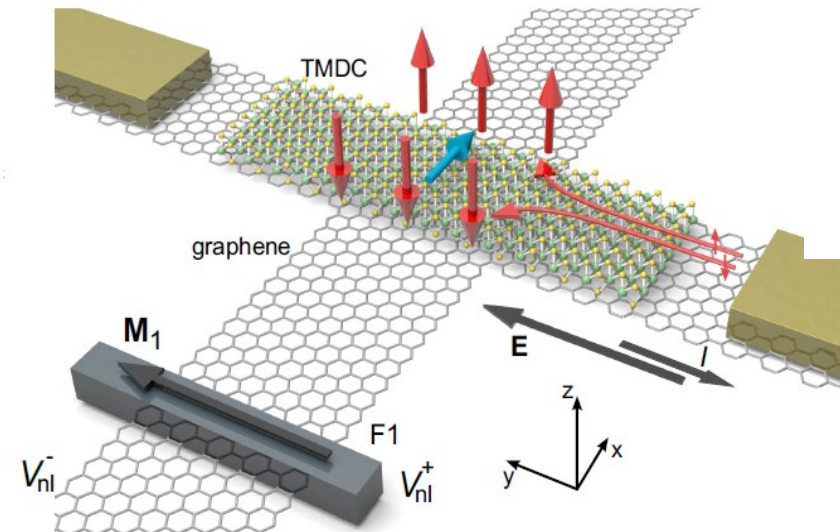
Nature Materials 19 (2), 170-175 (2020)

Tunable room-temperature spin galvanic and spin Hall effects in van der Waals heterostructures

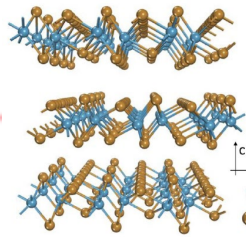
L. Antonio Benítez^{ID 1,2,4*}, Williams Sávero Torres^{ID 1,4*}, Juan F. Sierra¹, Matias Timmermans^{ID 1,2}, Jose H. Garcia^{ID 1}, Stephan Roche^{1,3}, Marius V. Costache¹ and Sergio O. Valenzuela^{ID 1,3*}



$$\lambda_s \theta_{sH}^\alpha \sim 5 - 10 \text{ nm}$$



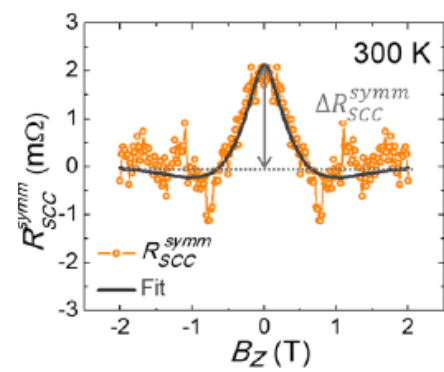
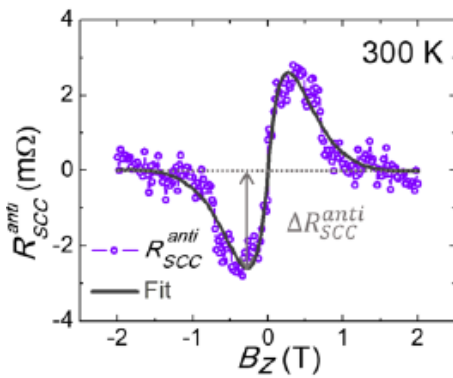
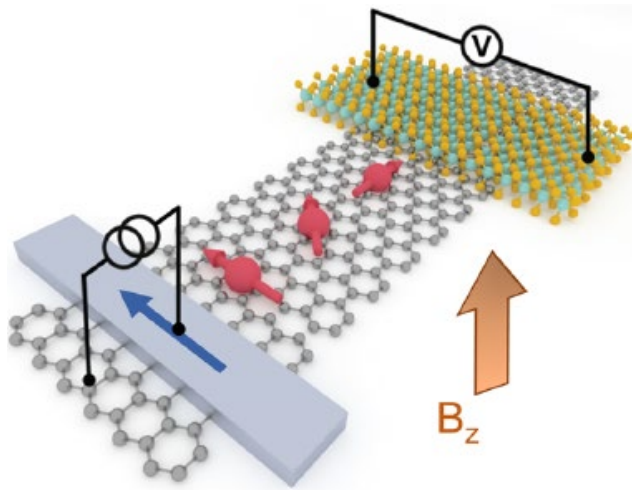
SHE in Low-symmetry multilayers TMDs



C. K. Safeer, et al. *Nano Letters* **19** (12), 8758-8766 (2019)

Multidirectional spin-to-charge conversion in **multilayers MoTe₂** (*11 nm thick sample*)

$$\Delta R_{sH} \sim \theta_{sH}^2 \rho \frac{W}{\lambda_s} e^{-L/\lambda_s}$$



$$\lambda_s \cdot \theta_{sH} \sim 1 \text{ nm}$$

P. Song et al. *Nat. Mater.* **19**, 292–298 (2020)

$$\theta_{sH} \sim 30\%$$

$$\lambda_s \sim 1 \mu\text{m}$$

$$\lambda_s \cdot \theta_{sH} \sim 300 \text{ nm} !!$$



4-band symmetry-based model TMD- 1T_d

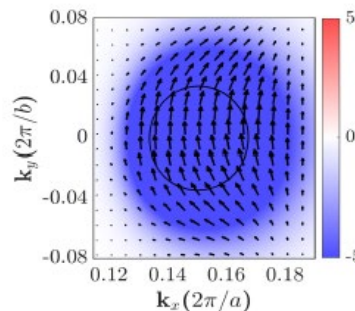
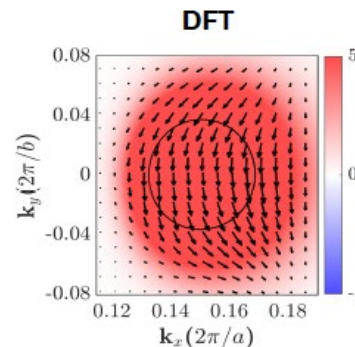
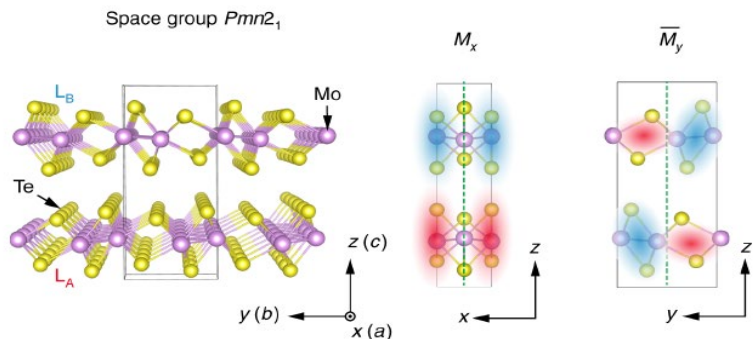
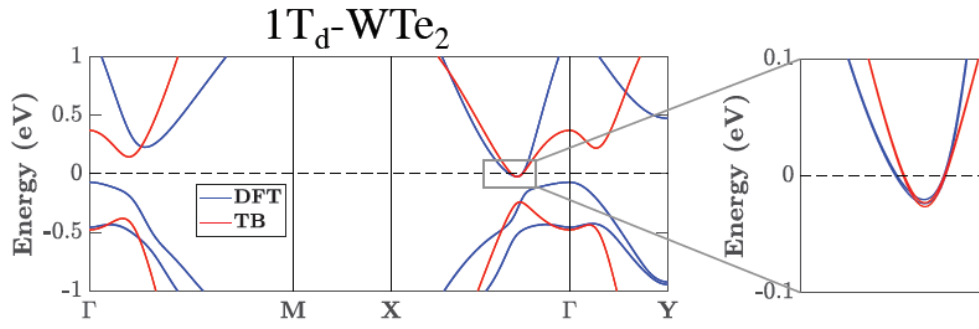
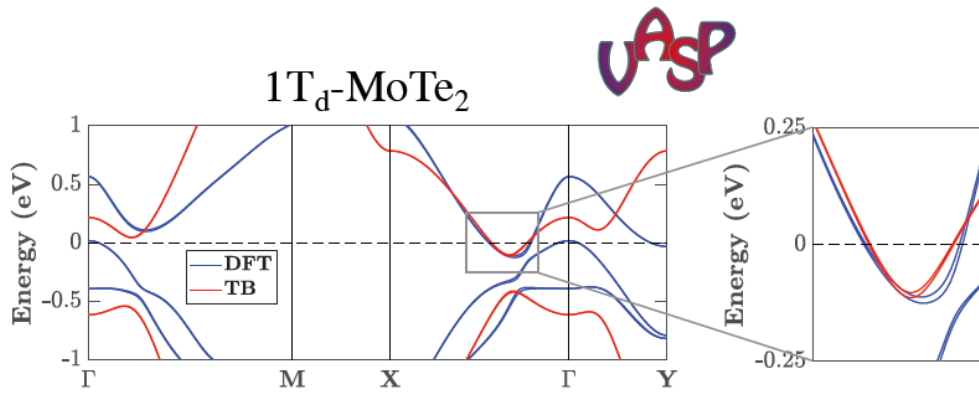
Bulk crystal structure of 1T_d -TMD

(mirror symmetry in the yz plane (M_x)
& a glide mirror symmetry (M_y) along
the perpendicular z direction)



Centre for
Advanced 2D Materials

Monolayer 1T_d -TMD: *Lowering symmetry*
2D structure loses translational symmetry along the z direction



Persistent-canted
spin texture (yz)
(k-independent)

$$\langle \vec{S} \rangle_{E_F} \approx \langle S_0 \rangle_{E_F} \hat{u}(\theta)$$

4-band symmetry-based model TMD- $\mathbf{1T_d}$

4-band real space tight binding model (*interpolated in Wannier basis (Wanier90) generated by two orbitals (plus spin) / unit cell - p_y of the chalcogens and d_{yz} of the metal ions*)

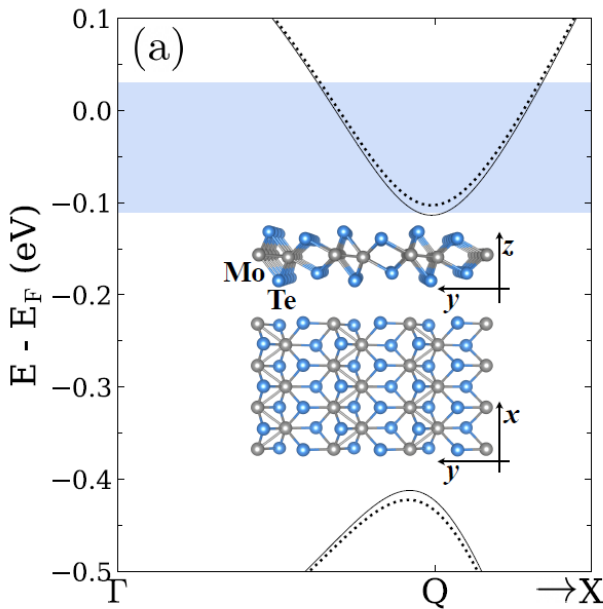
$$\begin{aligned} H = & \sum_i (\Delta_E + 4m_d + \delta) c_{i,s}^\dagger c_{i,s} - \sum_{\langle i,j \rangle} (m_p + m_d) c_{i,s}^\dagger c_{j,s} \\ & + \sum_i (\Delta_E - 4m_d - \delta) d_{i,s}^\dagger d_{i,s} - \sum_{\langle i,j \rangle} (m_p - m_d) d_{i,s}^\dagger d_{j,s} \\ & - \sum_{\langle i,j \rangle} \frac{\beta}{2} (\hat{l}_{ij} \cdot \hat{y}) c_{i,s}^\dagger d_{j,s} + \sum_i \eta c_{i,s}^\dagger d_{i,s} \\ & \text{---} \sum_{\langle i,j \rangle} \frac{i}{2} (\Lambda \times \hat{l}_{ij}) \cdot (\hat{y} + \hat{z}) c_{i,s}^\dagger d_{j,s}, \end{aligned}$$

Spin-orbit coupling

$$\Lambda \equiv (\Lambda_x \sigma_x, -\Lambda_y \sigma_y, \Lambda_z \sigma_z)$$

Spin texture:

Arrows: *in-plane spin projection*
Color: *spin projection along z*

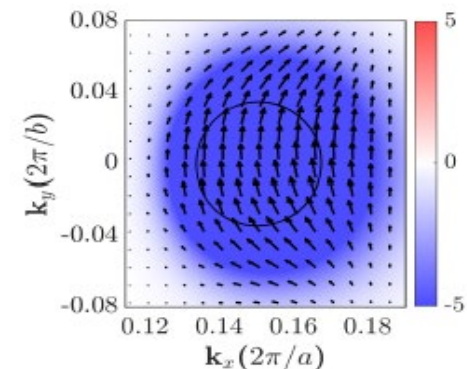
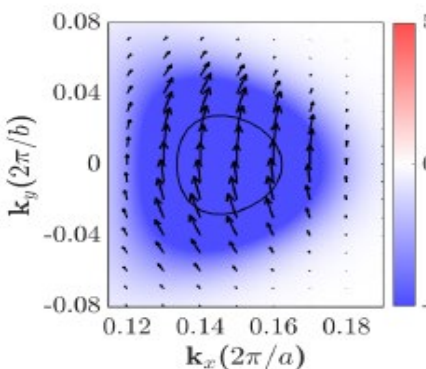
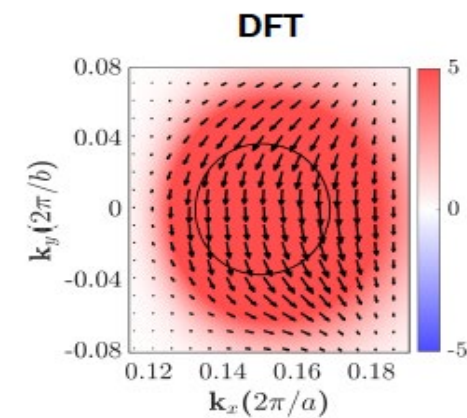
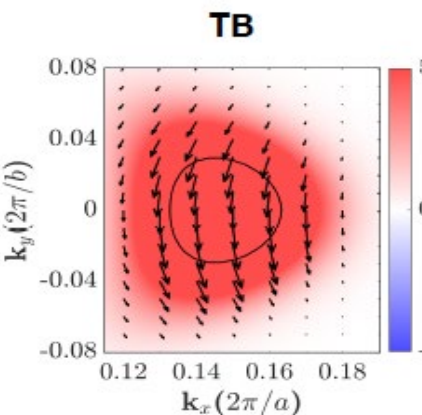


MoTe₂

CB2

WTe₂

CB1



Anisotropic spin dynamics in MoTe₂

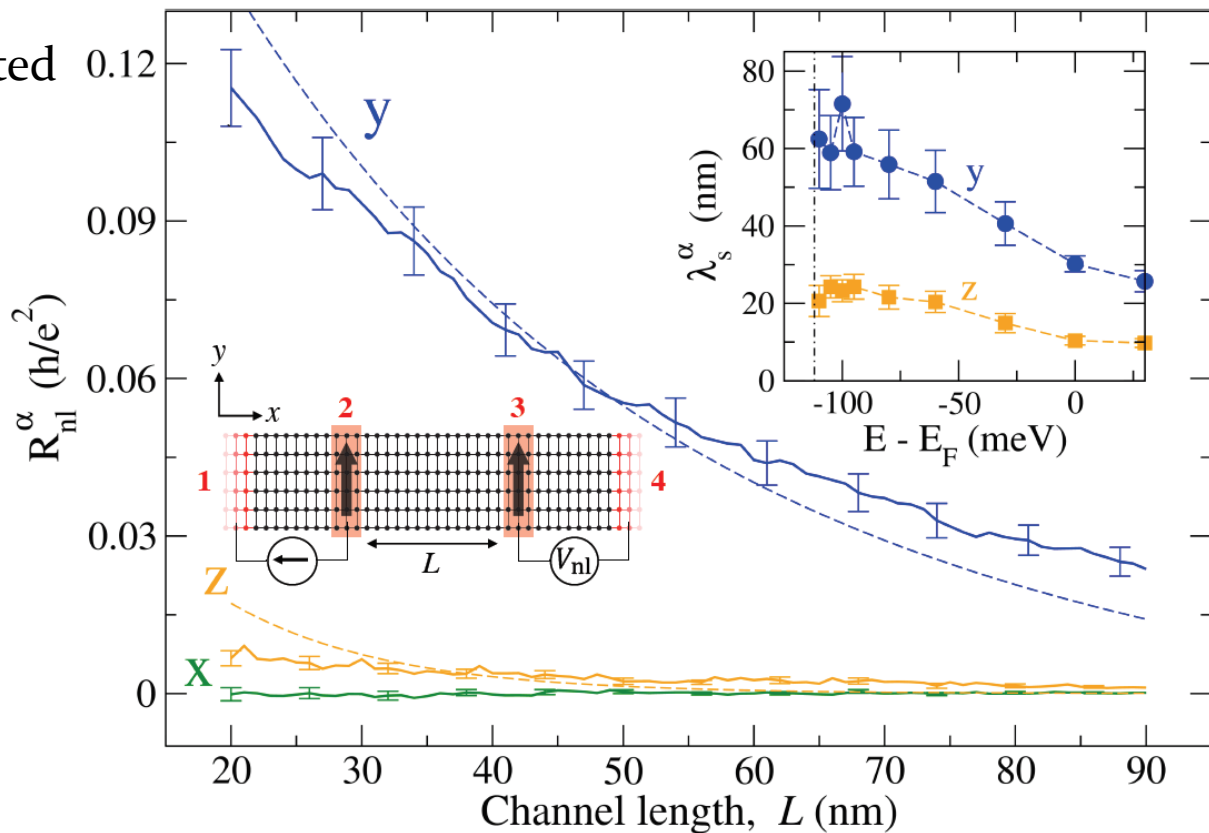
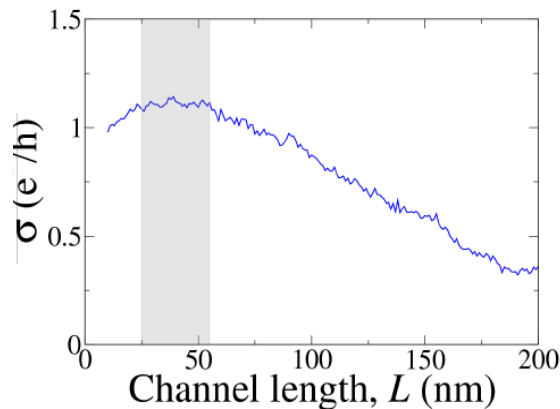
Study of the nonlocal resistance versus channel length to extract spin diffusion length

$$I_0^\alpha \quad \alpha \in \{x, y, z\}$$

Spin α -polarized current injected

$$R_{\text{nl}}^\alpha \equiv V_{\text{nl}} / I_0^\alpha$$

+Anderson disorder
Diffusive regime (MFP < L)



Extract of λ_s by fitting to the solution of a 1D spin diffusion equation

$$\lambda_S^y > \lambda_S^z \gg \lambda_S^x$$

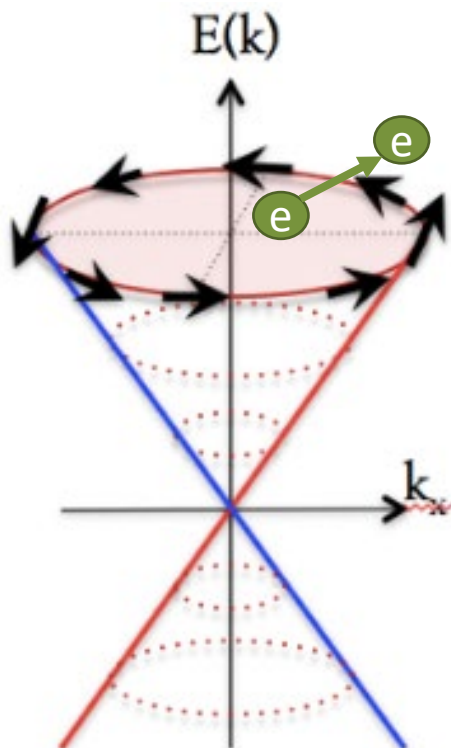
Anisotropic spin dynamics in MoTe₂

In 2D Rashba SOC materials

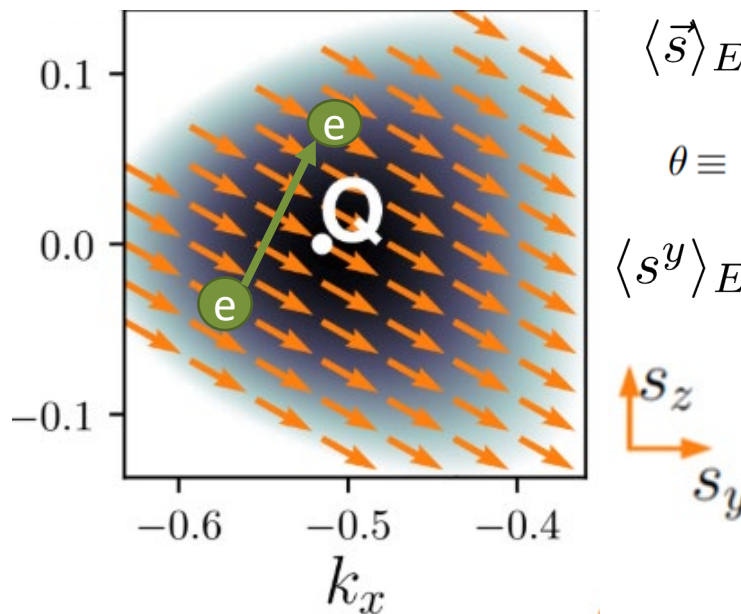
Spin-momentum locking

*scattering changes effective (in-plane)
magnetic field randomly*

$$\lambda_s^z \sim \frac{1}{2} \lambda_s^y = \frac{1}{2} \lambda_s^x$$



In 2D Weyl semimetal TMD
Persistent (cantèd) spin texture



$$\langle \vec{s} \rangle_{E_F} \sim \langle S_0 \rangle_{E_F} \hat{u}(\theta)$$

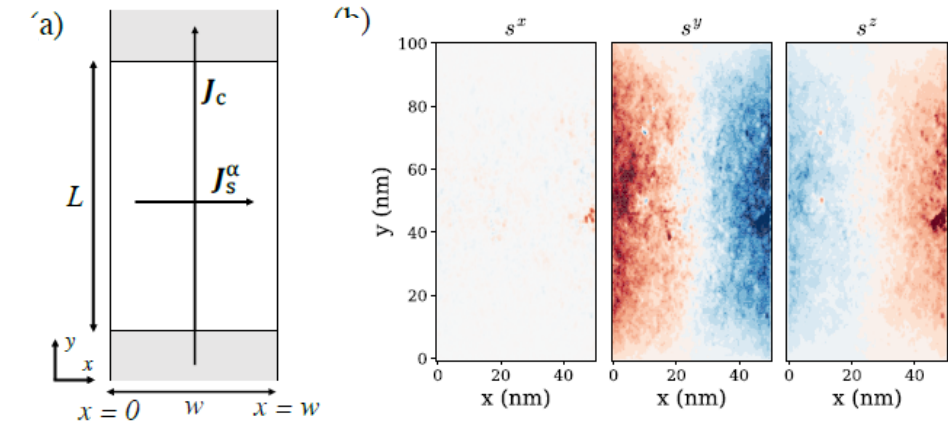
$$\theta \equiv \arctan(\Lambda_z/\Lambda_y) \approx -56^\circ$$

$$\langle s^y \rangle_E > \langle s^z \rangle_E \gg \langle s^x \rangle_E$$

Effective magnetic field is fixed (pointing in the yz plane)
x-polarized spins precess much faster- shorter spin diffusion
z-polarized spins precess faster than y-polarized

$$\lambda_s^y > \lambda_s^z \gg \lambda_s^x$$

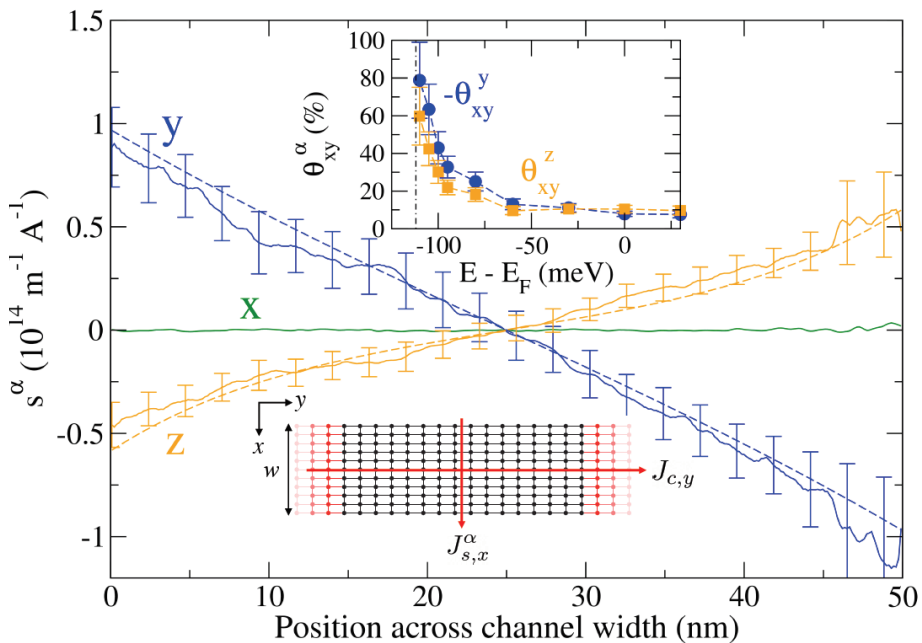
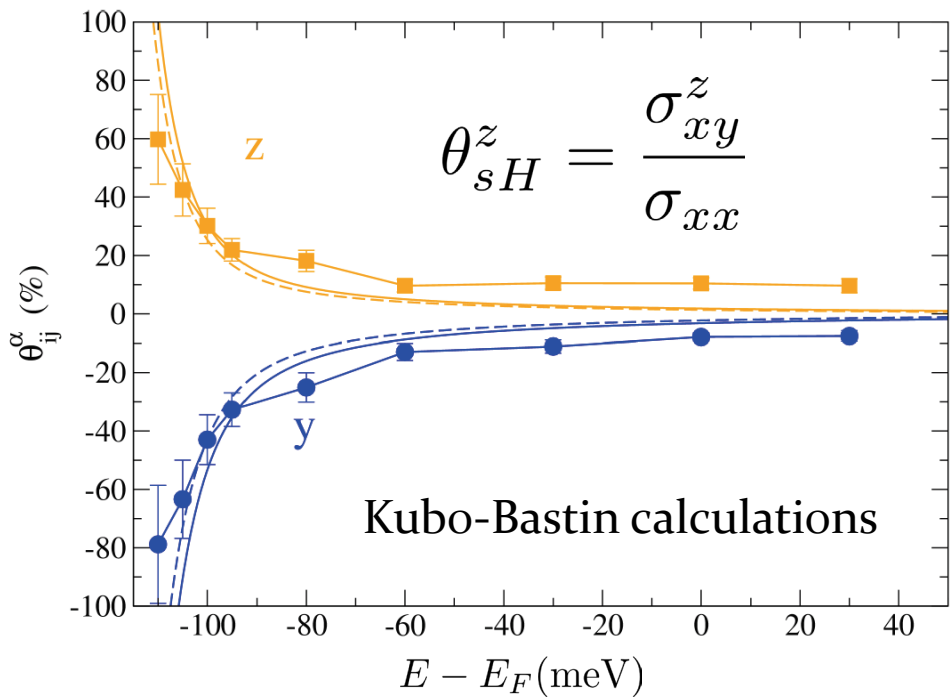
Spin accumulation & (Giant) Spin Hall angle



Extract the spin accumulation across the channel

Fitting the results with solution of the *Spin drift-diffusion equation*

$$\frac{s^\alpha(x)}{J_c} = -\frac{\theta_{xy}^\alpha \lambda_s^\alpha}{|e| D_s} \frac{\sinh(\frac{w-2x}{2\lambda_s^\alpha})}{\cosh(\frac{w}{2\lambda_s^\alpha})},$$



$$\lambda_s \theta_{sH}^\alpha \sim 10 - 50 \text{ nm}$$

Experimental fingerprints (Hanle)

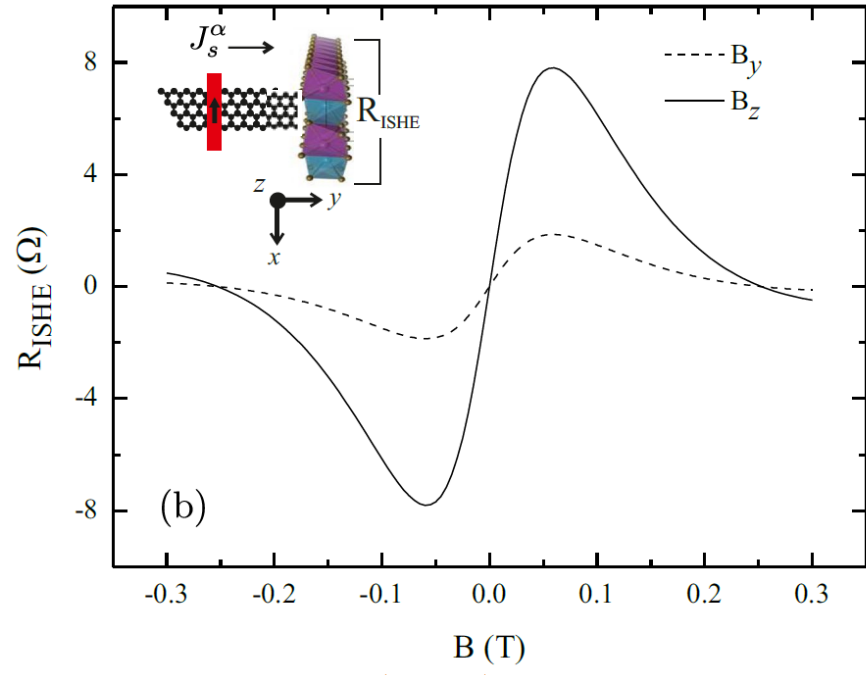
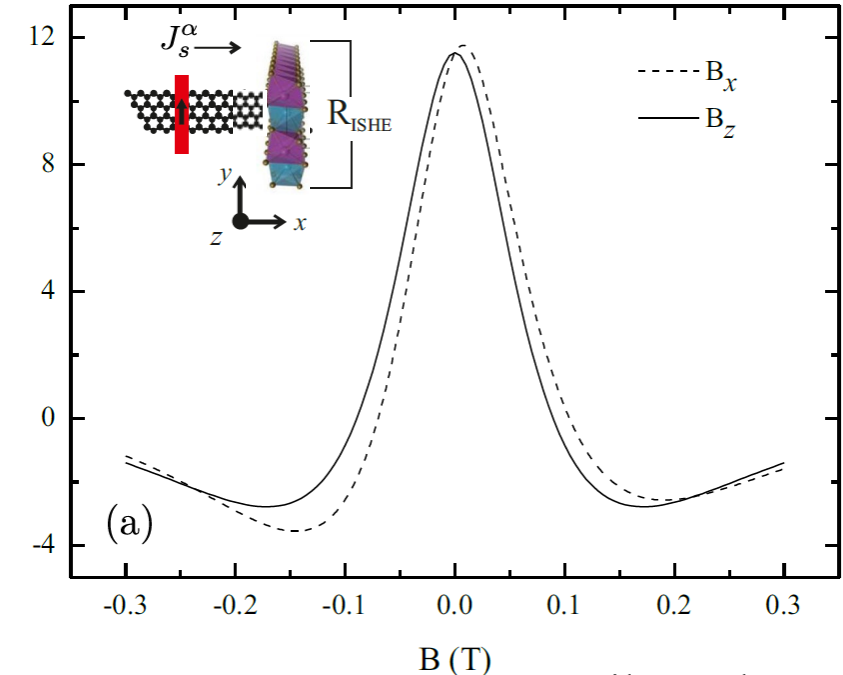
Simulated response of the inverse SHE (R_{ISHE})
to spin precession for two orientations of the TMD crystal (full absorption limit)

spin current polarization reaching the TMD J_s^α controlled externally with a magnetic field orientation

Anisotropic spin diffusion

$$R_{ISHE} = V_{ISHE}/I_0^y$$

- up to 3 orders of magnitude larger than other SHE materials (large SHA)
- symmetric or antisymmetric depending on crystal orientation



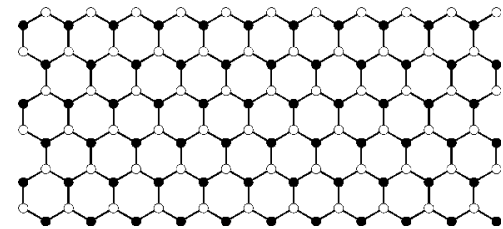
Low symmetry topological materials

Canted Quantum Spin Hall Effect (WTe₂ monolayer)

J.H. Garcia et al. **Phys. Rev. Lett.** 125, 256603 (2020)

J.H. Garcia et al. **Phys. Rev. B** 106 (16), L161410 (2022)

Quantum Spin Hall Effect

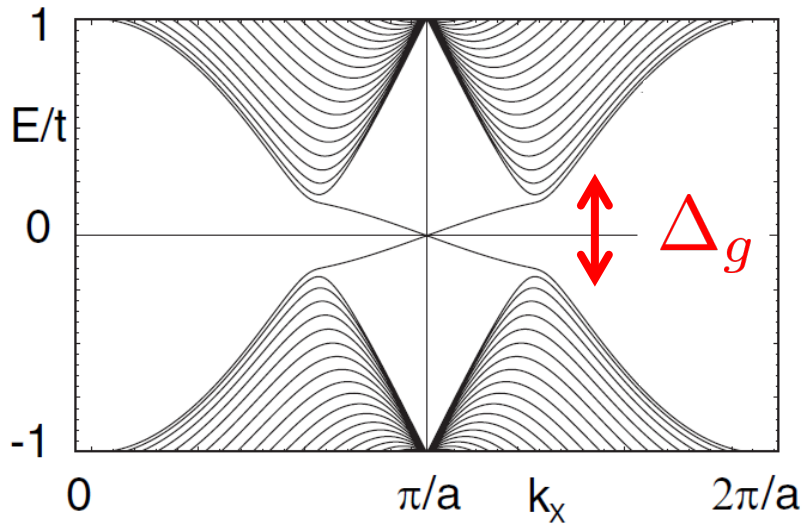
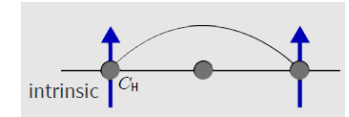


C.L. Kane and E. J. Mele,
Phys. Rev. Lett. 95, 26801 (2005)

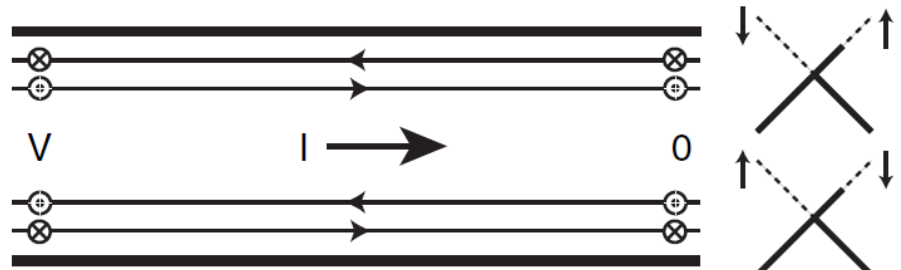


Zigzag graphene ribbon with intrinsic SOC

$$\mathcal{H} = t \sum_{\langle ij \rangle} c_i^\dagger c_j + i(8\lambda_{SO}/a^2) \sum_{\langle\langle ij \rangle\rangle} c_i^\dagger \mathbf{s} \cdot (\mathbf{d}_{ij}^1 \times \mathbf{d}_{ij}^2) c_j$$



Gapless helical edge states
States with opposite spins
counterpropagate at the edges



“QHE” in absence of magnetic field
Towards dissipation current (TRS invariant)....

$$\Delta_g \sim 0.1 \text{ meV}$$

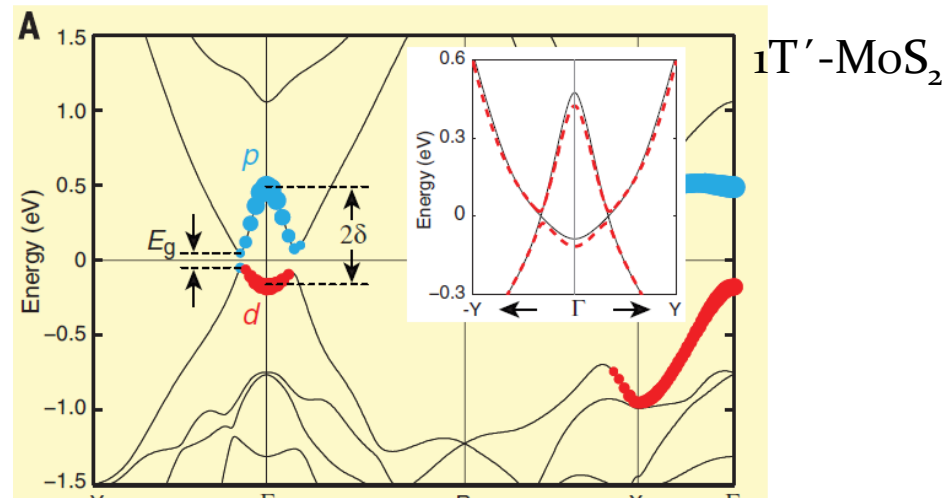
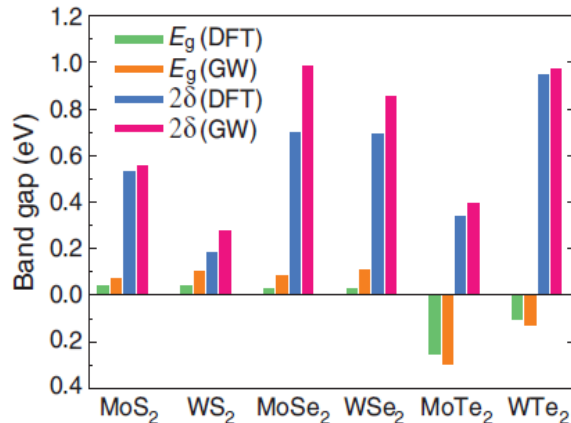
$1T'$ -TMD monolayer as QSH insulators



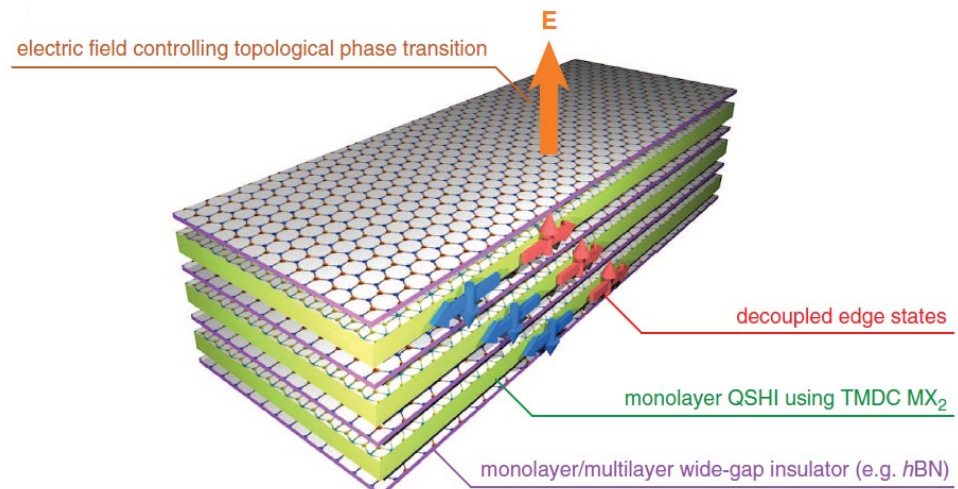
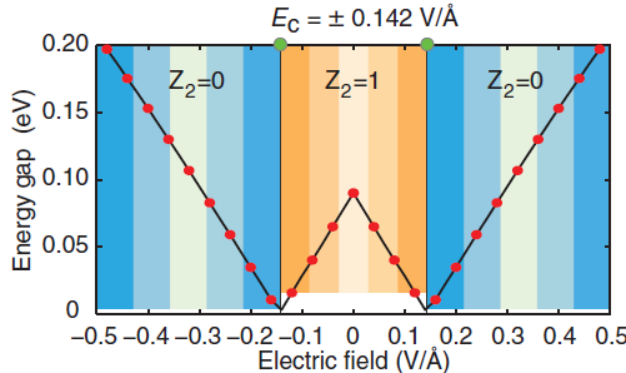
X. Qian, J. Liu, L. Fu, J. Li, **Science 346, 1344 (2014)**

Structural distortion causes an intrinsic band inversion between chalcogenide-p and metal-d bands (gap in order of 0.1 eV)

Prediction in 2014



Topological field effect transistor (low-power quantum electronics)



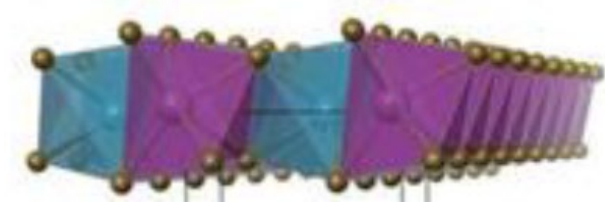
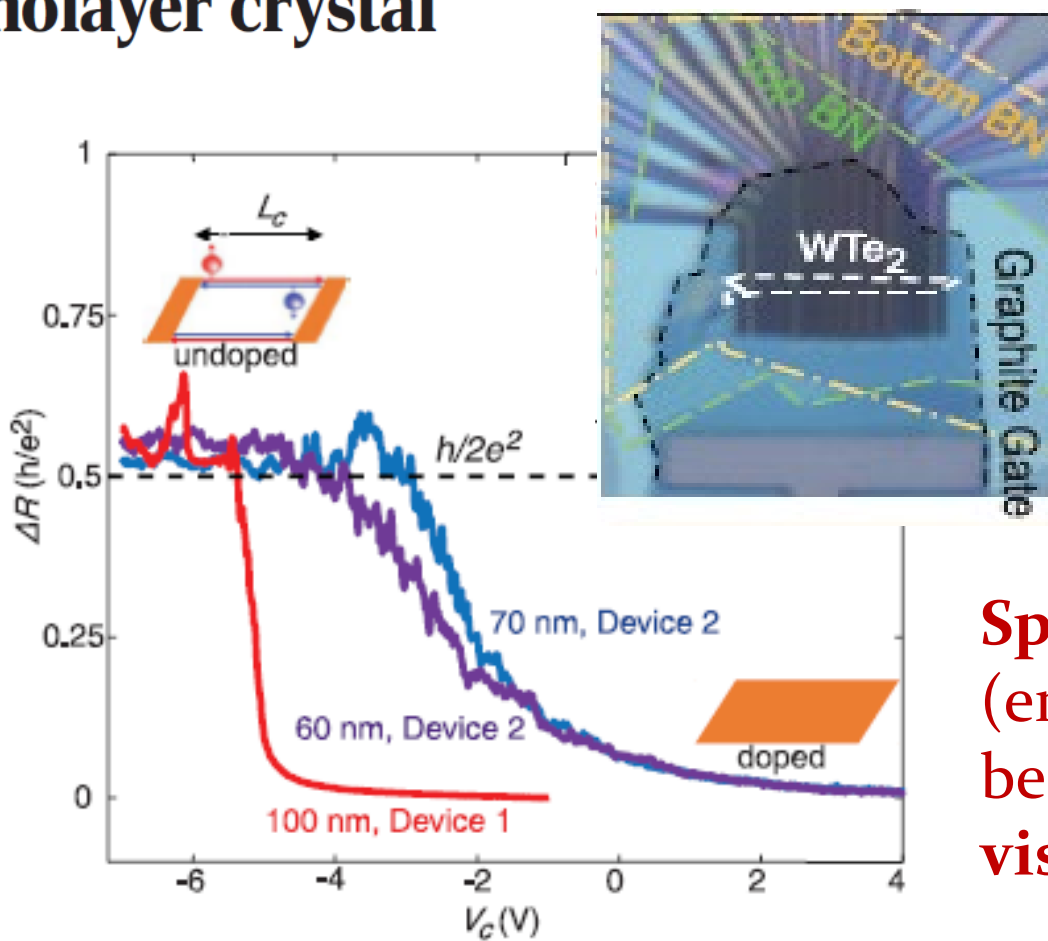
1T-WTe_2 as Quantum Spin Hall insulator

TOPOLOGICAL MATTER

Observation of the quantum spin Hall effect up to 100 kelvin in a monolayer crystal

Wu et al.

Science 359, 76-79 (2018)

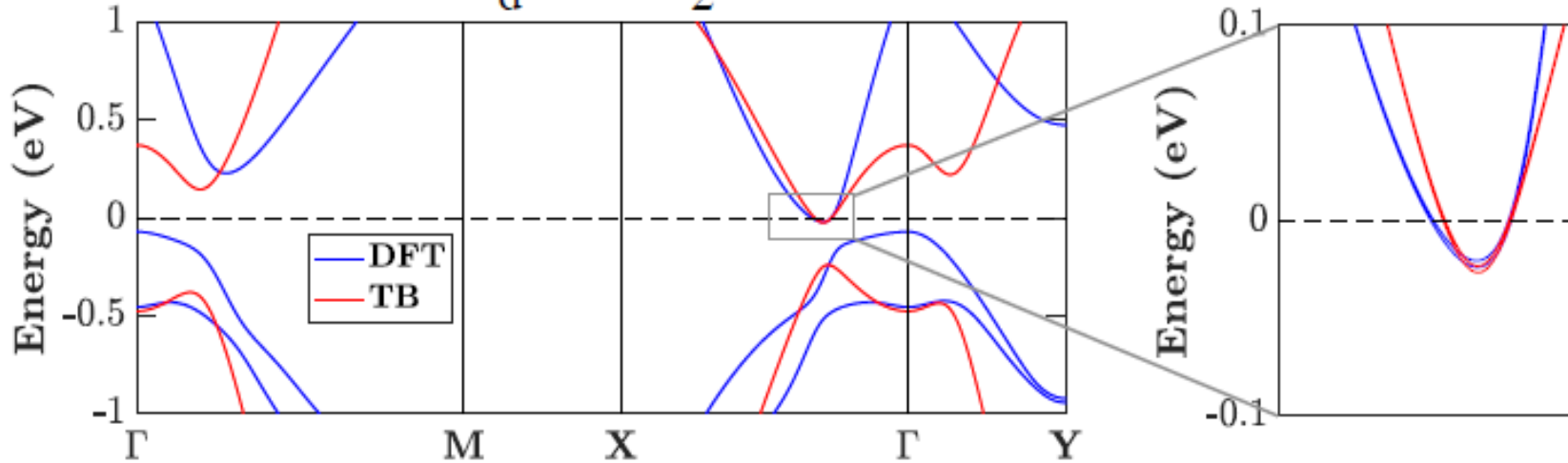


Purely electrical measurements

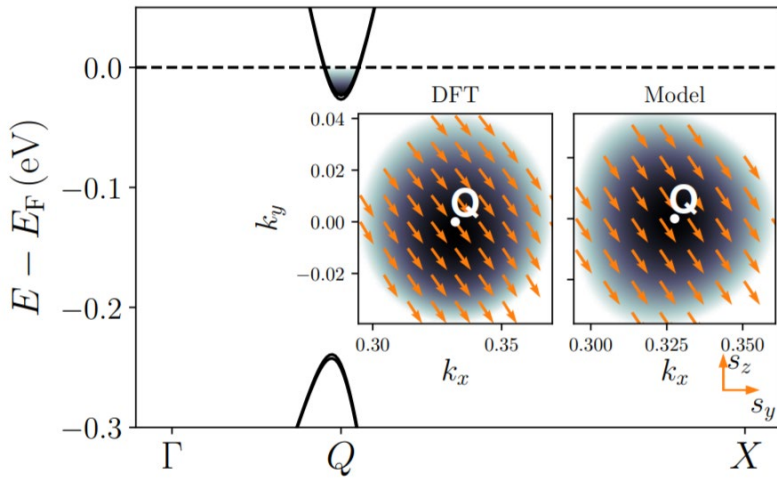
Spin-momentum locking (entanglement) has not yet been directly visualized/demonstrated

QSHE in WTe₂

1T_d-WTe₂



$$\mathcal{H}_0 \simeq (k_x^2 + k_y^2)(m_p\tau_0 + m_d\tau_z) + \beta k_y\tau_y + \delta\tau_z + \eta\tau_x$$



$$\mathcal{H}_{\text{SOC}} \simeq (\Lambda_x k_y \sigma_x + \Lambda_y k_x \sigma_y + \Lambda_z k_x \sigma_z) \otimes \tau_x$$

$$\theta \equiv \arctan(\Lambda_z/\Lambda_y) \approx -56^\circ$$

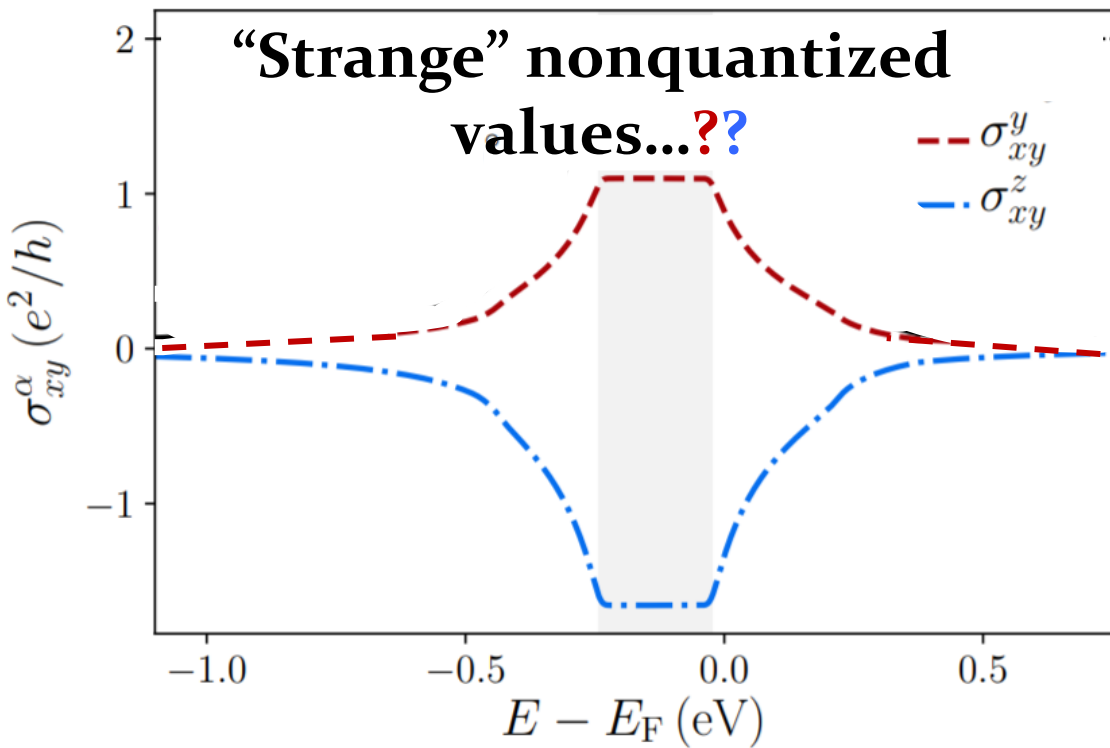
Spin Hall conductivity for WTe₂

Spin Hall conductivity tensor (Kubo-Bastin formula)

$$\sigma_{ij}^{\alpha}, \alpha = x, y, z$$

$$\sigma_{ij}^{\alpha} = -2\hbar\Omega \int_{-\infty}^{E_F} dE \operatorname{Im} \left(\operatorname{Tr} \left[\delta(E - \mathcal{H}) J_{s,i}^{\alpha} \frac{dG^+}{dE} J_j \right] \right)$$

measures of the spin projection onto α



Simulations on a system with **4 Millions atoms** (*energy broadening = 5 meV*)

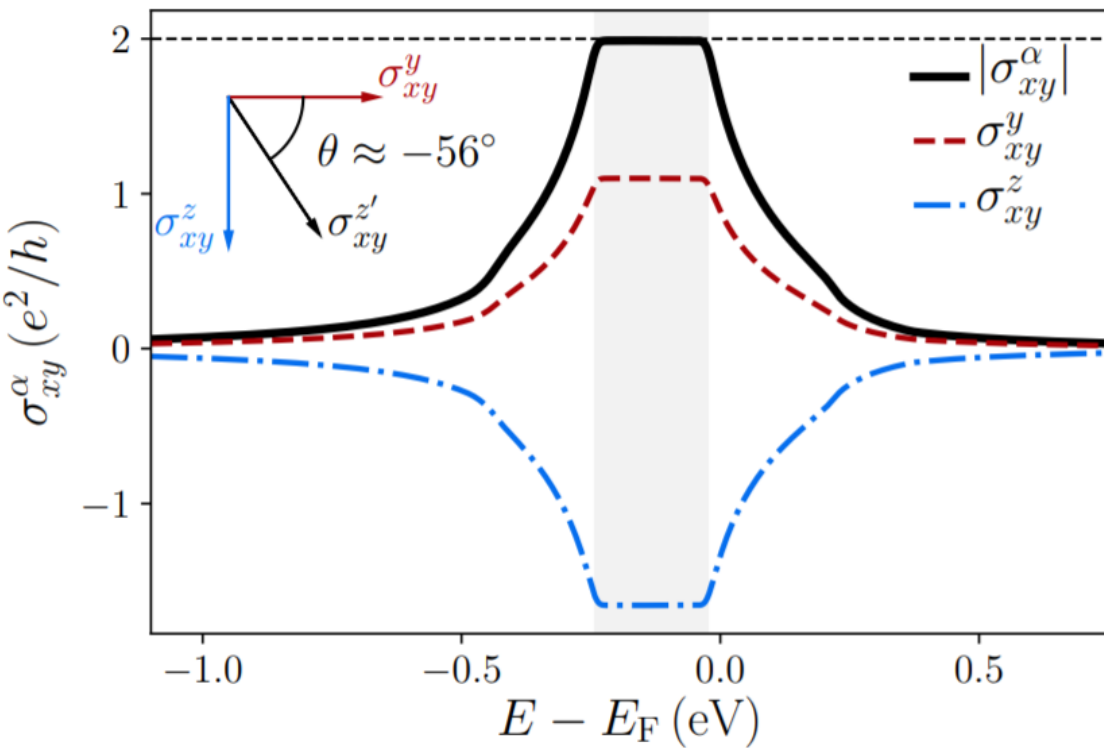
Spin Hall conductivity for WTe₂

Spin Hall conductivity tensor
(Kubo-Bastin formula)

$$\sigma_{ij}^{\alpha}, \alpha = x, y, z$$

measures of the spin projection onto α

$$\sigma_{ij}^{\alpha} = -2\hbar\Omega \int_{-\infty}^{E_F} dE \operatorname{Im} \left(\operatorname{Tr} \left[\delta(E - \mathcal{H}) J_{s,i}^{\alpha} \frac{dG^+}{dE} J_j \right] \right)$$



In the gap, a combination of SHC in y and z directions

$$|\sigma_{xy}^{\alpha}| \equiv \sqrt{(\sigma_{xy}^y)^2 + (\sigma_{xy}^z)^2} = \frac{2e^2}{h}$$

$$\arctan(\sigma_{xy}^z / \sigma_{xy}^y) = -56^\circ$$

Two spin-canted topological states
sustaining QSHE in WTe₂

Spin quantization axis

$$\mathcal{H}'_{\text{SOC}} \equiv U^\dagger(\theta) \mathcal{H} U(\theta) = \Lambda_x k_y \sigma_x + \Lambda_r k_x \sigma_{z'} \tau_x$$

$$U(\theta) \equiv \cos[(2\theta - \pi)/4] \sigma_0 - i \sin[(2\theta - \pi)/4] \sigma_x$$

$$[\mathcal{H}', \sigma_{z'}] \approx 0$$

(spin preserved along z')

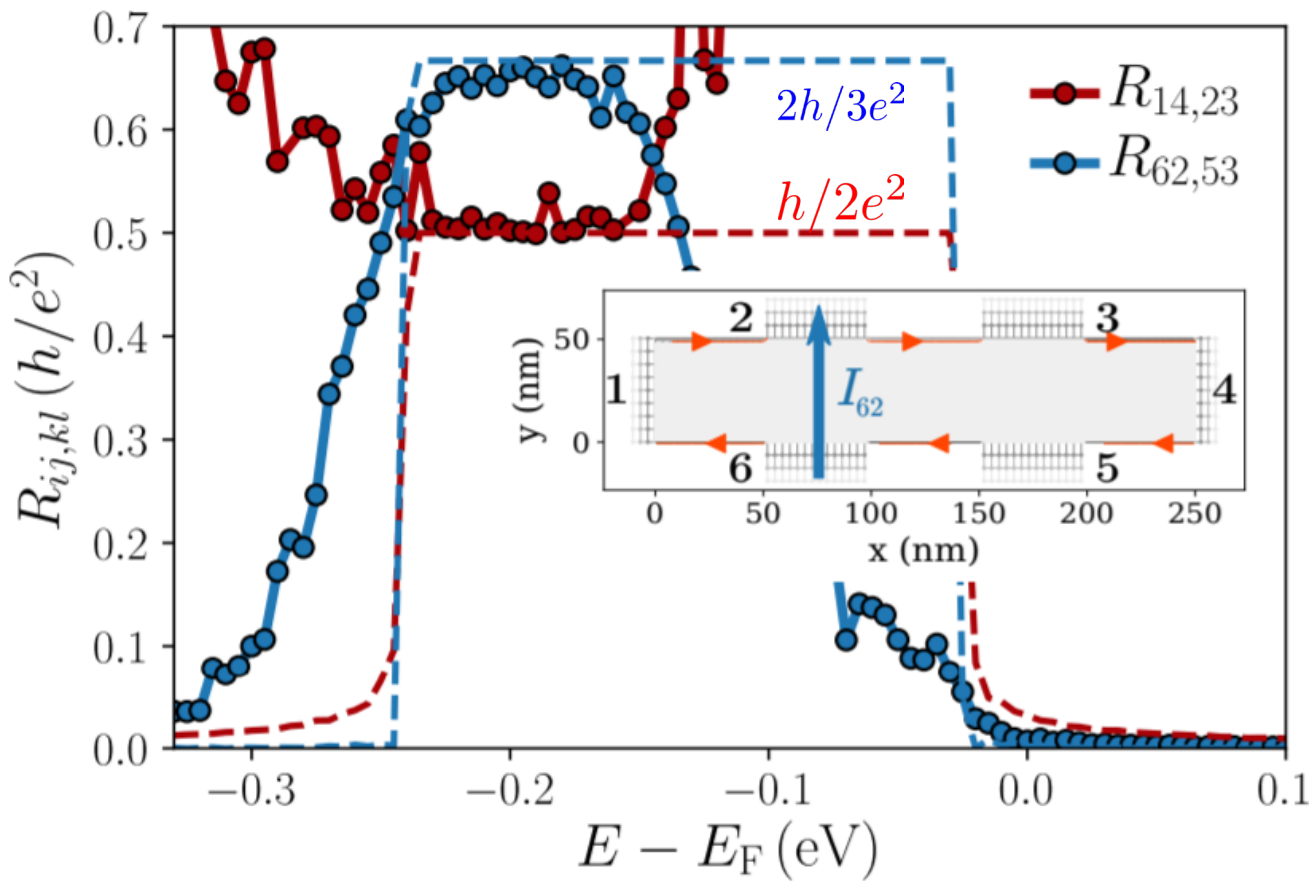
Nonlocal resistance calculations

*Topologically
protected edge-states*

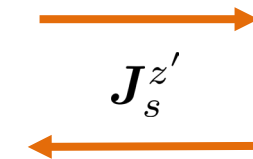
Quantized two-terminal resistance (2 channels) $h/2e^2$

Quantized nonlocal resistance $2h/3e^2$

Robustness to disorder (Anderson model 1 eV)



Bond-projected spin currents
for spins polarized along the
(rotated) z' direction



Bond-projected spin currents
for spins polarized along the
(rotated) y' direction



“vanishing contribution”

Determination of the helical edge and bulk spin axis in quantum spin Hall insulator WTe₂

Wenjin Zhao^{1†}, Elliott Runburg^{1†}, Zaiyao Fei¹, Joshua Mutch¹, Paul Malinowski¹, Bosong Sun¹, Xiong Huang^{2,3}, Dmytro Pesin⁴, Yong-Tao Cui^{2,3}, Xiaodong Xu^{1,5}, Jiun-Haw Chu¹, David H. Cobden^{1*}

¹Department of Physics, University of Washington, Seattle WA 98195, USA

²Department of Physics and Astronomy, University of California, Riverside, Riverside CA 92521, USA

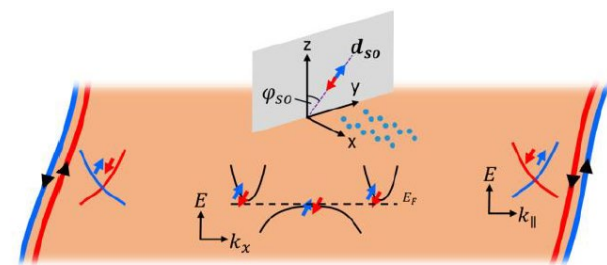
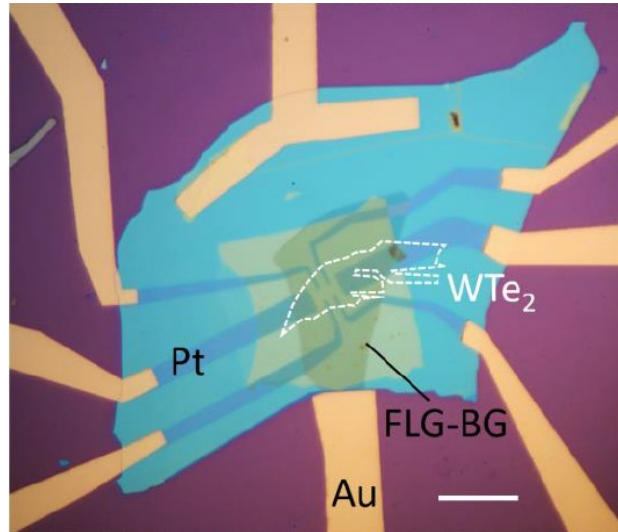
³Department of Materials Science and Engineering, University of California, Riverside, Riverside CA 92521, USA

⁴Department of Physics, University of Virginia, Charlottesville, Virginia 22904, USA

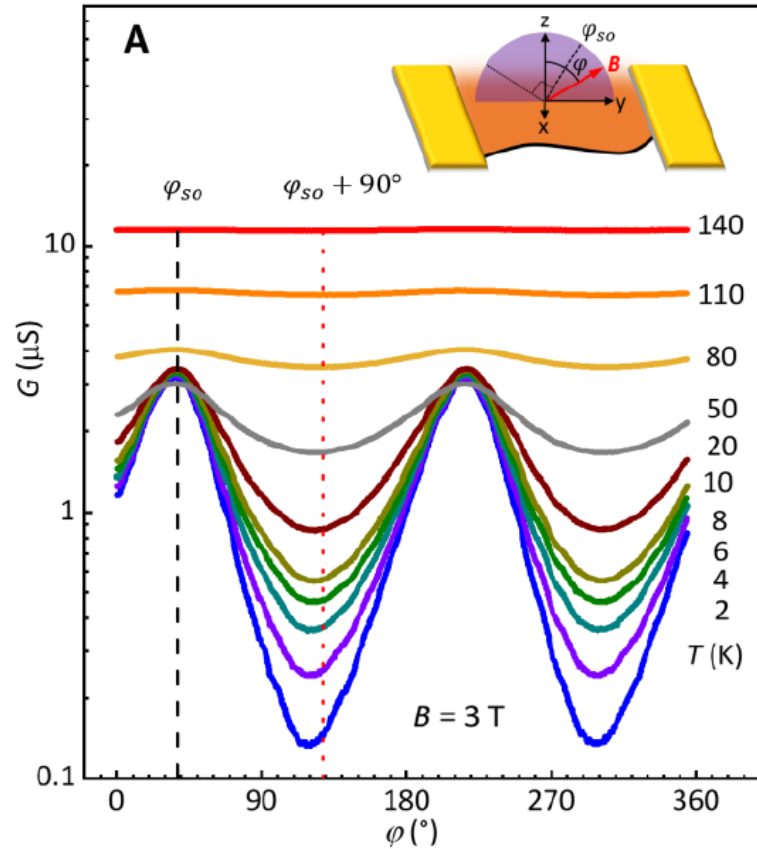
⁵Department of Materials Science and Engineering, University of Washington, Seattle WA 98195, USA

†These authors contributed equally

*Corresponding author: cobden@uw.edu



Phys. Rev. X 11, 041034 (2021)



Electrical control of spin-polarized topological currents in monolayer WTe₂

Jose H. Garcia,¹ Jinxuan You,^{1,2} Mónica García-Mota,² Peter Koval,² Pablo Ordejón,¹ Ramón Cuadrado,¹ Matthieu J. Verstraete,³ Zeila Zanolli,^{4,1} and Stephan Roche^{1,5}

¹Catalan Institute of Nanoscience and Nanotechnology - ICN2,
(CSIC and BIST), Campus UAB, Bellaterra, 08193 Barcelona, Spain

²Simune Atomistics S.L., Tolosa Hiribidea, 76, 20018 Donostia-San Sebastian, Spain

³nanomat/QMAT/CESAM and European Theoretical Spectroscopy Facility Universite de Liege,
Allee du 6 Aout 19 (B5a), 4000 Liege, Belgium

⁴Dept. of Chemistry, Debye Institute for Nanomaterials Science, and ETSF, Utrecht University, The Netherlands

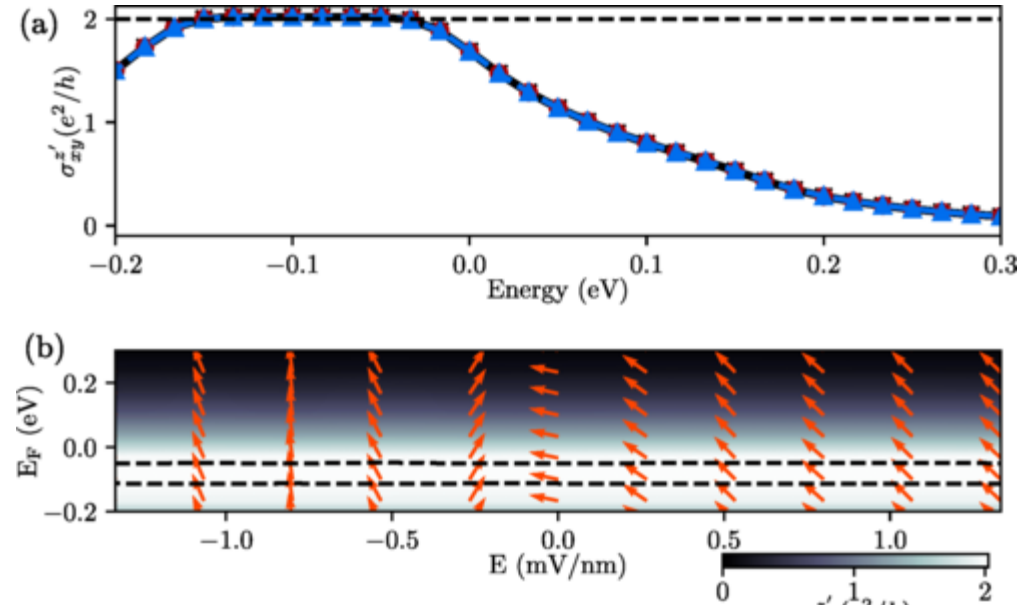
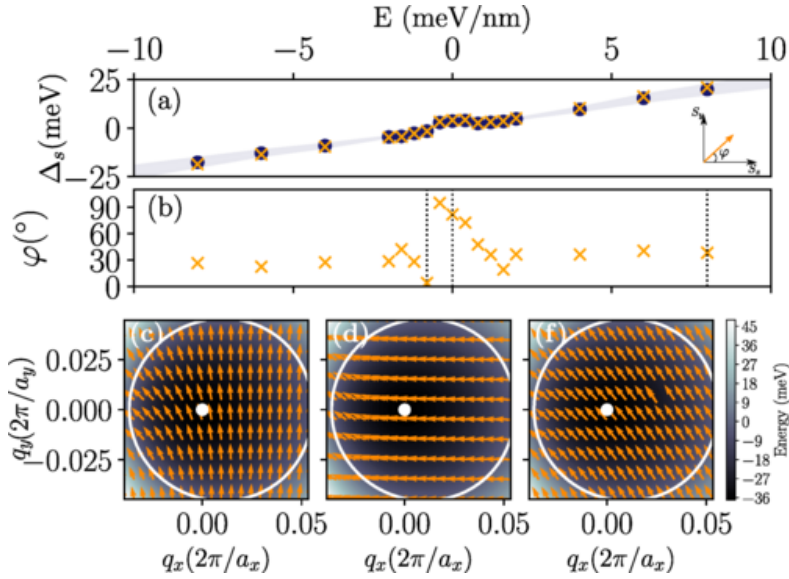
⁵ICREA-Institució Catalana de Recerca i Estudis Avançats, 08010 Barcelona, Spain

(Dated: May 25, 2022)



We evidence the possibility for coherent electrical manipulation of the spin orientation of topologically protected edge states in a low-symmetry quantum spin Hall insulator. By using a combination of *ab-initio* simulations, symmetry-based modeling, and large-scale calculations of the spin Hall conductivity, it is shown that small electric fields can efficiently vary the spin textures of edge currents in monolayer 1T'-WTe₂ by up to a 90-degree spin rotation, without jeopardizing their topological character. These findings suggest a new kind of gate-controllable spin-based device, topologically protected against disorder and of relevance for the development of topological spintronics.

Physical Review B 106 (16), L161410 (2022)



Increasing the variety of *spin-orbit torque components*

José Garcia

*By lowering the symmetry of the crystals
& heterostructures (twist degree of freedom..)*

nature
REVIEWS
PHYSICS

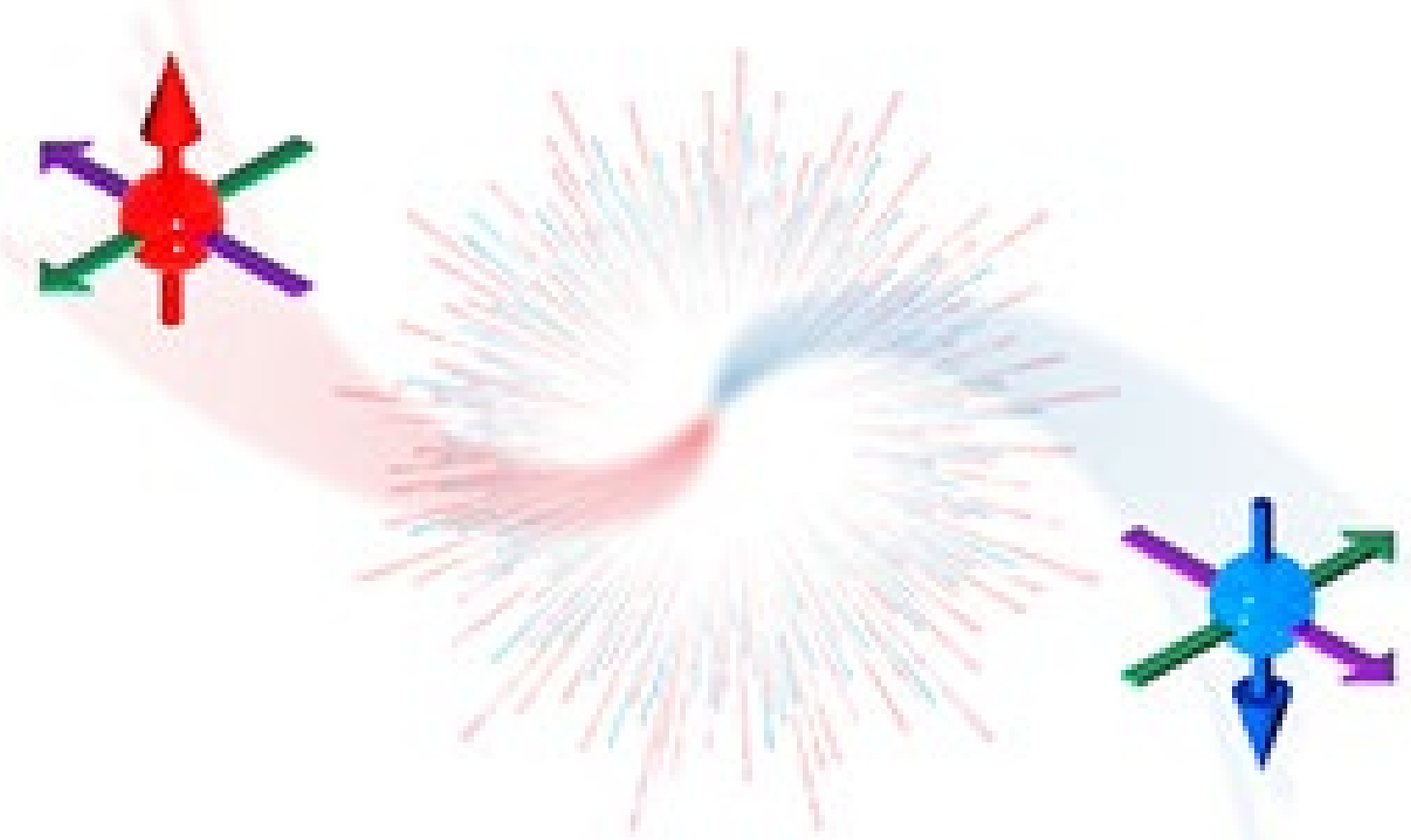
H. Kurebayashi, J. H. Garcia,
S Khan, J. Sinova & S. Roche



Joaquin medina

Repr. Mat.	Space Group	Crystal System	\mathbf{H}^e	\mathbf{H}^o
MX_3^*	$\text{P}\bar{6}2\text{m}$ (189)			$\tau_{\text{DL}} \mathbf{m} \times (\mathbf{J} \times \hat{\mathbf{z}}) + \tau_z m_z \mathbf{J} + \tau_{\text{ani}} \nabla_{\mathbf{m}} [J_y m_x m_y + J_x (m_y^2 - m_x^2)] / 2$
$\text{Fe}_3\text{GeTe}_2^*$	$\text{P}\bar{6}\text{m}2$ (187)	Hexagonal	$\tau_{\text{FL}} \mathbf{J} \times \hat{\mathbf{z}}$	$\tau_{\text{DL}} \mathbf{m} \times (\mathbf{J} \times \hat{\mathbf{z}}) + \tau_z m_z \mathbf{J} + \tau_{\text{ani}} \nabla_{\mathbf{m}} [J_x m_x m_y + J_y (m_x^2 - m_y^2)] / 2$
MnBi_2Te_2	$\text{P}\bar{3}\text{m}1$ (164)			
MXY^\dagger	$\text{P}3\text{m}1$ (156)			$\tau_{\text{DL}} \mathbf{m} \times (\mathbf{J} \times \hat{\mathbf{z}}) + \tau_z m_z \mathbf{J} + \tau_{\text{ani}} \nabla_{\mathbf{m}} [J_x m_x m_y + J_y (m_x^2 - m_y^2)] / 2$
Fe_5GeTe_2	$\text{R}\bar{3}\text{m}$ (147)	Trigonal	$\tau_{\text{FL}} \mathbf{J} \times \hat{\mathbf{z}}$	
CrI_3	$\text{P}\bar{3}1\text{m}$ (162)			$\tau_{\text{DL}} \mathbf{m} \times (\mathbf{J} \times \hat{\mathbf{z}}) + \tau_z m_z \mathbf{J} + \tau_{\text{ani}} \nabla_{\mathbf{m}} [J_y m_x m_y + J_x (m_y^2 - m_x^2)] / 2$
CrGeTe_3	$\text{P}\bar{3}$ (147)	Trigonal	$\tau_{\text{FL}}^I \mathbf{J} \times \hat{\mathbf{z}} + \tau_F^{II} \mathbf{J}$	$\begin{aligned} & \tau_{\text{DL}}^I \mathbf{m} \times (\mathbf{J} \times \hat{\mathbf{z}}) + \tau_z m_z \mathbf{J} + \tau_{\text{ani}}^I \nabla_{\mathbf{m}} \left[J_y m_x m_y + \frac{J_x (m_x^2 - m_y^2)}{2} \right] \\ & + \tau_{\text{ani}}^{II} \nabla_{\mathbf{m}} \left[J_y m_x m_y + \frac{J_x (m_x^2 - m_y^2)}{2} \right] + \tau_o^{II} [(\mathbf{J} \times \mathbf{m}) \cdot \hat{\mathbf{z}}] \hat{\mathbf{z}} \end{aligned}$
FeTe^\dagger	$\text{P}4/\text{nmm}$ (129)	Tetragonal	$\tau_{\text{FL}} \mathbf{J} \times \hat{\mathbf{z}}$	$\tau_o \mathbf{m} \times (\mathbf{J} \times \hat{\mathbf{z}}) + \tau_z m_z \mathbf{J}$
CrI_2	$\text{P}\bar{4}\text{m}2$ (115)	Orthorhombic	$\begin{pmatrix} 0 & \tau_{\text{FL}}^{xy} \\ \tau_{\text{FL}}^{yx} & 0 \end{pmatrix} \mathbf{J}$	$(\mathbf{M} \cdot \hat{\mathbf{z}}) \begin{pmatrix} \tau_z^x & 0 \\ 0 & \tau_z^y \end{pmatrix} \mathbf{J} + \mathbf{M} \cdot \begin{pmatrix} \tau_o^x & 0 \\ 0 & \tau_o^y \end{pmatrix} \mathbf{J} \hat{\mathbf{z}}$
CrSBr	$\text{P}n\text{mm}$ (59)	Orthorhombic	$\begin{pmatrix} 0 & \tau_{\text{FL}}^{xy} \\ \tau_{\text{FL}}^{yx} & 0 \end{pmatrix} \mathbf{J}$	$(\mathbf{M} \cdot \hat{\mathbf{z}}) \begin{pmatrix} \tau_z^x & 0 \\ 0 & \tau_z^y \end{pmatrix} \mathbf{J} + \mathbf{M} \cdot \begin{pmatrix} \tau_o^x & 0 \\ 0 & \tau_o^y \end{pmatrix} \mathbf{J} \hat{\mathbf{z}}$
NiPS_3	$\text{C}2/\text{m}$ (12)	Monoclinic	$\begin{pmatrix} 0 & \tau_{\text{FL}}^{xy} & 0 \\ \tau_{\text{FL}}^{yx} & 0 & 0 \\ 0 & \tau_{\text{FL}}^{yz} & 0 \end{pmatrix} \mathbf{J}$	$\begin{pmatrix} M_x \tau_o^{x,xx} + M_z \tau_o^{z,xx} & M_y \tau_o^{y,yx} & 0 \\ M_y \tau_o^{y,xy} & M_x \tau_o^{x,yy} + M_z \tau_o^{z,yy} & 0 \\ M_z \tau_o^{z,xz} & 0 & 0 \end{pmatrix} \mathbf{J} + \mathbf{M} \cdot \begin{pmatrix} \tau_o^{xx} & 0 & 0 \\ 0 & \tau_o^{yy} & 0 \\ 0 & 0 & 0 \end{pmatrix} \mathbf{J} \hat{\mathbf{z}}$

“Spukhafte Fernwirkung!”



"Spukhafte Fernwirkung!"

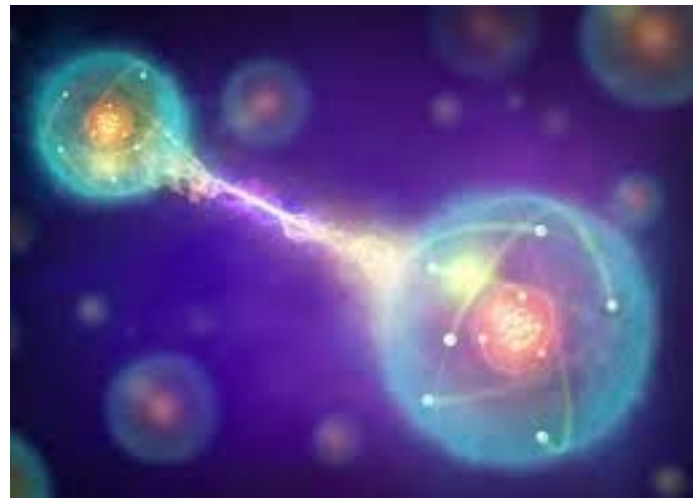
Letter to Max Born(1947),
about the statistical approach to quantum mechanics

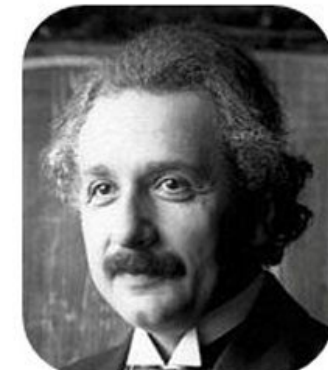
"I cannot seriously believe in "it" because the theory cannot be reconciled with the idea that physics should represent a reality in space and time, free from spooky action at a distance..."

(A. Einstein)



Spooky Action At A Distance





A. Einstein



B. Podolsky



N. Rosen

MAY 15, 1935

PHYSICAL REVIEW

VOLUME 47

Can Quantum-Mechanical Description of Physical Reality Be Considered Complete?

A. EINSTEIN, B. PODOLSKY AND N. ROSEN, *Institute for Advanced Study, Princeton, New Jersey*
(Received March 25, 1935)

In a complete theory there is an element corresponding to each element of reality. A sufficient condition for the reality of a physical quantity is the possibility of predicting it with certainty, without disturbing the system. In quantum mechanics in the case of two physical quantities described by non-commuting operators, the knowledge of one precludes the knowledge of the other. Then either (1) the description of reality given by the wave function in

quantum mechanics is not complete or (2) these two quantities cannot have simultaneous reality. Consideration of the problem of making predictions concerning a system on the basis of measurements made on another system that had previously interacted with it leads to the result that if (1) is false then (2) is also false. One is thus led to conclude that the description of reality as given by a wave function is not complete.



of them with a representative of its own. I would not call that *one* but rather *the* characteristic trait of quantum mechanics, the one that enforces its entire departure from classical lines of thought. By the interaction the two representatives (or ψ -functions) have become entangled. To disentangle them we must gather further information by experiment, although we knew as much as any-

30 years after (1964)...., John Bell proved that no theory of nature that obeys locality and realism can reproduce all the predictions of quantum theory



VOLUME 49, NUMBER 2

PHYSICAL REVIEW LETTERS

12 JULY 1982

**Experimental Realization of Einstein-Podolsky-Rosen-Bohm *Gedankenexperiment*:
A New Violation of Bell's Inequalities**

Alain Aspect, Philippe Grangier, and Gérard Roger

*Institut d'Optique Théorique et Appliquée, Laboratoire associé au Centre National de la Recherche Scientifique,
Université Paris-Sud, F-91406 Orsay, France*

(Received 30 December 1981)

The linear-polarization correlation of pairs of photons emitted in a radiative cascade of calcium has been measured. The new experimental scheme, using two-channel polarizers (i.e., optical analogs of Stern-Gerlach filters), is a straightforward transposition of Einstein-Podolsky-Rosen-Bohm *gedankenexperiment*. The present results, in excellent agreement with the quantum mechanical predictions, lead to the greatest violation of generalized Bell's inequalities ever achieved.

(practical?) Quantum Computers

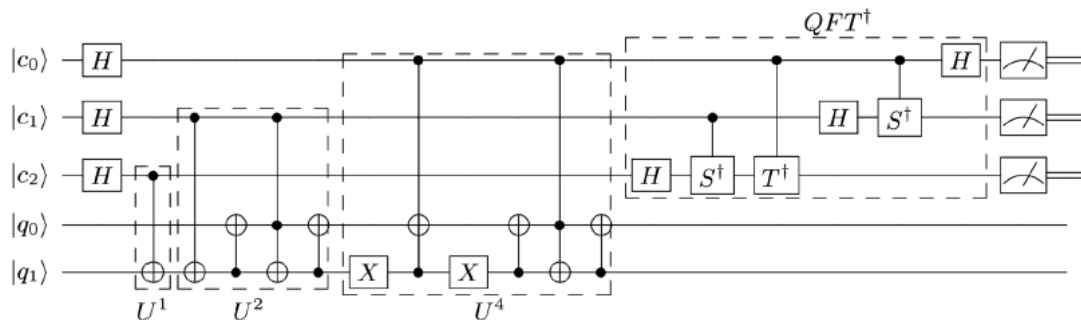
- **IBM** – 400 Qubits plus quantum processor (2022)
- **D-Wave** 5000 Qubits quantum annealer
- **Microsoft** –Quantum Lab-Delft.... **“Chi l’ha visto?”**
- **Google** –Quantum Artificial Intelligence Lab
- **Bristlecone**: 72-qubit quantum chip..



aims to build quantum processors and develop novel quantum algorithms to dramatically accelerate computational tasks for machine learning

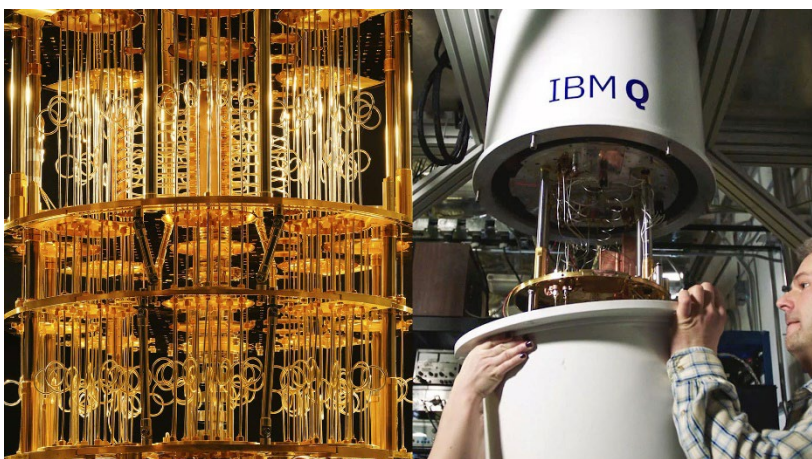
What available IBM quantum computer can do today?

Useful Quantum algorithm (Shor's algorithm) factorizing very large number in prime numbers... ("quantum cryptography...")



exponentially faster than the most efficient known classical factoring algorithm....

27-qubit quantum processor **ibmq_toronto** **scientific reports**



OPEN

Demonstration of Shor's factoring algorithm for $N = 21$ on IBM quantum processors

Unathi Skosana & Mark Tame

We report a proof-of-concept demonstration of a quantum order-finding algorithm for factoring the integer 21. Our demonstration involves the use of a compiled version of the quantum phase estimation routine, and builds upon a previous demonstration. We go beyond this work by using a configuration of approximate Toffoli gates with residual phase shifts, which preserves the functional correctness and allows us to achieve a complete factoring of $N = 21$. We implemented the algorithm on IBM quantum processors using only five qubits and successfully verified the presence of entanglement between the control and work register qubits, which is a necessary condition for the algorithm's speedup in general. The techniques we employ may be useful in carrying out Shor's algorithm for larger integers, or other algorithms in systems with a limited number of noisy qubits.

"Observation of topological phenomena in a programmable lattice of 1,800 qubits"

A.D. King et al **Nature 560, 456 (2018)**



Topological quantum transition (Kosterlitz-Thouless)

Reproduced with Large scale simulation in a network of 1,800 **in situ programmable superconducting niobium flux qubits**

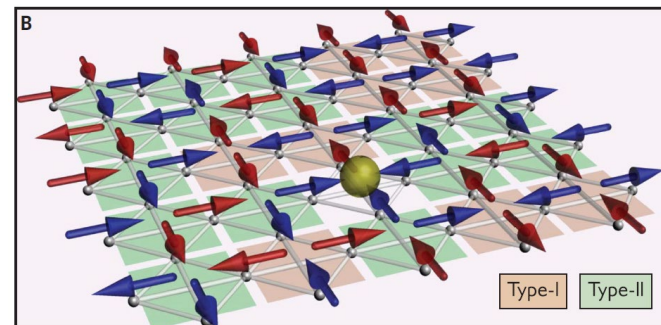
A. D King et al., **Science 373, 576–580 (2021)**

MAGNETISM

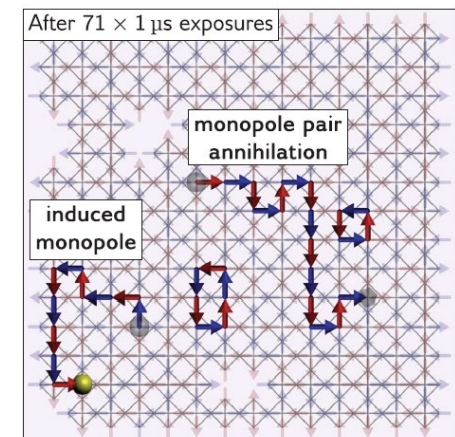
Qubit spin ice

Andrew D. King^{1*}, Cristiano Nisoli^{2*}, Edward D. Dahl¹,
Gabriel Poulin-Lamarre¹, Alejandro Lopez-Bezanilla²

$$\mathcal{H} = \mathcal{J} \left(\sum_{\langle ij \rangle} J_{ij} \hat{\sigma}_i^z \hat{\sigma}_j^z + \sum_i h_i \hat{\sigma}_i^z \right) - \Gamma \sum_i \hat{\sigma}_i^x$$



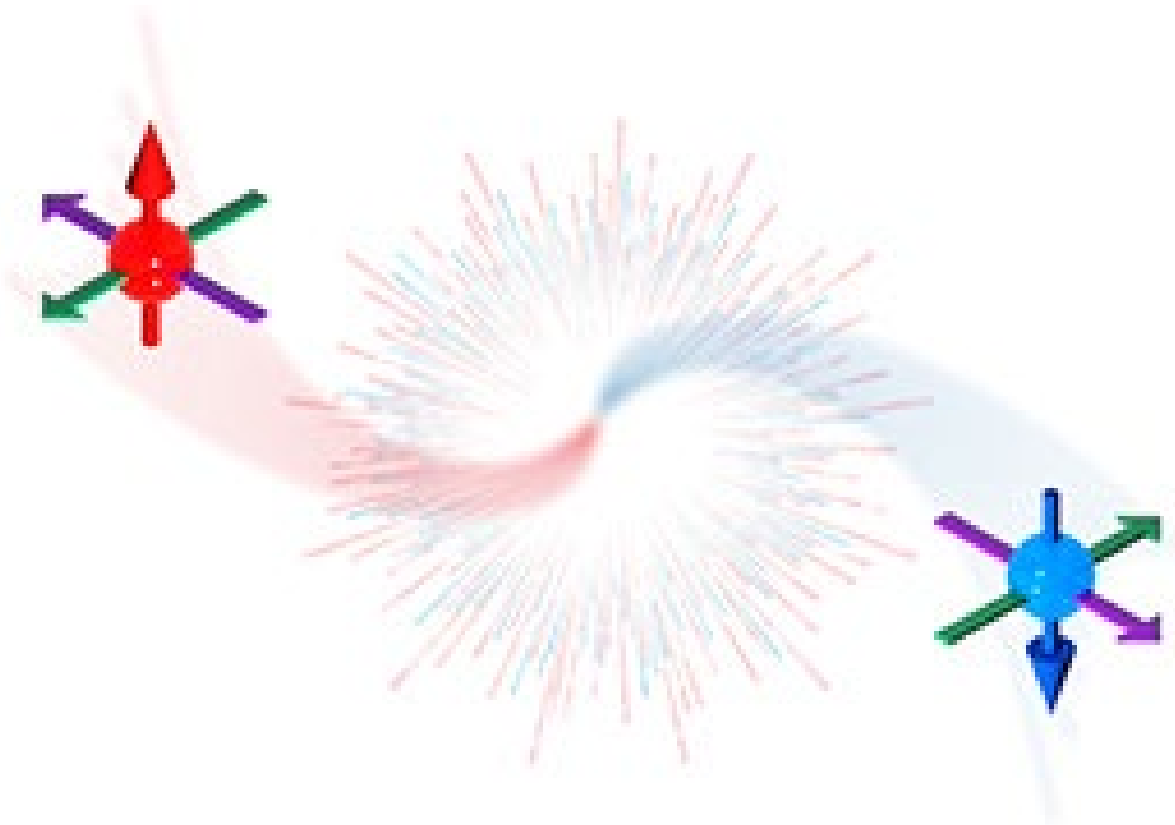
Artificial spin ices are frustrated spin systems that can be engineered, in which fine tuning of geometry and topology has allowed the design and characterization of exotic emergent phenomena at the constituent level. Here, we report a realization of spin ice in a lattice of superconducting qubits. Unlike conventional artificial spin ice, our system is disordered by both quantum and thermal fluctuations. The ground state is classically described by the ice rule, and we achieved control over a fragile degeneracy point, leading to a Coulomb phase. The ability to pin individual spins allows us to demonstrate Gauss's law for emergent effective monopoles in two dimensions. The demonstrated qubit control lays the groundwork for potential future study of topologically protected artificial quantum spin liquids.



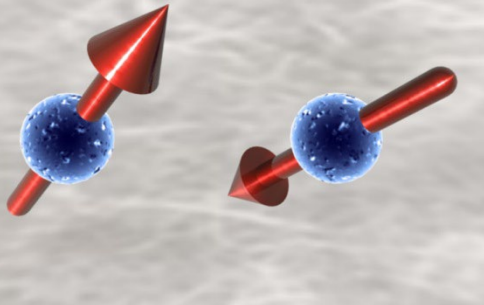
Entanglement in Quantum Matter

as a ressource for

Quantum information



Particles in Graphene

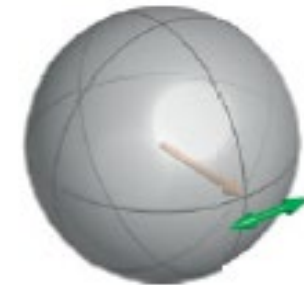


Three intraparticle (quantum) degrees

Spin

Valley “isospín”

Sublattice “pseudospin”



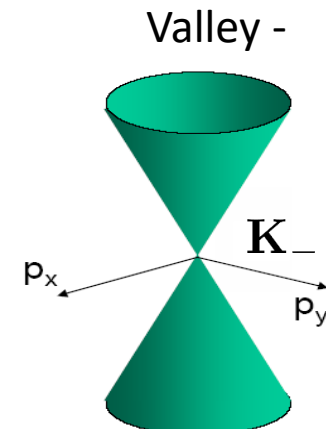
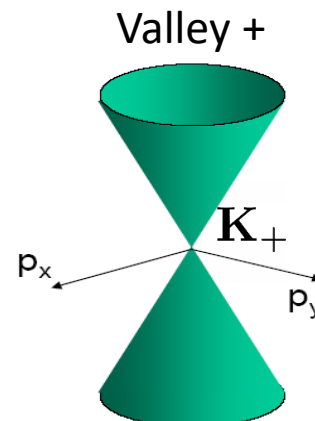
8-components wavefunction

$$\begin{pmatrix} 0 & p_x - ip_y & 0 & 0 & 0 & 0 & 0 & 0 \\ p_x - ip_y & 0 & 0 & 0 & 0 & 0 & 0 & 0 \\ 0 & 0 & 0 & -p_x + ip_y & 0 & 0 & 0 & 0 \\ 0 & 0 & -p_x + ip_y & 0 & 0 & 0 & 0 & 0 \\ 0 & 0 & 0 & 0 & 0 & p_x - ip_y & 0 & 0 \\ 0 & 0 & 0 & 0 & p_x - ip_y & 0 & 0 & 0 \\ 0 & 0 & 0 & 0 & 0 & 0 & 0 & -p_x + ip_y \\ 0 & 0 & 0 & 0 & 0 & 0 & -p_x + ip_y & 0 \end{pmatrix} \begin{pmatrix} \Psi_{A,+}^{\uparrow} \\ \Psi_{B,+}^{\uparrow} \\ \Psi_{A,-}^{\uparrow} \\ \Psi_{B,-}^{\uparrow} \\ \Psi_{A,+}^{\downarrow} \\ \Psi_{B,+}^{\downarrow} \\ \Psi_{A,-}^{\downarrow} \\ \Psi_{B,-}^{\downarrow} \end{pmatrix}$$

No intervalley/spin mixing- Valleys degenerate..
No disorder, No spin-orbit interaction

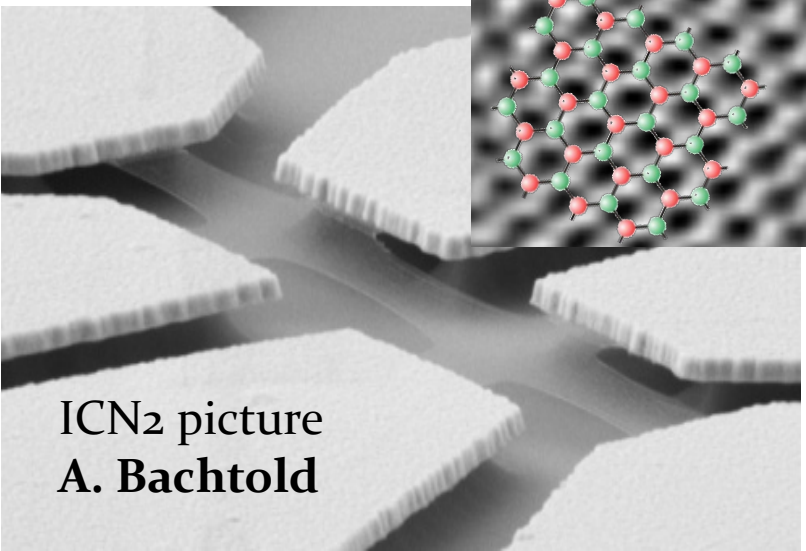
$$\mathcal{H}_{K_+} = v_F \vec{\sigma} \cdot \vec{p}$$

DIRAC Fermions
GAPLESS Linear energy dispersion
and velocity $10^6 m/s$

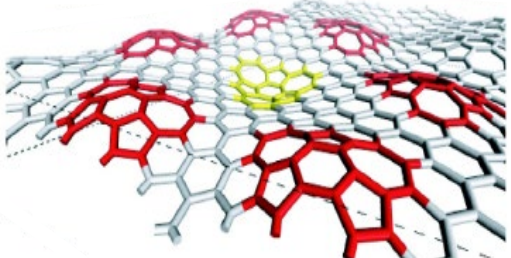


“Unique properties of Clean graphene”

$$\mathcal{H}_{K_+} = v_F \vec{\sigma} \cdot \vec{p}$$



Long range potential
Intravalley scattering
(short momentum transfer)

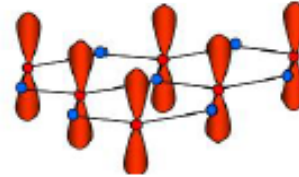


$$\mathcal{H}_{K_+} |\Psi_{\vec{p}}\rangle = E_{\vec{p}} |\Psi_{\vec{p}}\rangle$$

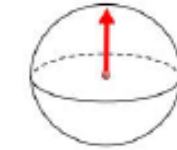
$$\Psi_{\vec{p}} = \frac{1}{\sqrt{2}} \left(\Psi_{\vec{p}}(A) \begin{pmatrix} 1 \\ 0 \end{pmatrix} + \Psi_{\vec{p}}(B) \begin{pmatrix} 0 \\ 1 \end{pmatrix} \right)$$

pseudospin

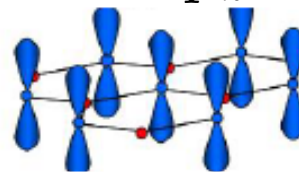
A sublattice : p_z



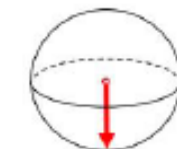
$$|\Psi_A\rangle$$



B sublattice : p_z



$$|\Psi_B\rangle$$



Spinor Representation

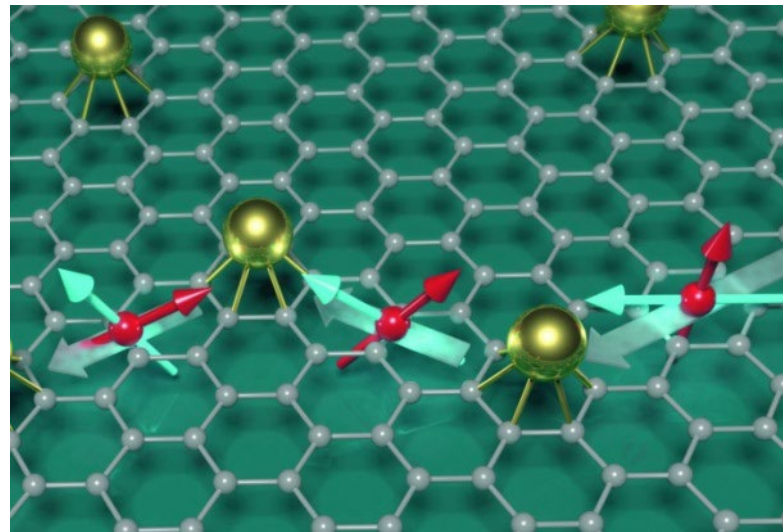
And related Berry's phase

Anomalous quantum transport

- Ballistic conductivity $\sigma \sim 4e^2/\pi h$
- Klein tunneling
- Diverging zero-energy Mean free path/mobility
- Weak antilocalization (quantum interferences)
- Anomalous vs conventional QHE
- **Spin transport ?**

Pseudospin-driven spin relaxation mechanism in graphene

Dinh Van Tuan^{1,2}, Frank Ortmann^{1,3,4}, David Soriano¹, Sergio O. Valenzuela^{1,5} and Stephan Roche^{1,5*}



$$\vec{P}(E, t) = \frac{\langle \psi_{\uparrow}(t) | [1_{\sigma} \otimes \vec{s}] \delta(E - \mathcal{H}^{\text{eff}}) + \delta(E - \mathcal{H}^{\text{eff}}) [1_{\sigma} \otimes \vec{s}] | \psi_{\uparrow}(t) \rangle}{2 \langle \psi_{\uparrow}(t) | \delta(E - \mathcal{H}^{\text{eff}}) | \psi_{\uparrow}(t) \rangle}$$

Spin-Pseudospin entanglement

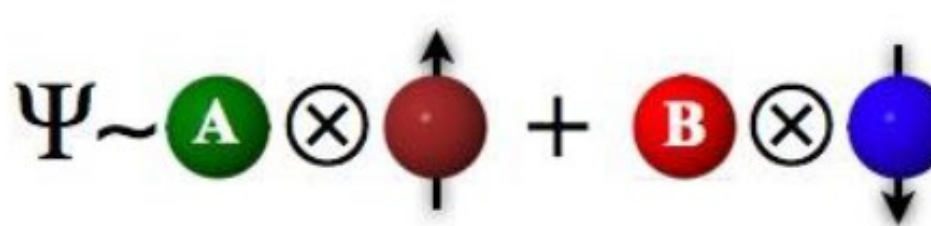
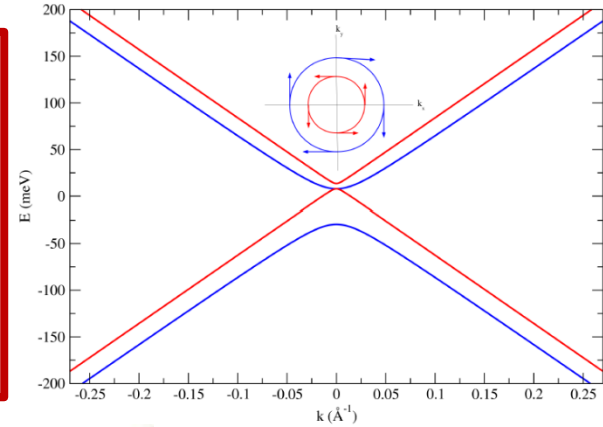
$$h_0(\vec{k}) = \hbar v_F (\eta \sigma_x k_x + \sigma_y k_y) \otimes 1_s$$

$$h_R(\vec{k}) = \bar{\lambda}_R (\eta [\sigma_x \otimes s_y] - [\sigma_y \otimes s_x])$$

$$h_I(\vec{k}) = \bar{\lambda}_I \eta [\sigma_z \otimes s_z]$$

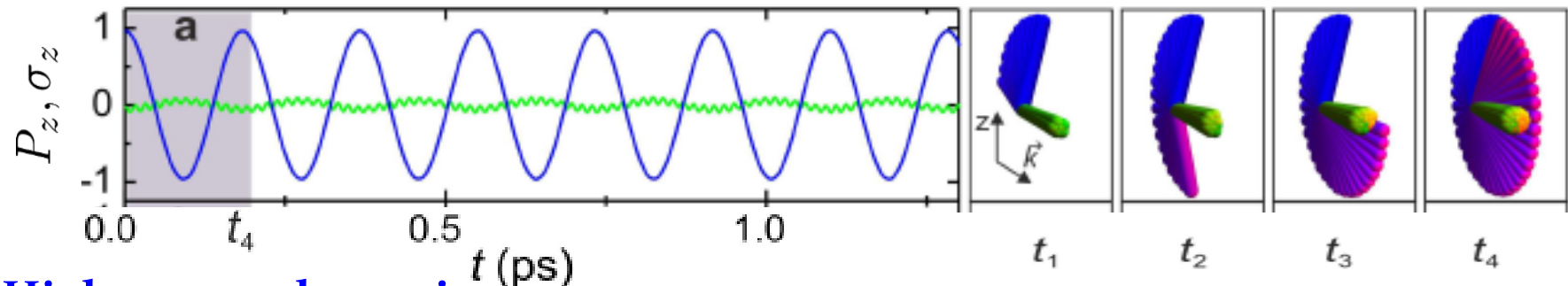
$$\Psi_{\vec{k},\pm}^I = \begin{pmatrix} 0 \\ 1 \end{pmatrix} \otimes |\uparrow\rangle \pm \begin{pmatrix} i \\ 0 \end{pmatrix} \otimes |\downarrow\rangle$$

$$\Psi_{\vec{k},\pm}^{II} = \begin{pmatrix} 1 \\ 0 \end{pmatrix} \otimes |\uparrow\rangle \pm \begin{pmatrix} 0 \\ i \end{pmatrix} \otimes |\downarrow\rangle$$



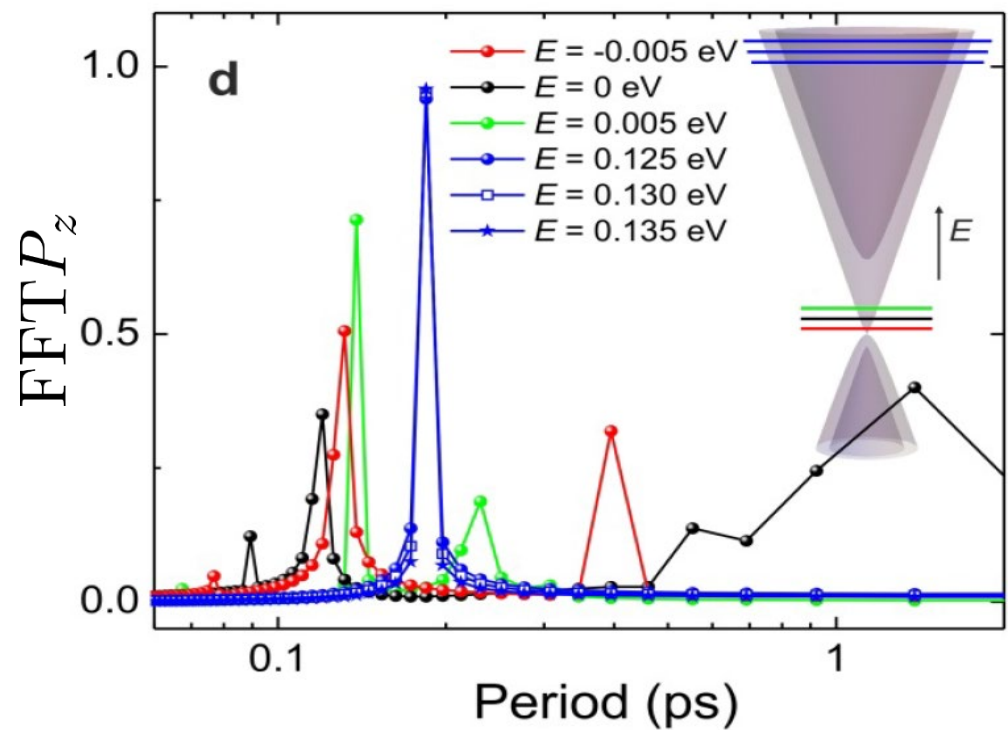
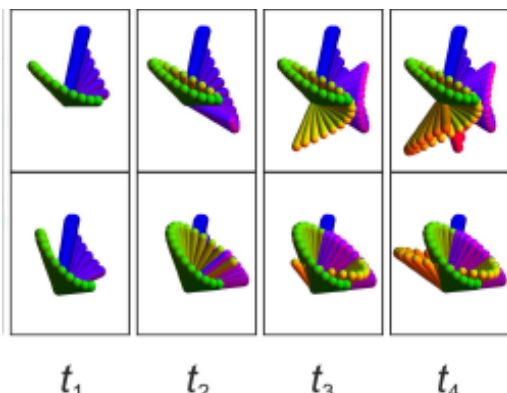
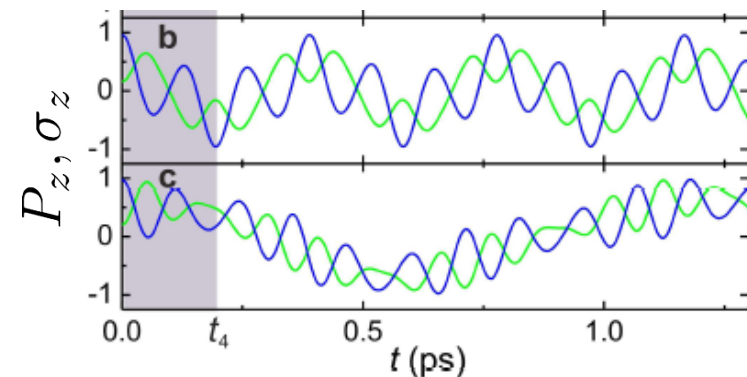
a change in sublattice (pseudospin) index entails a change in spin index
Low energy spin and pseudospin are completely locked

Spin-Pseudospin dynamics



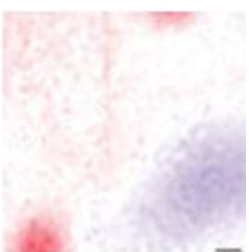
High energy dynamics

Low-energy dynamics



Stronger dephasing at Dirac point

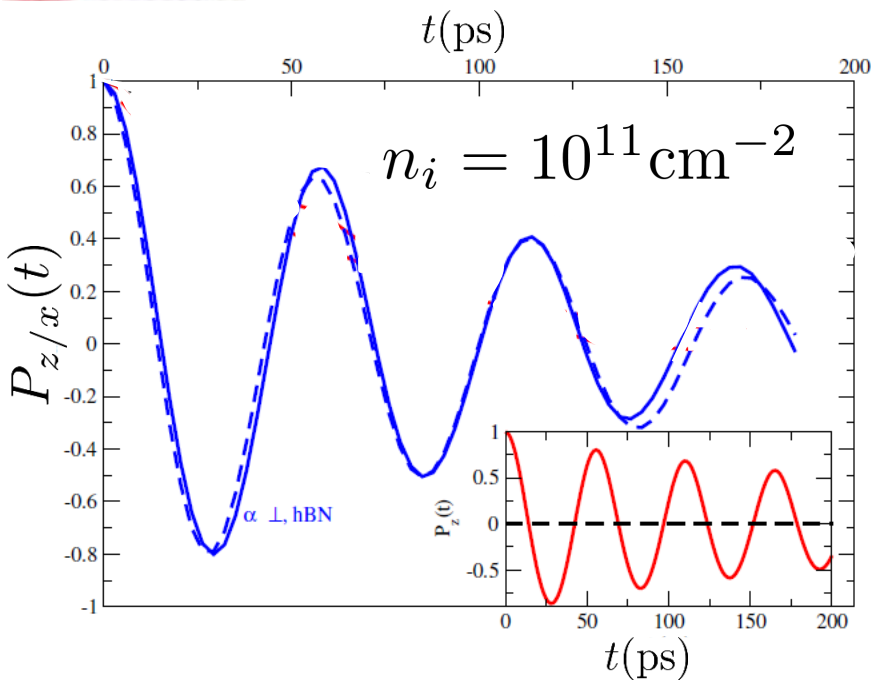
Dephasing results combination of non-uniform spin precession freq and broadening



Graphene on hBN

electron-hole puddles drive the relaxation

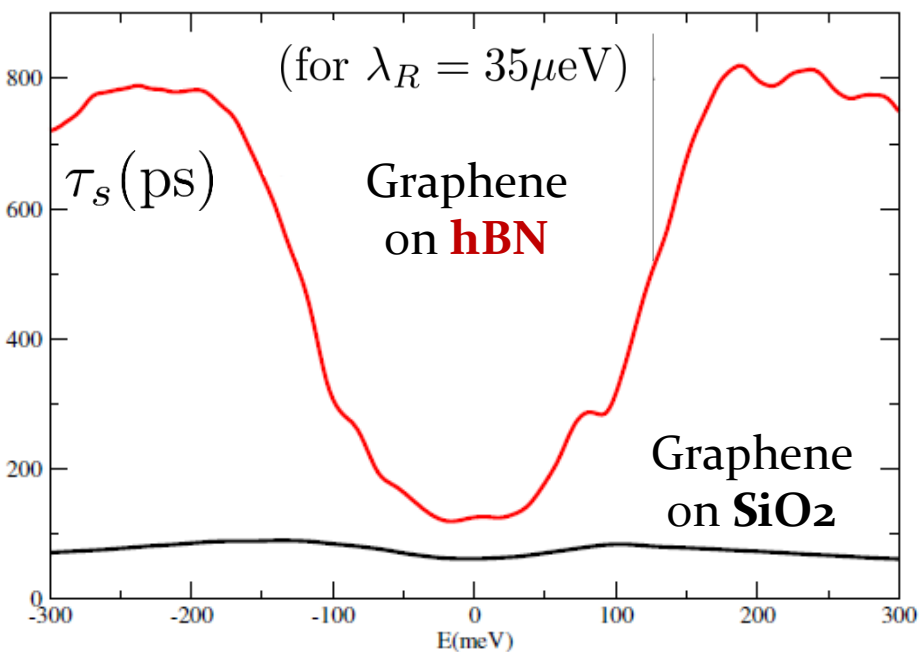
$$\tau_p^{\text{hBN}} / T_\Omega \geq 1$$



Dephasing driven by an
entangled dynamics between
spin and pseudospin

D. Van Tuan et al, **Nature Physics 10, 857 (2014)**
„ **Sci. Reports 6, 21046 (2016)**
A.W. Cummings and SR, **PRL 116, 086602 (2016)**

$$P_{z/x}(t) \sim \cos\left(\frac{2\pi t}{T_\Omega}\right) e^{-t/\tau_s}$$



$$\tau_s(E) \approx 4T_\Omega \approx 4 \frac{\pi\hbar}{\lambda_R}$$

$$\tau_s \simeq 1 - 10 \text{ ns}$$

(for $\lambda_R \rightarrow 5 \mu\text{eV}$)

Emergence of intraparticle entanglement and time-varying violation of Bell's inequality in Dirac matter

Bruna Gabrielly de Moraes^{1,2}, Aron W. Cummings¹, Stephan Roche^{1,3,*}

¹Catalan Institute of Nanoscience and Nanotechnology (ICN2), CSIC and BIST, Campus UAB, Bellaterra, 08193 Barcelona, Spain

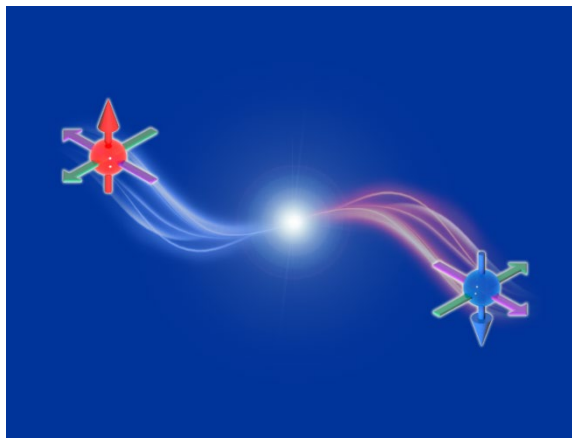
²Department of Physics, Universitat Autònoma de Barcelona, Campus UAB, Bellaterra, 08193 Barcelona, Spain

³Institució Catalana de Recerca i Estudis Avançats (ICREA), 08010 Barcelona, Spain



(Received 2 June 2020; revised 16 July 2020; accepted 17 July 2020; published 30 July 2020)

We demonstrate the emergence and dynamics of intraparticle entanglement in massless Dirac fermions. This entanglement, generated by spin-orbit coupling, arises between the spin and sublattice pseudospin of electrons in graphene. The entanglement is a complex dynamic quantity but is generally large, independent of the initial state. Its time dependence implies a dynamical violation of a Bell inequality, while its magnitude indicates that large intraparticle entanglement is a general feature of graphene on a substrate. These features are also expected to impact entanglement between pairs of particles, and may be detectable in experiments that combine Cooper pair splitting with nonlocal measurements of spin-spin correlation in mesoscopic devices based on Dirac materials.



*Emerging entanglement properties
between intraparticle degrees of freedom
Robustness against decoherence
Possibility of nonlocal manipulation...*

Concurrence (entanglement degree)

$$R = \sqrt{\rho_{1,2}(\sigma_{1y} \otimes \sigma_{2y})\rho_{1,2}^*(\sigma_{1y} \otimes \sigma_{2y})}$$

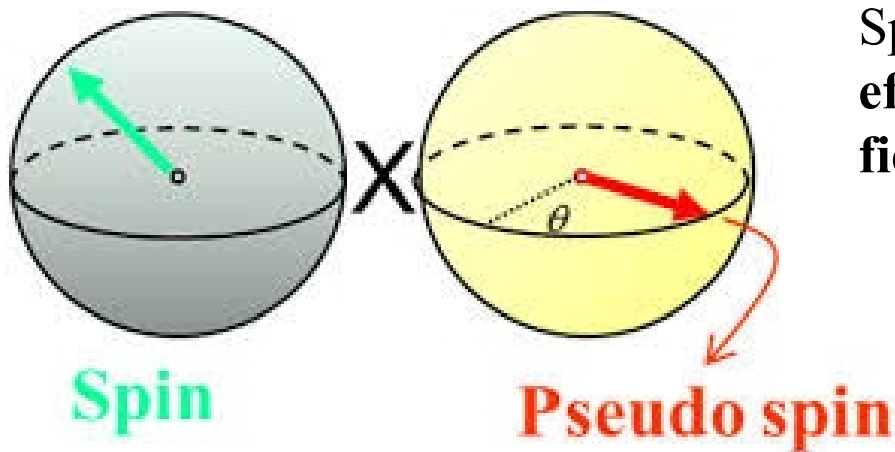
diagonalising an operator R which is built from the general **two-qubit density matrix**

$$C(\phi) = \max\{0, \tilde{\lambda}_1 - \tilde{\lambda}_2 - \tilde{\lambda}_3 - \tilde{\lambda}_4\}$$

Concurrence has a one-to-one correlation with the entanglement of formation, and ranges between 0 (separable state) and 1 (maximally entangled state)

Concurrence (spin-pseudospin) for electronic states propagating in Graphene/substrate (SiO_2 or hBN)

$$\hat{\mathcal{H}} = \hbar v_F (\tau \hat{\sigma}_x k_x + \hat{\sigma}_y k_y) \otimes \hat{s}_0 + \lambda_R (\tau \hat{\sigma}_x \otimes \hat{s}_y - \hat{\sigma}_y \otimes \hat{s}_x)$$



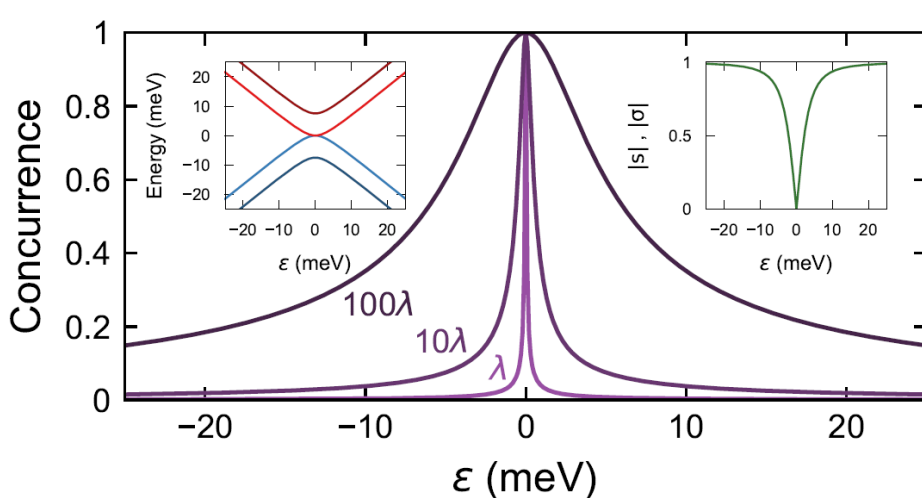
Spin and pseudospin will precess around **effective magnetic and pseudomagnetic fields** (oscillation freq. $\omega_R = 2\lambda_R/\hbar$)

$$\mathbf{B}_s^{\text{eff}}(t) = \lambda_R (-\langle \hat{\sigma}_y \rangle(t), \langle \hat{\sigma}_x \rangle(t), 0),$$

$$\begin{aligned} \mathbf{B}_{\sigma}^{\text{eff}}(t) &= \lambda_R (\langle \hat{s}_y \rangle(t), -\langle \hat{s}_x \rangle(t), 0) \\ &\quad + \varepsilon (1, 0, 0), \end{aligned}$$

Hamiltonian (Rashba SOC) & Concurrence (spin-pseudospin)

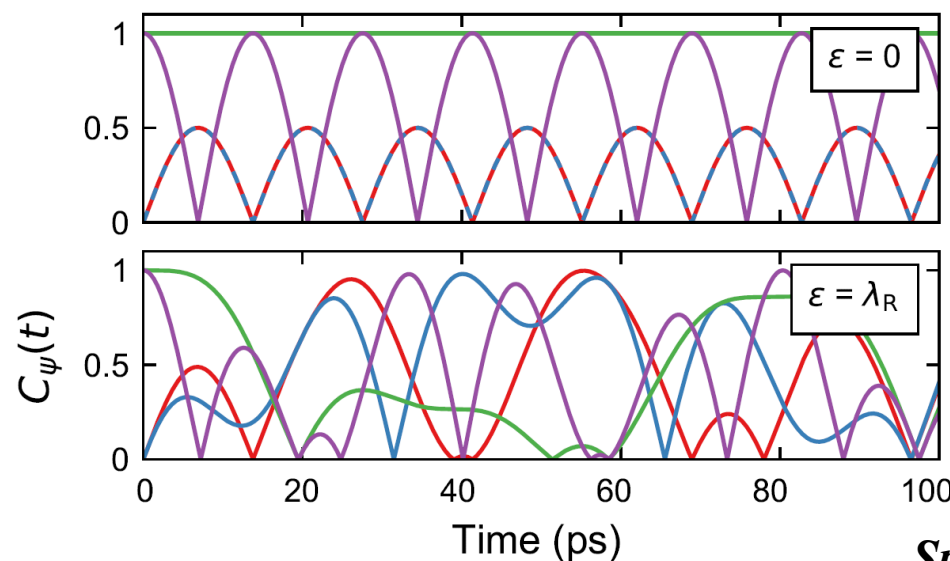
$$\hat{\mathcal{H}} = \hbar v_F (\tau \hat{\sigma}_x k_x + \hat{\sigma}_y k_y) \otimes \hat{s}_0 + \lambda_R (\tau \hat{\sigma}_x \otimes \hat{s}_y - \hat{\sigma}_y \otimes \hat{s}_x)$$



$$[|A\uparrow\rangle \quad |B\uparrow\rangle \quad |A\downarrow\rangle \quad |B\downarrow\rangle]^T$$

In the eigenstates basis of H

$$C_{\phi_{\pm}^{\text{e,h}}} = \lambda_R / \sqrt{\varepsilon^2 + \lambda_R^2}$$



$$\begin{array}{c} \textcolor{red}{|}\psi_x^\uparrow\rangle \textcolor{blue}{|}\psi_y^\uparrow\rangle \textcolor{green}{|}\psi_{\text{Bell}}^1\rangle \textcolor{purple}{|}\psi_{\text{Bell}}^2\rangle \end{array}$$

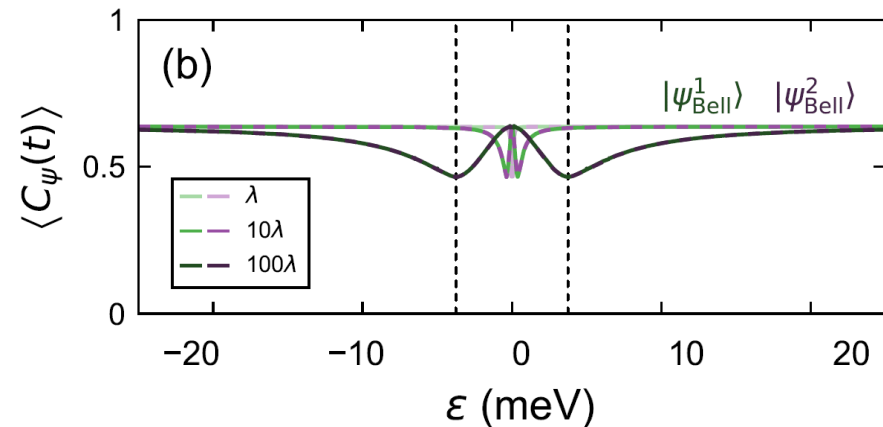
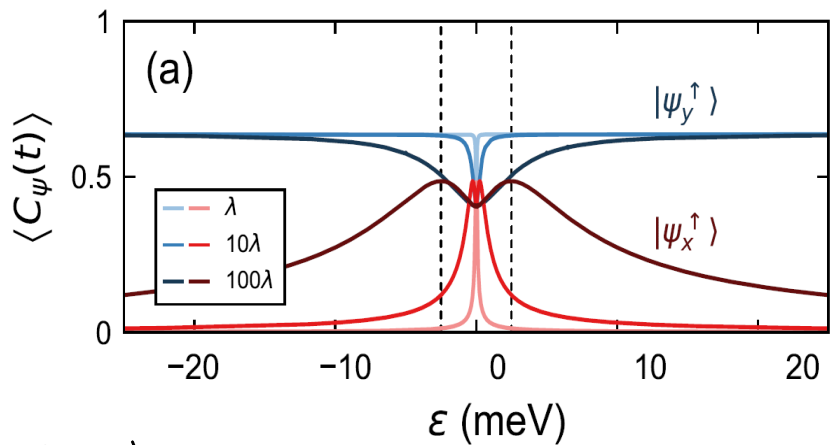
Time-evolution of concurrence
for different initial states

$$\frac{1}{\sqrt{2}} [1 \quad 1 \quad 0 \quad 0]^T = \frac{1}{\sqrt{2}} (|A\rangle + |B\rangle) \otimes |\uparrow\rangle = |\psi_x^\uparrow\rangle$$

pseudospin along x, spin along z

States initially unentangled acquired
Spin-pseudospin entanglement during propagation

Emergence, persistent & robust spin-pseudospin entanglement

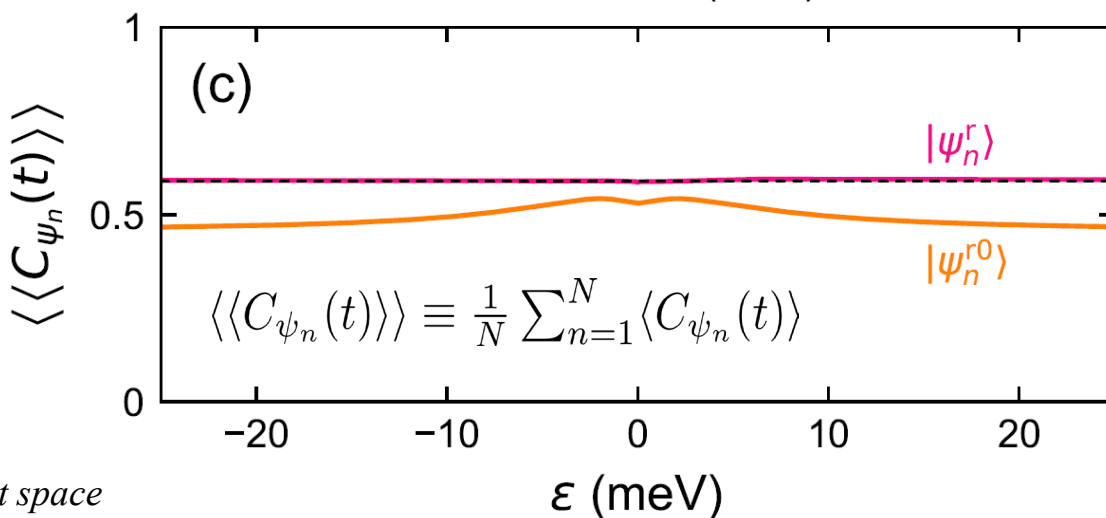


$|\psi_n^{r0}\rangle$

is a separable state with random spherical angles defining the orientations of the pseudospin and spin on the Bloch sphere

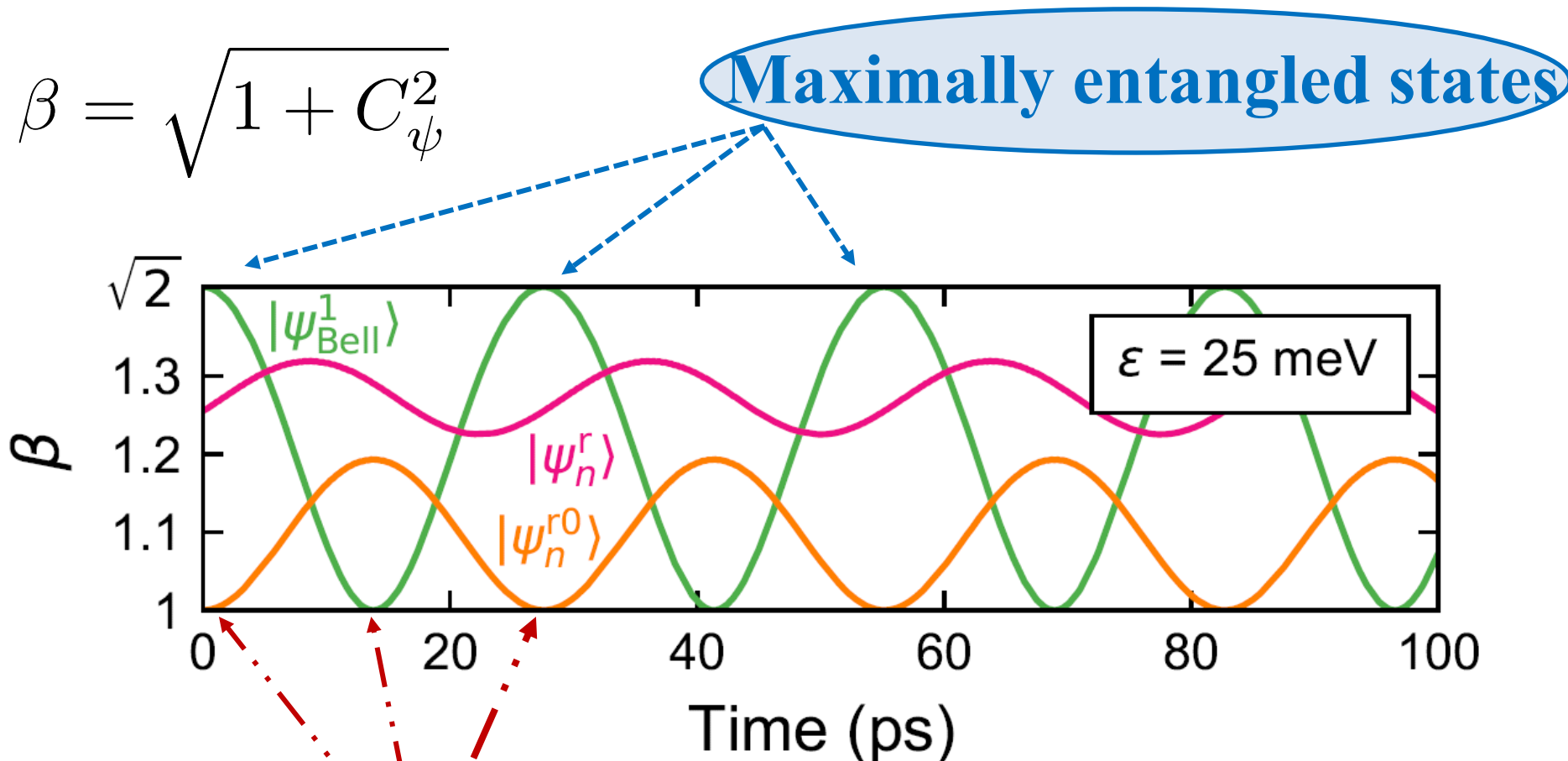
$$|\psi_n^r\rangle = [a \quad b \quad c \quad d]^T$$

States that are equivalent to the action of a random unitary matrix on some reference state, which are uniform over the four-dimensional Hilbert space



Even arbitrarily initial state develops a final entanglement
(entanglement resilient to scattering)

Time-dependent violation of the Bell inequality (CHSH variant)



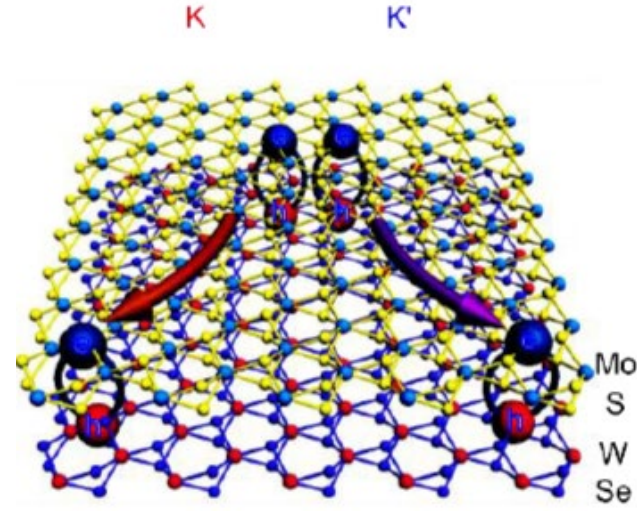
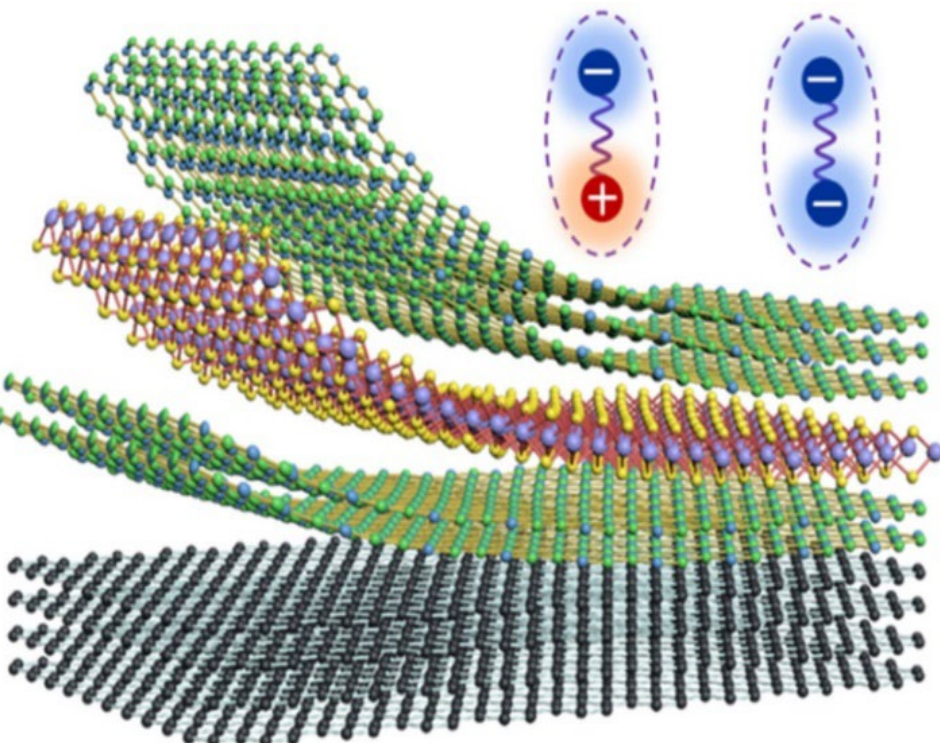
Unentangled states

Whatever the initial state
There is always an emerging
intraparticle entanglement resource
generated during the dynamics

Van der Waals heterostructures Dirac-Topological Matter

opportunities to *manipulate DoFs by external fields*
(electromagnetic, deformation fields, proximity effects...)

Two (more)-particle entanglement
generation, manipulation & detection
using intraparticle vs interparticle DoFs



Time-evolution of non-local
correlations

Conference and Advanced School on Low-Dimensional Quantum Systems



Slides available upon request

Stephan.roche@icn2.cat

Connect with me on !!



*“...Semejante a un rebaño de nubes, arrastrando la cola inmensa
y turbia de lo desconocido
tu alma enorme rebasa tus hechos y tus cantos,
y es lo mismo que un viento terrible y milenario encadenado
a una matita de suspiros...”*

Pablo de Rokha

